

**Interactions of *BLADE-ON-PETIOLE1* and 2 with
TALE Homeobox Genes in the Regulation of Flowering
and Inflorescence Architecture in *Arabidopsis thaliana***

By: Madiha Khan

A thesis submitted to the Faculty of Graduate and Postdoctoral Affairs in partial
fulfillment of the requirements for the degree of

Doctor of Philosophy

In

Biology

Carleton University

Ottawa, Ontario, Canada

© 2013

Madiha Khan

ABSTRACT

Plants have evolved a diversity of inflorescence architectures and variations in flowering time to maximize reproductive success within their environment. BLADE-ON-PETIOLE 1, 2 (*BOP1/2*) are a class of BTB-ankryin transcription factors with homology to the defense regulator NONEXPRESSOR OF PATHOGENESIS-RELATED GENES1 (*NPR1*). *BOP* activity is concentrated at meristem-organ junctions (“lateral organ boundaries”) where it functions to control the morphology of leaves, flowers, fruits, and inflorescences. Loss-of-function studies have elucidated how *BOP1/2* control leaf development, but how *BOP1/2* regulate inflorescence architecture is still relatively unknown. Gain-of-function *BOP1/2* plants mimic loss-of-function in *KNOX* and *BELL* three-amino-acid-loop extension (*TALE*) homeodomain proteins. *BEL1*-like (*BELL*) genes *PENNYWISE* (*PNY*) and *POUNDFOOLISH* (*PNF*) are required for *Arabidopsis* (*Arabidopsis thaliana*) competence to flower, whereas the *KNOTTED1*-like *HOMEODOMAIN* (*KNOX*) gene *BREVIPEDICELLUS* (*BP*) in conjunction with *PNY* control internode elongation and stem patterning in inflorescences.

In this thesis, I used *BOP* gain-of-function as an approach to uncover interactions with *TALE* homeobox genes in regulation of flowering and inflorescence architecture. Firstly, I showed that *BP* and *PNY* in stems restrict *BOP1/2* expression to boundaries at the base of the floral shoot to promote internode elongation and vascular patterning. Expression analysis revealed *bp* and *pny* inflorescence defects are caused by misexpression of *BOP1/2*. Furthermore, I showed that *BOP1/2* antagonize *BP/PNY* activities by activating the lateral organ boundary gene *KNOTTED-like from ARABIDOPSIS THALIANA6* (*KNAT6*). My research also revealed that *BOP1/2* function downstream of *BP/PNY* in

opposing fashion, through reciprocal regulation of downstream target genes, including biosynthetic enzymes required for lignin deposition in stems.

Secondly, I identified another boundary gene *ARABIDOPSIS THALIANA HOMEBOX GENE1 (ATH1)* as required by BOP1/2 to antagonize BP/PNY activity. Rescue experiments showed that *ATH1* misexpression was the cause of *bp* and *pnf* inflorescence defects. These studies revealed that BOP1/2 induce the expression of boundary genes *ATH1* and *KNAT6*, whose interacting products form a complex that opposes BP-PNY activity.

Lastly, I found that PNY/PNF in the meristem repress *BOP1/2* to promote competence to flower. I showed *pnf pny* mutants are unable to complete the transition to flowering because *BOP1/2* and its downstream effectors *KNAT6* and *ATH1* are misexpressed in the meristem. Inactivation of these genes rescues *pnf pny* competence to flower. Using a steroid-induction system, I identified *ATH1* and *PRXR9GE (PRXR9)*, a lignin peroxidase gene, as direct transcriptional targets of BOP1 in lateral organ boundaries. BOP1/2 lack a DNA-binding domain and associate with promoter DNA by binding to TGACG (TGA) bZIP transcription factors. I identified TGA1 and TGA4 bZIP factors required by BOP1/2 to exert changes in flowering and inflorescence architecture.

Collectively, these findings shed light on how interplay between BOP1/2 and KNOX-BELL complexes in the meristem and lateral organ boundaries governs flowering and inflorescence architecture in a model plant species.

ACKNOWLEDGEMENTS

In the name of God, the Most Gracious, the Most Merciful

First and foremost, Allhumdulillah!

I would like to express my sincere gratitude to my supervisor, Dr. Shelley Hepworth for her support, guidance and patience. Her constant encouragement and belief in my abilities, since I was an undergraduate student in her lab, have brought me to where I am today. I am very thankful for the opportunities she provided me and the knowledge I have gained from her.

I am grateful to Dr. Douglas Johnson, Dr. Brian Miki and Dr. John Vierula for their guidance as my committee advisors and for providing me with suggestions to help me succeed with my research. I would also like to thank Dr. Owen Rowland for his help throughout my graduate studies.

My time in the Hepworth lab would not have been as interesting without the company of so many wonderful former and current graduate students. Special thanks to Mingli Xu for her patience in teaching me experimental techniques when I first started out as an undergraduate student. I would like to thank Lama Musa and Paul Tabb for bearing with my frustrations with plants. I would also like to acknowledge Jhadeshwar Murmu, Ian Pulsifier, Eryang Li, Shabnam Gholoobi, Alexander Edwards, Sollapura Vishwanath, Huasong Xu, Natalie Woerlen and Bhaswati Devi for their assistance in the lab.

Last, but not least, I would like to thank my family for their love, support and encouragement. I am forever indebted to Mamma and Pappa for all the sacrifices they have had to make to provide us with a good education and for all the prayers and emotional support that has helped me succeed. I am grateful for the motivation and encouragement from Khala Jaan, Bari Khala, Mana, Bushra, Khalo Jaan, Talha, Mum Fariza and the rest of my family and family in-law throughout these years. I owe my deepest gratitude to my husband, Abdool Shafaaz Yasseen III, for his love, support and understanding. I am blessed to have these wonderful people in my life without whom, I could not have succeeded in accomplishing this goal.

PREFACE

This thesis identifies novel roles of BLADE-ON-PETIOLE1 and 2 (BOP1 and BOP2) in flowering time, inflorescence architecture, secondary cell wall biosynthesis, and fruit patterning. This work has resulted in two first-author publications. I was involved in obtaining most of the experimental results included in this work. However, some parts which were carried out in collaboration with other students have been listed in detail below.

Publications included in thesis:

Chapter 2

1. **Khan M**, Xu M, Murmu J, Tabb P, Liu Y, Storey K, McKim SM, Douglas CJ, Hepworth SR (2012) Antagonistic interaction of BLADE-ON-PETIOLE1 and 2 with BREVIPEDICELLUS and PENNYWISE regulates Arabidopsis inflorescence architecture. *Plant Physiol.* **158**: 946-960.

Chapter 3

2. **Khan M**, Tabb P, Hepworth SR (2012) *BLADE-ON-PETIOLE1* and 2 regulate Arabidopsis inflorescence architecture in conjunction with homeobox genes *KNAT6* and *ATH1*. *Plant Signal. Behav.* **7**: 788-792.

Statement of contributions:

1. Chapter 2

Madiha Khan: stained and sectioned *BOP2:GUS* in stems and fruits, characterized the expression pattern of *KNAT2:GUS* and *KNAT6:GUS* in stems and fruits, crossed and obtained homozygous *bp pny* double mutants and characterized the phenotypes of *35S:BOP1/2* and *bp pny* plants, identified homozygous lines of *bop1 bop2 pny*, *bop1 bop2 bp1*, *bop1 bop2 bp-2* and characterized the rescue both qualitatively and quantitatively, created *bp-2 BOP1:GUS*, *bp-2 BOP2:GUS*, *bp-2 KNAT6:GUS*, *pny BOP1:GUS*, *pny BOP2:GUS*, *pny KNAT6:GUS*, *35S:BOP2 KNAT6:GUS*, *bop1 bop2 PNY:GUS* and *35S:BOP2 PNY:GUS* lines and stained them, created homozygous *bp-2*

as2-1 and *pnv as2-1* mutants, created *35S:BOP2/+ Col/+*, *35S:BOP2/+ knat2/+*, *35S:BOP2/+ knat6/+* and *35S:BOP2/+ knat2/+ knat6/+* lines, quantified their height and did qRT-PCR on them to check for transcript levels of *BOP2* in rosette leaves and inflorescence apices, made the cDNA for qRT-PCR of *KNAT6*, *BP* and *PNY* in internodes and pedicels and obtained the RNA from base of stems for qRT-PCR of lignin genes, phloroglucinol-HCl staining on all stem cross-sections and the toluidine blue staining on stem longitudinal sections, S.E.M of fruits, wrote the primary manuscript and aided in subsequent reviews.

Mingli Xu: made the initial crosses for *bop1 bop2 x pnv* and *bop1 bop2 x bp-2* mutants, provided stem sections of *bp-2 BOP2:GUS* and *pnv BOP2:GUS* lines, stained and sectioned *KNAT2:GUS* and *KNAT6:GUS* SD-grown seedlings, performed *in situ* for *KNAT6* and *BP* in the inflorescence and stems, and carried out qRT-PCR analysis of *KNAT6*, *BP*, and *PNY* transcripts in internodes, pedicels and inflorescence using cDNA provided by Madiha Khan.

Jhadeswar Murmu: constructed *tCUP:BOPI/2* and *35S:KNAT6* transgenic plants.

Paul Tabb: photographed *35S:KNAT6*, *bp-2 as2-1*, *pnv as2-1* plants and carried out yeast-two hybrid assays.

Dr. Carl Douglas and Yuanyuan Liu: qRT-PCR of lignin biosynthetic genes

Kathryn Storey: constructed *35S:BOPI* and *35S:BOP2* lines.

Sarah McKim: first identified and provided important insight into the rescue of ectopic lignification in *bp* by *bop1 bop2* mutations.

Dr. Shelley R. Hepworth: designed experiments, took photographs of *BOP2:GUS* stained plants, carried out toluidine blue of stems, carried out phloroglucinol staining of fruits, analyzed data, and prepared the manuscript in conjunction with MK and MX.

2. Chapter 3

Madiha Khan: did the majority of experimental work, analyzed the resulting data, wrote the primary manuscript, and assisted with subsequent editing and reviews.

Paul Tabb: constructed and characterized *bp-2 ath1-3* and *pnv ath1-3* double mutants.

Dr. Shelley R. Hepworth: assisted in experimental design, construction of double mutants, data analysis, and prepared the manuscript in conjunction with MK.

3. Chapter 4

Madiha Khan: did the majority of experimental work, analyzed the data, and wrote the primary manuscript for submission to Journal of Experimental Botany.

Paul Tabb: constructed and characterized *bop1 bop2 pny pnf*, *kna6 pny pnf*, *ath1-3 pny pnf* lines and associated control lines, analyzed *BOP2:GUS* expression in the *pnv pnf* IM, and made the *PRXR9:GUS* reporter construct.

Alexander Edwards: constructed *35S:BOP1-GR* lines with the help of Paul Tabb.

Patrick de Francesco: identified and stained *PRXR9:GUS* lines.

Dr. Shelley R. Hepworth: crossed and identified *pnv pnf ATH1:GUS* and *35S:BOP2 ATH1:GUS* lines. Responsible for editing and submission of the manuscript.

Copyrighted material:

Khan et al., (2012b) Plant Physiology **158**:946-60 is reprinted as Chapter 2 in this thesis with permission from the publisher (American Society of Plant Biologists). Permission to reprint this article was also granted by Mingli Xu (co-first author).

Khan et al., (2012a) Plant Signaling and Behavior **7**:788-792 is reprinted as Chapter 3 in this thesis with permission from the publisher (Landes Bioscience).

TABLE OF CONTENTS

ABSTRACT	2
ACKNOWLEDGEMENTS	4
PREFACE	5
TABLE OF CONTENTS	8
LIST OF ABBREVIATIONS	12
LIST OF TABLES	13
LIST OF FIGURES	14
CHAPTER 1 - INTRODUCTION	16
THESIS OVERVIEW	17
1.1 Model plant <i>Arabidopsis thaliana</i>	18
1.2 Life cycle and modular architecture of <i>Arabidopsis</i>	19
1.3 Vegetative development	20
1.3.1 Organization of the SAM.....	20
1.3.2 Establishment of the SAM.....	21
1.3.3 Maintenance of the SAM.....	22
1.3.3.1 A CLAVATA-WUSHEL feedback loop maintains the SAM	22
1.3.3.2 TALE homeodomain proteins maintain the SAM	23
1.3.4 Phyllotaxis	25
1.3.5 Establishment and maintenance of boundaries	26
1.4 Reproductive development	27
1.4.1 Reproductive plant architecture	28
1.4.2 The floral transition.....	28
1.4.3 Competence to flower	29
1.4.3.1 Photoperiod based regulation of flowering	29
1.4.3.2 <i>FLC</i>	30
1.4.3.3 Vernalization based regulation of flowering.....	30
1.4.3.4 Autonomous pathway based regulation of flowering	31
1.4.4 Floral integrators.....	31
1.4.5 Floral-meristem identity.....	32
1.4.6 Meristem regulators	33
1.4.7 Inflorescence architecture	34

1.4.7.1 BP and PNY promote internode elongation.....	35
1.4.7.2 Lateral-organ boundary genes restrict internode elongation.....	36
1.4.8 Vascular patterning and secondary cell wall biosynthesis.....	36
1.5 BOP1/2 regulation of plant development and defense.....	39
1.5.1 Leaf patterning.....	40
1.5.2 Flower development.....	41
1.5.3 Other species.....	43
1.5.4 Plant defense.....	45
1.5.5 Mechanism.....	45
1.6 Thesis rationale.....	47
CHAPTER 2 – Antagonistic interaction of BLADE-ON-PETIOLE1 and 2 with BREVIPEDICELLUS and PENNYWISE regulates Arabidopsis inflorescence architecture.....	54
2.1 Abstract.....	55
2.2 Introduction.....	56
2.3 Materials and methods.....	59
2.3.1 Plant material and growth conditions.....	59
2.3.2 Primers and genotyping.....	60
2.3.3 Construction of <i>35S::BOP1</i> , <i>35S::BOP2</i> , and <i>tCUP4::BOP1</i> transgenic lines.....	60
2.3.4 Phenotypic analysis of inflorescence structure.....	61
2.3.5 <i>In situ</i> hybridization and localization of GUS activity.....	61
2.3.6 Scanning electron microscopy (SEM).....	62
2.3.7 Lignin staining.....	62
2.3.8 qRT-PCR.....	63
2.3.9 Accession numbers.....	63
2.4 Results.....	64
2.4.1 Expression of <i>BOP1</i> and <i>BOP2</i> in lateral-organ boundaries.....	64
2.4.2 A spectrum of inflorescence architecture defects caused by <i>BOP1/2</i> gain of function.....	65
2.4.3 Inactivation of <i>BOP1/2</i> partially rescues the <i>bp</i> phenotype.....	66
2.4.4 Inactivation of <i>BOP1/2</i> completely rescues the <i>pnv</i> phenotype.....	67
2.4.5 <i>BOP1/2</i> expression domains are expanded in <i>bp</i> and <i>pnv</i> mutants.....	68
2.4.6 <i>BOP1/2</i> promote <i>KNAT6</i> expression.....	69
2.4.7 <i>BOP1/2</i> exert their function through <i>KNAT6</i>	70
2.4.8 <i>BOP1/2</i> and <i>BP/PNY</i> are antagonistic regulators of stem lignification.....	71

2.4.9 BOP1/2 activate genes repressed by BP	73
2.5 Discussion	74
2.5.1 BOP1/2 differentially regulate KNOX activity in leaves and inflorescences	75
2.5.2 Misexpression of <i>BOP1/2</i> restricts growth to create variations in inflorescence architecture.....	75
2.5.3 BOP1/2 and KNAT6 function in the same genetic pathway	76
2.5.4 ARABIDOPSIS THALIANA HOMEBOX GENE1 is a potential KNAT6 cofactor.....	78
2.5.5 BP and BOP1/2 antagonistically regulate secondary cell wall biosynthesis	79
CHAPTER 3- <i>BLADE-ON-PETIOLE1</i> and 2 regulate Arabidopsis inflorescence architecture in conjunction with homeobox genes <i>KNAT6</i> and <i>ATH1</i>	113
3.1 Abstract	114
3.2 Introduction	115
3.3 Results and discussion	117
3.3.1 BOP1/2 promote <i>ATH1</i> expression.....	117
3.3.2 Inactivation of <i>ATH1</i> rescues <i>pnf</i> and partially rescues <i>bp</i> inflorescence defects.....	118
3.3.3 BOP1/2 require <i>ATH1</i> activity to exert changes in inflorescence architecture	119
3.3.4 Roles for <i>KNAT6</i> and <i>ATH1</i> in secondary stem development	119
3.3.5 BOP1/2 are positive regulators of a <i>KNAT6-ATH1</i> boundary module.....	120
CHAPTER 4 – PENNYWISE and POUNDFOOLISH co-ordinate flowering by antagonizing <i>BLADE-ON-PETIOLE</i> mediated activation of lateral organ boundary genes	128
4.1 Abstract	129
4.2 Introduction	130
4.3 Materials and methods	134
4.3.1 Plant material and growth conditions.....	134
4.3.2 Primers and genotyping	135
4.3.3 Construction of <i>4CL:BOPI-GR</i> , <i>D35S:BOPI-GR</i> , <i>35S:BOPI-GR</i> and <i>PRXR9:GUS</i> transgenic lines	136
4.3.4 Histological analysis of GUS localization	137
4.3.5 qRT-PCR	138
4.3.6 Accession numbers	139
4.4 Results	139
4.4.1 Inactivation of BOP1/2, KNAT6, or ATH1 rescues the <i>pnf pnf</i> phenotype.....	139
4.4.2 <i>BOP1/2</i> , <i>ATH1</i> , and <i>KNAT6</i> expression domains are expanded in <i>pnf pnf</i> meristems	140
4.4.3 <i>PRXR9</i> is co-expressed with other lateral organ boundary genes.....	141

4.4.4 BOP1/2 directly activates lateral organ boundary genes <i>ATH1</i> and <i>PRXR9</i>	142
4.4.5 BOP1/2 promote <i>TGA1</i> and <i>TGA4</i> expression	144
4.4.6 BOP1/2 exert their function through TGA1/4	144
4.5 Discussion	145
4.5.1 PNY and PNF in the meristem repress BOP1/2 to promote floral evocation	146
4.5.2 BOP1/2 are direct transcriptional regulators of lateral organ boundary genes <i>ATH1</i> and <i>PRXR9</i>	148
4.5.3 BOP1/2 activity is dependent on TGA1 and TGA4	149
CHAPTER 5 – Conclusions and future directions	165
5.1 General conclusions	166
5.2 Future directions	168
REFERENCES	171

LIST OF ABBREVIATIONS

35S CaMV	Cauliflower Mosaic Virus 35S promoter
4CL	4-COUMARATE:CoA LIGASE
AGL24	AGAMOUS-like24
AP1	APETELA1
ASI, 2	ASYMMETRIC LEAVES1 and 2
ATH1	ARABIDOPSIS THALIANA HOMEBOX GENE1
BELL	BEL1-LIKE
BLR	BELLRINGER
BOP1/2	BLADE-ON-PETIOLE1 and 2
BP	BREVIPEDICELLUS
BTB/POZ	Bric-a-Brac/POX virus and Zinc finger
C4H	cinnamate 4-hydroxylase
CAD	cinnamyl alcohol dehydrogenase
CCoAOMT	caffeoyl CoA O-methyltransferase
CCR	cinnamoyl CoA reductase
CHX	Cyclohexamide
CLV	CLAVATA
CO	CONSTANS
COCH	COCHLEATA
Col	Columbia
COMT	Caffeic acid O-methyltransferase
CUC1, 2, 3	CUP-SHAPED COTYLEDONS1, 2 and 3
Cys521 and 529	Cysteine 521 and 529
CZ	Central Zone
DEX	Dexamethasone
FLC	FLOWERING LOCUS C
FLM	FLOWERING LOCUS M
FRI	FRIGIDA
FT	FLOWERING LOCUS T
FUL	FRUITFUL
G	Guaiacyl
GR	GLUCOCORTICOID
H	p-hydroxyphenyl
HCT	BAHD family acyltransferase
IM	Inflorescence meristem
KNAT2	KNOTTED-like FROM ARABIDOPSIS THALIANA2
KNAT6	KNOTTED-like FROM ARABIDOPSIS THALIANA6
KNOX	KNOTTED1-like HOMEBOX
Ler	Landsberg erecta

<i>LFY</i>	<i>LEAFY</i>
<i>LOB</i>	<i>LATERAL ORGAN BOUNDARY</i>
<i>MAF2</i>	<i>MADS AFFECTING FLOWERING 2</i>
miR156	miRNA156
<i>NPRI</i>	<i>NONEXPRESSOR OF PATHOGENESIS RELATED GENES1</i>
<i>NOOT</i>	<i>NODULE ROOT</i>
<i>NtBOP2</i>	<i>Nicotiana tabacum BLADE-ON-PETIOLE2</i>
OC	Organizing center
<i>PAL</i>	<i>PHENYLALANINE AMMONIA LYASE</i>
<i>PME5</i>	<i>PECTIN METHYL-ESTERASE5</i>
<i>PNF</i>	<i>POUNDFOOLISH</i>
<i>PNY</i>	<i>PENNYWISE</i>
<i>Pp-miR534</i>	<i>Physcomitrella patens microRNA534</i>
<i>PR</i>	<i>PATHOGENESIS RELATED</i>
<i>PRXR9</i>	<i>ARABIDOPSIS THALIANA PEROXIDASE9GE</i>
<i>PtBL1/2</i>	<i>Populus trichocarpa BLADE-ON-PETIOLE1 and 2</i>
PZ	Peripheral zone
<i>REV</i>	<i>REVOLUTA</i>
RIM	Resistance-inducing ability of methyl jasmonate
RZ	Rib zone
S	Syringyl
SAM	Shoot apical meristem
SEM	Scanning electron microscopy
<i>SOCI</i>	<i>SUPPRESSOR OF OVEREXPRESSION OF CONSTANS1</i>
<i>SPL</i>	<i>SQUAMOSA PROMOTER BINDING PROTEIN-like</i>
<i>STM</i>	<i>SHOOTMERISTEMLESS</i>
<i>SVP</i>	<i>SHORT VEGETATIVE PHASE</i>
TALE	Three-amino-acid loop-extension
<i>TFL1</i>	<i>TERMINAL FLOWER1</i>
TGA	TGACG-motif binding
<i>VRN1, 2</i>	<i>VERNALIZATION1 and 2</i>
WT	Wild-type
<i>WUS</i>	<i>WUSHEL</i>

Genetic nomenclature in Arabidopsis

<i>BOP1</i>	Wild-type gene
<i>bop1</i>	Loss-of-function mutant
<i>bop1-6D</i>	Dominant gain-of-function mutation
BOP1	Wild-type protein

LIST OF TABLES

Table 2.1 Summary of inflorescence defects in plants overexpressing <i>BOP1</i> or <i>BOP2</i>	81
Table S2.1 List of general primers	99
Table S2.2 List of primers for qPCR analysis of lignin genes	100
Table S4.1 Summary of inflorescence defects in plants overexpressing <i>BOP1-GR</i>	162
Table S4.2 List of general primers	163

LIST OF FIGURES

Figure 1.1 Architecture of the model plant <i>Arabidopsis thaliana</i>	49
Figure 1.2 Organization of the SAM in <i>Arabidopsis thaliana</i>	50
Figure 1.3 Genetic interactions in the SAM of <i>Arabidopsis thaliana</i>	51
Figure 1.4 Genetic interactions regulating floral transition in <i>Arabidopsis thaliana</i>	52
Figure 1.5 Reorganization of <i>TALE</i> homeobox genes upon transition to inflorescence meristem.....	53
Figure 2.1 <i>BOP2:GUS</i> expression pattern in boundaries.	82
Figure 2.2 <i>BOP1</i> gain-of-function causes <i>bp</i> - and <i>pnf</i> -like defects in inflorescence architecture.	84
Figure 2.3 Phenotypic suppression of <i>bp</i> and <i>pnf</i> inflorescence defects by <i>bop1 bop2</i>	85
Figure 2.4 Quantitative analysis of <i>bp</i> phenotypic rescue of <i>bop1 bop2</i>	86
Figure 2.5 Quantitative analysis of <i>pnf</i> phenotypic rescue by <i>bop1 bop2</i>	88
Figure 2.6 <i>BOP2:GUS</i> expression in wildtype, <i>bp</i> , and <i>pnf</i> inflorescences.....	90
Figure 2.7 <i>KNAT6</i> expression in wild type, <i>bp-2</i> , <i>pnf</i> , and <i>BOP</i> gain-of-function mutants.....	93
Figure 2.8 Inactivation of <i>KNAT6</i> rescues compact internodes caused by <i>BOP2</i> gain-of-function.	95
Figure 2.9 Lignification pattern and lignin biosynthetic gene expression in wild-type and mutant stems.	97
Figure 2.10 Summary of genetic interactions between BP-PNY, BOP1/2, and KNAT6 in the inflorescence.....	98
Figure S2.1 Phenotypic suppression of <i>bp-2</i> inflorescence defects by <i>bop1 bop2</i>	101
Figure S2.2 Comparison of stem-pedicel junctions in wild type and mutants.	102
Figure S2.3 Loss-of-function <i>bop1 bop2</i> restores replum formation in <i>pnf</i> mutants.	104
Figure S2.4 <i>KNAT6:GUS</i> and <i>KNAT2:GUS</i> expression in WT plants.	105
Figure S2.5 <i>BOP1:GUS</i> expression pattern in WT, <i>bp-2</i> , and <i>pnf</i> inflorescences.....	106
Figure S2.6 Quantitative analysis of <i>BOP2</i> transcript in <i>35S:BOP2</i> lines crossed to wildtype and mutants	107
Figure S2.7 Inflorescence phenotype of <i>35S:KNAT6</i> transgenic plants and <i>bp as2-1</i> and <i>pnf as2-1</i>	108
Figure S2.8 Comparison of <i>BP</i> and <i>PNY</i> expression levels in wild-type, <i>bop1 bop2</i> and <i>bop1-6D</i>	110
Figure S2.9 Analysis of stem lignification pattern in WT and mutants of <i>pnf</i>	112
Figure 3.1 qRT-PCR of relative <i>ATH1</i> transcript levels in internodes	121
Figure 3.2 Phenotypic suppression of <i>pnf-40126</i> and <i>bp-2</i> inflorescence defects by <i>ath1-3</i> loss-of-function	123
Figure 3.3 Inactivation of <i>ATH1</i> rescues compact internodes in <i>BOP2</i> gain-of-function plants.....	124
Figure 3.4 Effect of <i>KNAT6</i> and <i>ATH1</i> inactivation on vascular patterning in <i>bp-2</i> stems	126
Figure 3.5 Summary of genetic interactions between BP-PNY, BOP1/2 and KNAT6-ATH1 in inflorescence.....	127
Figure 4.1 Phenotypic suppression of <i>pnf pnf</i> loss of flowering by <i>bop1 bop2</i> , <i>knat6</i> and <i>ath1-3</i>	152
Figure 4.2 <i>BOP2:GUS</i> and <i>ATH1:GUS</i> expression in the meristems of <i>pnf pnf</i> plants.....	154
Figure 4.3 <i>ATH1:GUS</i> expression in inflorescences apices of WT and <i>35S:BOP2</i> plants.....	155
Figure 4.4 <i>PRXR9:GUS</i> expression in boundaries	156
Figure 4.5 Transcript level comparisons of <i>ATH1</i> , <i>PRXR</i> , <i>KNAT6</i> , <i>TGA1</i> and <i>TGA4</i> in <i>D35S:BOP1-GR</i>	158
Figure 4.6 BOP1/2 require TGA1 and TGA4 to exert changes in inflorescence architecture.....	160
Figure 4.7 Summary of genetic interactions between PNY/PNF-STM, BOP1/2, ATH1 and KNAT6	161
Figure S4.1 Quantitative analysis of <i>35S:BOP2</i> rescue by <i>tga1</i> and <i>tga4</i>	164

CHAPTER 1

INTRODUCTION

THESIS OVERVIEW

Arabidopsis (*Arabidopsis thaliana*) serves as a simple model for the systematic study of factors that control plant architecture. All aerial organs of plants are derived from the shoot apical meristem (SAM) whose activity elaborates repeating modules called phytomers. A phytomer consists of three parts: a leaf with an axillary meristem, subtended by an internode. Elaboration of the different parts of a module varies widely between species and within species during different phases of development giving rise to architectural diversity. In many ways, the meristem can be regarded as a master regulator of plant architecture.

During vegetative development, the SAM generates leaves without internodes to form a compact rosette. Floral inductive signals acting on the SAM promote inflorescence meristem (IM) fate. The IM stops making leaves and initiates the production of axillary meristems that form flowers, separated by internodes. Nature produces a diversity of inflorescence architectures, designed to optimize reproductive success. Over the years, a handful of genes have been identified that regulate meristem transition to IM fate and that control the architecture of inflorescences, but how these genes interact and regulate each other to effect change in plant architecture is still relatively unknown.

In *Arabidopsis*, loss-of-function studies have identified two BTB-ankryin transcription factors encoded by *BLADE-ON-PETIOLE1* and 2 (*BOPI/2*) that control leaf, inflorescence, and flower development by controlling growth, differentiation, and meristem activity at lateral organ boundaries (Ha et al., 2003; Ha et al., 2004; Hepworth et al., 2005; Norberg et al., 2005; Ha et al., 2007; McKim et al., 2008; Jun et al., 2010;

Xu et al., 2010). Boundaries are specialized junctions that separate lateral organs from the meristem (Aida and Tasaka, 2006). Gain-of-function BOP1/2 results in shortened plants with clustered or downward-pointing flowers (Norberg et al., 2005; Ha et al., 2007). These phenotypes are reminiscent of double mutations in three-amino-acid-loop-extension (TALE) homeobox genes *PENNYWISE* (*PNY*; also called *BELLRINGER*, *REPLUMLESS*, and *VAMAANA*) from the *BEL1-like* (*BELL*) family and *BREVIPEDICELLUS* (*BP*; formerly *KNOTTED1-LIKE FROM ARABIDOPSIS THALIANA1 [KNAT1]*) from the *KNOTTED1-like HOMEBOX (KNOX)* family that maintain indeterminacy in the SAM (Smith and Hake, 2003). BP and PNY are also known to form heterodimers and play a role in internode patterning (Byrne et al., 2002; Smith and Hake, 2003). Another BELL gene, *POUNDFOOLISH (PNF)*, functions redundantly with *PNY* along with the KNOX partner SHOOTMERISTEMLESS (*STM*) to regulate the transition to flowering (Byrne et al., 2003; Smith et al., 2004; Gómez-Mena and Sablowski, 2008; Bhatt et al., 2004; Kanrar et al., 2006; Rutjens et al., 2009). The overall objectives of this thesis were to examine how BOP1/2 interactions with BP and PNY in stems and with PNY and PNF in the SAM regulate inflorescence architecture and flowering, and to identify downstream targets of BOP1/2 important for its activity in these processes.

1.1 Model plant *Arabidopsis thaliana*

Arabidopsis is a member of the *Brassicaceae* family which includes mustard, cabbage, horseradish. Since 1970's it has been used as a model organism to study plant molecular genetics, development, physiology and biochemistry due to its compact genome (125Mb) which has been completely sequenced with extensive genetic and physical maps of all 5

chromosomes available through The Arabidopsis Information Resource (TAIR; www.arabidopsis.org). Arabidopsis is a small (30-40 cm) plant with a 6-8 week life cycle and prolific seed production that is easily transformed using *Agrobacterium* (Meyerowitz, 1987). Gene knockout mutants are available through the Arabidopsis Biological Resource Center (ABRC) at little cost (www.arabidopsis.org). Knowledge gained from Arabidopsis has been successfully applied to improvement of economically viable crop species (Lavagi et al., 2012).

1.2 Life cycle and modular architecture of Arabidopsis

The life cycle of Arabidopsis consists of three main stages: the embryonic, vegetative and reproductive stages. Arabidopsis has both male and female gametes which are self-fertilizing. Embryogenesis begins with a single fertilized zygote that elongates giving rise to globular, triangular, heart, and torpedo stages. By late torpedo stage, cellular differentiation establishes all the tissues required for vegetative development. Under favorable environmental conditions, germination, the transition to vegetative development occurs. The Arabidopsis embryo resumes growth and the SAM produces a compact rosette of leaves without internode elongation (Fig. 1.1). Upon perception of appropriate environmental and endogenous cues, the SAM converts to a reproductive IM (Amasino and Michaels, 2010; Irish, 2010). The IM produces lateral branches, and subsequently flowers, which are separated by internodes (Fig. 1.1).

The body plan of Arabidopsis is based on meristem production of repeating modules called phytomers. Three types of phytomers arranged in a spiral phyllotactic pattern are produced during Arabidopsis development (Schultz and Haughn, 1991). Type 1

phytomers are comprised of an extremely short internode and a rosette leaf with the potential to form an axillary meristem (P1 in Fig. 1.1). Type 2 phytomers formed in the basal portion of the primary shoot consist of long internodes, cauline leaves, and axillary branches (P2 in Fig. 1.1). Type 3 phytomers constitute the terminal portion of the main inflorescence, consisting of intermediate-length internodes, no leaf, and a lateral flower (P3 in Fig. 1.1; Schultz and Haughn, 1991; Talbert et al., 1995). Flowers are viewed as specialized shoots with homology to axillary branches, that have floral organs in place of leaves (Talbert et al., 1995). The different types of phytomers present in *Arabidopsis* suggest that mechanisms exist to specify each type of module at the appropriate stage of development. For example, late-flowering mutants of *Arabidopsis* are delayed in their production of an inflorescence (type 2 and 3 phytomers) and produce type 1 rosette phytomers for an extended period. Thus, the transition from one type of phytomer to another is under tight genetic control (Schultz and Haughn, 1991).

1.3 Vegetative development

1.3.1 Organization of the SAM

The SAM is required to generate all aerial organs in a plant including leaves, stems, branches, and flowers. The SAM is organized into three parts. The central zone (CZ) lies at the shoot apex and contains a reservoir of enlarged, highly vacuolated stem cells that divide relatively infrequently (Fig. 1.2). The CZ is surrounded by the peripheral zone (PZ) comprised of small, dense cells that divide more frequently (Fig. 1.2). Beneath the CZ are columns of large vacuolated cells that comprise the rib zone (RZ) (Fig. 1.2).

These cells contribute to the meristem pith and produce the stem (Fletcher and Meyerowitz, 2000; Bäurle and Laux, 2003; Barton, 2010; Murray et al., 2012).

As stem cells in the CZ divide, they are pushed outwards into the PZ from where they are incorporated into leaves and side shoots. The PZ represents a transitional region of the SAM where the progeny of stem cells have the potential to acquire a more specified fate. Meanwhile, cell division in the RZ results in upwards growth of the shoots as differentiated cells give rise to the central tissues of the stem below (Fletcher and Meyerowitz, 2000; Bäurle and Laux, 2003; Barton, 2010; Murray et al., 2012).

The Arabidopsis SAM is further divided into a tunica-carpus structure consisting of two overlying layers: L1, the epidermal layer, and L2, the subepidermal layer (Fig. 1.2; Fletcher and Meyerowitz, 2000; Bäurle and Laux, 2003; Barton, 2010). These layers are a single cell thick and remain distinct because the cells generally divide in an anticlinal orientation (perpendicular to the meristem). Cells in the underlying L3 layer, divide anticlinally and periclinally generating the stem vasculature and pith as well as the innermost cells of leaves and floral organs (Fig. 1.2; Fletcher and Meyerowitz, 2000; Bäurle and Laux, 2003; Barton, 2010; Murray et al., 2012).

1.3.2 Establishment of the SAM

The SAM is established during embryogenesis. The earliest meristem maintenance gene to be activated is *WUSHEL* (*WUS*), which encodes a homeodomain transcription factor. *WUS* is first expressed in the apical subepidermal cells at the 16-cell stage of embryogenesis (Mayer et al., 1998). *CUP-SHAPED COTYLEDONS* (*CUC1*, 2, and 3) genes are activated soon after in an overlapping region in the late globular embryo

followed by *SHOOTMERISTEMLESS (STM)* at heart stage (Long and Barton, 1998; Aida et al., 1999). *STM* and *WUS* work synergistically in meristem development and are jointly required for the establishment and maintenance of SAM (reviewed in Sablowski, 2007). *CUC* and *STM* regulate each other to form the SAM and to separate cotyledons (Aida et al., 1999; Takada et al., 2001; Furutani et al., 2004). Studies have shown that apical region of the globular embryo is progressively subdivided during embryogenesis by these genes into a central region which produces the SAM, a peripheral region that produces cotyledons, and a boundary region where growth is suppressed to allow separation between the cotyledons and the meristem (reviewed in Bowman and Eshed, 2000; Capron et al., 2009).

1.3.3 Maintenance of the SAM

Several interacting pathways maintain the size of the SAM. Failure in this regulation results in an accumulation of stem cells in the SAM and meristem enlargement. Loss of cells from the SAM results in meristem consumption, with all of the cells incorporated into lateral organ primordia.

1.3.3.1 A CLAVATA-WUSHEL feedback loop maintains the SAM

In Arabidopsis, three *CLAVATA* genes (*CLV1*, 2, and 3) regulate the size of the stem cell reservoir in the SAM. Mutation of these genes results in an enlarged SAM (Clark et al., 1993; Clark et al., 1996; Kayes and Clark, 1998). *CLV3* encodes a small signaling peptide expressed in the L1 and L2 layers of the CZ whereas *CLV1* and 2 encode membrane-bound receptors expressed in the L3 layer. *CLV3* binds to *CLV1* and potentially *CLV2* triggering signaling that inhibits cell division in the CZ (Ogawa et al., 2008). Reddy and

Meyerowitz (2005) showed that *CLV3* positions the boundary between the central and peripheral zones in the SAM.

The WUS homeodomain transcription factor is normally expressed in the L3 layer just under the CZ in a region called the Organizing Center (OC) (Mayer et al., 1998). Mutations in the *CLV* genes expand the domain of *WUS* expression causing enlargement of the CZ (Brand, 2000; Schoof et al., 2000). Conversely, *wus* mutants lack the CZ, similar to plants that overexpress *CLV3* (Brand, 2000; Schoof et al., 2000). This shows that CLV signaling negatively regulates the stem cell population by restricting *WUS* expression. Compatible with this, *WUS* overexpression causes misexpression of *CLV3* and enlargement of the meristem (Fig. 1.3; Schoof et al., 2000). The WUS protein is mobile and moves from the L3 layer into the CZ where it directly activates *CLV3* transcription by binding to its promoter (Yadav et al., 2011). These findings show that WUS-CLV3 interactions establish a negative feed-back loop between stem cells in CZ and the OC to maintain meristem size (Schoof et al., 2000; Fletcher, 2002; Bäurle and Laux, 2003; Barton, 2010; Yadav et al., 2011).

1.3.3.2 TALE homeodomain proteins maintain the SAM

TALE homeodomain proteins in Arabidopsis comprise a superfamily that is divided into KNOX and BELL subfamilies (reviewed in Hamant and Pautot, 2010). Class I *KNOTTED1-like HOMEBOX (KNOX)* genes *SHOOTMERISTEMLESS (STM)*, *BREVIPEDICELLUS (BP)*, and *KNOTTED1-like FROM ARABIDOPSIS THALIANA2* and *6 (KNAT2 and 6)* play important role in SAM maintenance. *STM* is expressed throughout the SAM but is down-regulated in incipient organ primordia. Loss-of-function

stm mutants display fused organs lacking the SAM (Barton and Poethig, 1993; Endrizzi et al., 1996; Long et al., 1996). *BP* is expressed in the PZ and RZ and also down-regulated in incipient organ primordia to allow determinacy (Lincoln et al., 1994). *KNAT2* and *KNAT6* are expressed at the boundaries between the SAM and emerging organ primordia (Belles-Boix et al., 2006) with *KNAT2* additionally expressed in the RZ (Pautot et al., 2001; Belles-Boix et al., 2006). Loss-of-function *bp* and *knat6* mutants do not display SAM defects but enhance the phenotype of weak *stm* mutants in SAM maintenance and organ separation (Fig. 1.2; Byrne et al., 2002; Belles-Boix et al., 2006). Overexpression of *KNOX* genes results in the ectopic development of meristems on the adaxial surface and margins of leaves showing that all are sufficient to promote meristem formation (Lincoln et al., 1994; Chuck et al., 1996; Pautot et al., 2001; Gallois et al., 2002; Dean et al., 2004).

KNOX proteins function as heterodimers with BEL1-like (BELL) homeodomain proteins encoded by *PENNYWISE* (*PNY*), *POUNDFOOLISH* (*PNF*), and *ARABIDOPSIS THALIANA HOMEODOMAIN BOX1* (*ATH1*). Dimerization occurs through binding between the MEINOX and SKY domains in KNOX and BELL proteins respectively (Bellaoui et al., 2001; Byrne, 2003; Smith and Hake, 2003; Bhatt et al., 2004; Cole et al., 2006; Kanrar et al., 2006; Rutjens et al., 2009; Li et al., 2012). Heterodimerization has been shown to be important for nuclear localization of KNOX factors including STM (Cole et al., 2006). *PNY* expression can be observed in the CZ; *PNF* is expressed in the CZ and PZ of the SAM, whereas *ATH1* is expressed throughout the SAM, leaf primordia and base of developing leaves (Fig. 1.2; Smith et al., 2004; Proveniers et al., 2007; Gómez-Mena and Sablowski, 2008). *PNY* and *PNF* regulate the integrity of the CZ since the expression

domain of *STM* is narrower in *pny pnf* double mutants (Ung and Smith, 2011). Triple mutants of *ath1 pny pnf* produce a phenotype similar to weak *stm* mutants (Rutjens et al., 2009). This might be due to the depletion of nuclear localized BELL-STM complexes in the SAM (Rutjens et al., 2009).

Clark et al. (1996) found evidence of genetic interactions between *STM* and *CLV*. *clv* mutations partially suppress *stm* phenotypes and vice versa suggesting they are both sensitive to the levels of each other's activity and work in parallel pathways to maintain boundary between the CZ and PZ in the SAM (Clark et al., 1996; Kayes and Clark, 1998; reviewed in Fletcher, 2002). In addition, *CLV3* and *WUS* expression are expanded in the SAM of *pny pnf* mutants and *clv* mutation or *WUS* overexpression rescues lack of flowering in *pny pnf* mutants. *STM* expression shows that leaf initial cells impinge on the CZ in the absence of PNY and PNF suggesting that PNY/PNF-STM complexes establish the boundary between the CZ and PZ in the SAM (Fig. 1.2; Smith et al., 2004; Ung et al., 2011).

1.3.4 Phyllotaxis

The SAM generates organ primordia on its flanks in a regular arrangement known as phyllotaxis. This pattern contributes to the architecture of plants during vegetative and reproductive growth. Arabidopsis plants have spiral phyllotaxy with successive organs separated by an angle of $\sim 137.5^\circ$, also known as the “golden angle” (Murray et al., 2012). Auxin, a plant hormone, is required for proper positioning of organs. Experimental results suggest an autoregulatory loop between auxin, polar localization of PIN-FORMED1 auxin transporter proteins, and polar transport of auxin, creates auxin

maxima which can activate downstream processes to produce organ primordia. New primordia maintain a distance by depleting auxin in their proximity (Smith et al., 2006; reviewed in Capron et al., 2009; Murray et al., 2012; Gallavotti, 2013; Sassi and Vernoux, 2013).

1.3.5 Establishment and maintenance of boundaries

Lateral organ primordia on the flanks of the SAM are separated from surrounding tissues by boundaries comprised of cells with a reduced rate of division. Boundaries including meristem-organ and organ-organ boundaries maintain separation between organs and the meristem (reviewed in Aida and Tasaka, 2006). Several gene classes are known to play a role in boundary establishment and/or maintenance including *CUC*, *KNAT6*, and *BOP* genes (reviewed in Aida and Tasaka, 2006; Rast and Simon, 2008).

Lateral organ boundary identity is provided by NAC-domain transcription factors (reviewed in Aida and Tasaka, 2006). *CUC1* and *CUC2* genes are activated at the early- to mid-globular stages of embryogenesis in the presumptive SAM and become restricted to the boundaries between the SAM and cotyledons (Aida et al., 1999). *CUC* genes play an important role in establishing and maintaining the SAM since mutations in these genes impairs formation of the embryonic meristem and cause organ fusion (Aida et al., 1999; Takada et al., 2001; Hibara et al., 2003; Vroemen et al., 2003). *CUC1* promotes expression of *STM* to form the SAM. In turn, *STM* in conjunction with auxin-based signaling in the leaf restrict *CUC* expression to the boundary, which promotes cotyledon separation (Fig. 1.3; Aida et al., 1999; reviewed in Vernoux et al., 2010),

KNAT6 expression can be seen as early as in the triangular stage in the presumptive SAM but is later restricted to the boundaries between the SAM and cotyledons (Belles-Boix et al., 2006). Loss-of-function *knat6* mutants enhance *stm-2* defects resulting in organ fusion and loss of *CUC3* expression from the boundaries in the SAM. *CUC1/2* are redundantly required for *KNAT6* expression. This suggests a role for KNAT6 in promoting boundary maintenance via the *STM/CUC* pathway (Fig. 1.3; Belles-Boix et al., 2006).

BOP1/2 expression at lateral organ boundaries promotes the expression of LATERAL ORGAN BOUNDARY (LOB) domain-containing transcription factors, including *ASYMMETRIC LEAVES2 (AS2)*. *BOP1/2* maintains repression of *KNOX* genes in developing leaves through direct activation of *AS2*, whose product directly represses *BP* and *KNAT2* (Fig. 1.3; Ha et al., 2003; Ha et al., 2007; Jun et al., 2010; Guo et al., 2008). *AS2* forms a complex with *AS1* that promotes stable repression of *KNOX* genes via recruitment of Polycomb-repressive Complex2 proteins (Guo et al., 2008; Lodha et al., 2013). *STM* in the SAM represses *BOP1/2*. Inactivation of *BOP1/2* rescues *stm* defects through formation of functional meristems at the base of fused cotyledons (Jun et al., 2010). These data reveal that mutually antagonistic interactions between meristematic *KNOX* genes and lateral organ boundary genes are important for the maintenance of transcriptionally distinct compartments in the vegetative shoot apex (summarized in Fig. 1.3).

1.4 Reproductive development

1.4.1 Reproductive plant architecture

In response to internal and environmental cues, *Arabidopsis* transitions from vegetative to reproductive development. The meristem switches from the production of type 1 phytomers (rosette leaves) to the production of type 2 phytomers (long internodes and axillary branches subtended by a cauline leaf) and type 3 phytomers (intermediate-length internodes, an axillary flowers without subtending bract) (Fig 1.1; Talbert et al., 1995). The architecture of the inflorescence depends on the internode length, phyllotaxy, branching pattern, and orientation of flowers.

1.4.2 The floral transition

The transition to flowering is tightly regulated to maximize reproductive success. Flowering time is controlled by a variety of internal and external cues. The major external inputs for regulation include the vernalization pathway, which promotes flowering after long exposure to cold, the long-day photoperiod pathway, which promotes flowering in response to long hours of daylight, and the autonomous pathway, which promotes flowering in response to hormone and age-related signals (reviewed in Amasino and Michaels, 2010; Srikanth and Schmid, 2011). Regulation of the photoperiod pathway is primarily controlled by the transcription factor *CONSTANS* (*CO*) whereas regulation of the vernalization and autonomous pathways is controlled by the floral repressor *FLOWERING LOCUS C* (*FLC*) (reviewed in Amasino and Michaels, 2010). Inputs from these flowering-time pathways converge to regulate a small number of genes with floral integrator activity including *LEAFY* (*LFY*), *FLOWERING LOCUS T* (*FT*), and *SUPPRESSOR OF OVEREXPRESSION OF CONSTANS1* (*SOC1*), whose upregulation

in shoot apices promotes flowering. An important role of floral integrators is the activation of floral-meristem identity (FMI) genes, *LFY* and *APETELA1* (*API*). Expression of *LFY* and *API* in lateral organ primordia confers floral fate (reviewed in Amasino and Michaels, 2010).

1.4.3 Competence to flower

1.4.3.1 Photoperiod based regulation of flowering

The long-day pathway is regulated by the floral promoter *CONSTANS* (*CO*) whose transcription is regulated by the circadian clock. CO proteins are stabilized by light and degrade in darkness and thus accumulate only during long days to promote flowering. Loss-of-function *co* mutants are late-flowering in long days whereas *CO* overexpression leads to early flowering in all photoperiods (Koornneef et al., 1991; Onouchi et al., 2000). *CO* is expressed in the vasculature of leaves where it directly activates *FT*, whose protein travels from the vasculature of leaves to the SAM (Corbesier et al., 2007; Tamaki et al., 2007). In the SAM, FT forms a complex with bZIP protein FD and initiates flowering by promoting other floral integrators such as *SOC1* and FMI genes such as *API* (Michaels, 2009; Amasino and Michaels, 2010). *CO* additionally promotes *SOC1* and *LFY* expression (Simon et al., 1997; Samach, 2000). These data show that CO in the long-day photoperiod pathway promotes flowering by activating floral integrators (Fig. 1.4).

1.4.3.2 *FLC*

FLC encodes a MADS box transcriptional repressor that maintains the meristem in a vegetative state. *FLC* is expressed in shoot apices and leaf vasculature and is a target of both the vernalization and autonomous pathways (Bastow et al., 2004; Sung and Amasino, 2004). Constitutive *FLC* expression delays or blocks flowering in a dosage-dependent manner (Michaels and Amasino, 1999; Sheldon et al., 2000; Werner et al., 2005).

SHORT VEGETATIVE PHASE (SVP) is another MADS box protein that represses flowering in conjunction with *FLC* by binding to the *FT* and *SOC1* promoters (Hartmann et al., 2000; Lee et al., 2007). SVP and *FLC* form a complex (Li et al., 2008; reviewed in Srikanth and Schmid, 2011). *FLC* directly inhibits the expression of floral integrators *FD*, *FT*, and *SOC1* by binding to their regulatory regions (Hepworth et al., 2002; Searle et al., 2006; Michaels, 2009; Amasino and Michaels, 2010; Jarillo and Piñeiro, 2011). Thus, down-regulation of *FLC* is necessary for promotion of floral integrator expression and flowering (Fig. 1.3).

1.4.3.3 Vernalization based regulation of flowering

Vernalization is the exposure to prolonged winter cold rendering the plant competent to flower (Kim et al., 2009). In winter-annual accessions of *Arabidopsis*, *FLC* mRNA and protein levels are down-regulated by vernalization thereby permitting flowering. In summer-annual accessions of *Arabidopsis* like Col-0 or L.er., natural variation has selected for *flc* mutations or mutations in regulatory genes that down-regulate *FLC* expression, thus allowing plants to flower in the absence of vernalization (Johanson et al.,

2000; Gazzani et al., 2003; Michaels et al., 2003). *VERNALIZATION1* and 2 (*VRN1* and 2) genes encode nuclear-localized zinc-finger proteins that function in a chromatin-modifying complex to retain *FLC* in an inactive chromatin state (Bastow et al., 2004). They are part of the cellular machinery that provides a memory for vernalization and maintains repression of *FLC* even after exposure to warm temperatures (Gendall et al., 2001; reviewed in Putterill et al., 2004). Thus, vernalization represses *FLC* to promote flowering (Fig. 1.3).

1.4.3.4 Autonomous pathway based regulation of flowering

The autonomous pathway comprises a combination of RNA processing and epigenetic factors that are required to down regulate *FLC*. Since *FLC* antagonizes the activity of pathways that promote flowering, the autonomous pathway promotes flowering indirectly by lowering *FLC* levels (Koornneef et al., 1991; Sheldon et al., 2000; Michaels and Amasino, 2001). In winter-annuals where there is a requirement for vernalization, the activity of *FRIGIDA (FRI)* overcomes autonomous-pathway mediated repression of *FLC* until a period of cold has occurred (Michaels and Amasino, 1999; Sheldon et al., 2000; He and Amasino, 2005). Therefore, the vernalization and autonomous pathways both down regulate *FLC* to promote flowering (Fig. 1.4).

1.4.4 Floral integrators

The long-day, vernalization, and autonomous pathways converge to upregulate floral integrators such as *LFY*, *FT*, and *SOC1* to promote flowering. *FT* is expressed in phloem companion cells and its expression is increased in long days and according to a circadian pattern (Harmer, 2000; Suárez-López et al., 2001; Takada and Goto, 2003). *CO* from the

long-day pathway is a direct positive regulator of *FT* (Kobayashi et al., 1999; Samach et al., 2000; Yamaguchi et al., 2005). *FT* interacts with the meristem-specific bZIP transcription factor *FD* and might play a role in conveying the information to initiate flowering from the leaves to the apex (Abe et al., 2005; Wigge et al., 2005; Srikanth and Schmid, 2011). An *FT-FD* complex activates *SOC1* which in turn acts with the inflorescence meristem identity gene *AGAMOUS-LIKE24 (AGL24)*, whose product is a positive regulator of *LFY* (Lee et al., 2008a; Liu et al., 2008). SQUAMOSA PROMOTER BINDING PROTEIN-LIKE (SPL) transcription factors which are post-transcriptionally regulated by microRNA156 (miR156) also positively regulate *SOC1* and work in parallel with *FT* to specify flowers during reproductive development (Wang et al., 2009; Yamaguchi et al., 2009; Amasino and Michaels, 2010).

In the vernalization and autonomous pathways, *FLC* directly represses *SOC1* and *FT* by binding to recognition sites in their respective promoters (Hepworth et al., 2002; Helliwell et al., 2006). *FLC* is expressed in the hypocotyl and cotyledons of young seedlings where *FT* is transcribed. *SOC1* is a likely target of *FLC* in the shoot meristem (Wang et al., 2009). Thus, *LFY*, *SOC1*, and *FT* emerge as key nodes of convergent regulation for endogenous and exogenous pathways that control flowering (Fig. 1.4).

1.4.5 Floral-meristem identity

Inputs from multiple flowering-time pathways converge to regulate *LFY* and *API* whose expression in lateral organ primordia confers floral fate. Mutations in both genes results in the formation of “flowers” with inflorescence-like characteristics (references from Xu et al., 2010). *FT*, *SOC1*, and SPLs directly promote *LFY* expression (Schmid et al., 2003;

Yamaguchi et al., 2005; Lee et al., 2008a). In turn, LFY directly promotes *API* expression by binding to its promoter (Parcy et al., 1998; Wagner et al., 1999; William et al., 2004). FT-FD induces *API* synergistically with LFY (reviewed in Srikanth and Schmid, 2011). *API* maintains *LFY* expression by creating a positive feed-back loop (Bowman et al., 1993; Schultz and Haughn, 1993; Liljegren et al., 1999).

A group of MADS-box transcription factors including *AGL24*, *SVP*, and *SOC1* maintain indeterminacy in the IM. These genes are initially expressed in the floral meristem but are down-regulated to ensure that the floral meristem becomes determinate (reviewed in Liu et al. 2009). *API* directly represses genes conferring inflorescence meristem identity including *AGL24*, *SVP*, and *SOC1* to promote determinacy of the floral shoot. Mutation in *apl* leads to partial conversion of flowers to inflorescences (Liu et al., 2008). *TERMINAL FLOWER1 (TFL1)* which encodes a FT homolog represses *LFY* and *API* in the IM so that it remains indeterminate and capable of producing floral meristems. *TFL1* may influence LFY's ability to induce *API* since when *TFL1* is constitutively expressed, *LFY* and *FT*-dependent activation of *API* does not occur (Ratcliffe et al., 1998).

1.4.6 Meristem regulators

PNY, *PNF*, and *ATH1* belong to the BELL subfamily of TALE transcription factors and are required for SAM competence to respond to floral inductive signals and for specification of floral meristems (Smith et al., 2004; Kanrar et al., 2008; Rutjens et al., 2009). At the transition to flowering, *PNY* and *PNF* remain in the IM but expression of *ATH1* is down-regulated (Fig. 1.4; Smith et al., 2004; Kanrar et al., 2006; Gómez-Mena and Sablowski, 2008). In *pny pnf* mutants, the SAM does not fully attain IM identity and

is trapped in a vegetative state where it continues to produce leaves (Smith et al., 2004). Transcripts of floral integrators *SOC1* and *FT* accumulate in *pnf pnf* but are non-functional in the absence of PNY/PNF activity. Transcripts of floral-meristem identity genes *LFY* and *API* fail to accumulate in *pnf pnf* shoot apices (Smith et al., 2004; Kanrar et al., 2008). It is suggested that STM heterodimerization with PNY/PNF is required for FT-dependent specification of flower meristem identity (Kanrar et al., 2008; Rutjens et al. 2009; Smith et al., 2011). PNY and PNF also appear to regulate floral-meristem specification by direct upregulation of *SPLs* and by repression of miR156 (Lal et al., 2011). While *pnf pnf* mutants display morphological and molecular changes consistent with receiving floral inductive signals, the transition to IM fate is incomplete (Smith et al., 2004). Inactivation of *ATH1* rescues flowering defects in *pnf pnf* mutants suggesting that down-regulation of *ATH1* is crucial for meristem competence to flower (Rutjens et al., 2009; Tabb, 2011). There is some evidence to suggest that *ATH1* prevents floral competency by upregulation of *FLC* (Proveniers et al. 2007). Thus, *ATH1*-dependent up-regulation of *FLC* in *pnf pnf* mutants might antagonize competence to flower (Fig. 1.4). It is interesting that *ATH1* and PNY/PNF function redundantly in the SAM but antagonistically in SAM competence to flower.

1.4.7 Inflorescence architecture

In Arabidopsis, the transition to flowering is synchronized with the elongation of internodes to form an inflorescence. Loss-of-function studies have identified a number of genes whose interactions regulate phyllotaxy, internode elongation, and pedicel orientation in Arabidopsis.

1.4.7.1 BP and PNY promote internode elongation

BP, a class I KNOX protein, forms heterodimers with the BELL protein PNY. At the transition to flowering, *BP* is down regulated in the meristem and becomes expressed in the stem cortex. *PNY* expression is retained in the meristem but also expands to the stem cortex (Fig. 1.5; Lincoln et al., 1994; Byrne, 2003; Smith and Hake, 2003). BP and PNY heterodimers are predicted to regulate a common set of genes that govern inflorescence architecture (Smith and Hake, 2003). Microarrays suggest that their activities regulate genes involved in cell wall metabolism (Mele et al., 2003; Etchells et al., 2012). Loss-of-function *bp* mutants display shortened internodes with downward-pointing flowers (Douglas et al., 2002; Venglat et al., 2002; Ragni et al., 2008). Loss-of-function *pny* mutants display shortened internodes with irregular phyllotaxy (Byrne, 2003; Smith and Hake, 2003; Ragni et al., 2008). These mutants combined show a synergistic phenotype with severely shortened internodes and irregular phyllotaxy and pedicel orientation (Smith and Hake, 2003; Ragni et al., 2008). This suggests that BP and PNY play similar but also independent roles during inflorescence development.

The altered phyllotaxy defects in *pny* mutants have been linked to loss of repression of *PECTIN METHYL-ESTERASE 5 (PME5)*, a cell wall modifying enzyme whose activity is required to promote phyllotaxy and internode elongation. *pme5* mutants display clustered siliques similar to *pny* mutants (Peaucelle et al., 2011). Microarray data with *PNY* overexpression lines shows *PNY* is required for transcriptional repression of *PME5* (Etchells et al., 2012). Further research is required to discover which genes are directly controlled by BP and PNY to promote internode elongation.

1.4.7.2 Lateral-organ boundary genes restrict internode elongation

Recent work has revealed potential transcription factor targets of BP-PNY in regulating inflorescence architecture (Ragni et al., 2008; Rutjens et al., 2009; Li et al., 2012). *KNOX* genes *KNAT2* and *KNAT6* are expressed in the axils of pedicels in the inflorescence, a lateral organ boundary (Ragni et al., 2008). Both *knat2* and *knat6* loss-of-function mutants display wild-type inflorescence architecture (Belles-Boix et al., 2006; Ragni et al., 2008). BP and PNY in the stem confine *KNAT2* and *KNAT6* expression to the pedicel axils since *KNAT2* and *KNAT6* are misexpressed in *bp* and *pny* stems (Ragni et al., 2008). In addition, *bp* and *pny* mutant phenotypes are rescued by inactivation of *KNAT2* and *KNAT6* (Ragni et al., 2008). This suggests that BP-PNY and *KNAT2/6* functions in the inflorescence are antagonistic. The *BELL* gene *ATH1* is also expressed in the inflorescence and at the base of cauline leaves (Gómez-Mena and Sablowski, 2008). During the course of our work, it was reported that an *ath1-1* mutation partially rescues *bp* and *pny* mutant phenotypes and that overexpression of *ATH1* inhibits internode elongation (Gómez-Mena and Sablowski, 2008; Rutjens et al., 2009; Li et al., 2012). Plants overexpressing *BOP1/2* display shortened internodes similar to *35S:ATH1* and *bp pny* mutants (Norberg et al., 2005; Jun et al., 2010). These were some of the factors that led us to test if BP-PNY regulate *BOP1/2* or vice versa and to examine the relationship between *BOP1/2* and *ATH1-KNAT2/6* in inflorescence patterning.

1.4.8 Vascular patterning and secondary cell wall biosynthesis

In stems of wild-type *Arabidopsis* plants, cells are organized in a radial pattern starting with epidermis on the outside, followed by the cortex, then equally spaced vascular

bundles separated by interfascicular cells and finally, pith cells in the center of the stem. The vascular bundles contain phloem on the outside and xylem on the inside separated by meristematic cambium cells. Lignin is mainly deposited in the walls of xylem cells and interfascicular fiber cells in wild-type stems.

Lignin is an aromatic polymer required by plants for water transport, mechanical support, and for defense against pathogens. Lignin consists of *p*-hydroxyphenyl (H), guaiacyl (G) and syringyl (S) monolignols that are synthesized through the phenylpropanoid pathway, a common pathway for other secondary metabolites such as flavonoids and coumarins (see Figure 2 from Bonawitz and Chapple, 2010; Figure 1 from Zhao and Dixon, 2011).

PHENYLALANINE AMMONIA LYASE (PAL) catalyzes the first step in production of monolignols, which is the deamination of phenylalanine to cinnamate. A P450-dependent monooxygenase, CINNAMATE 4-HYDROXYLASE (C4H), then catalyzes the next step to *p*-coumarate. 4-COUMARATE:Coenzyme A LIGASE (4CL) is an ATP-dependent CoA ligase that catalyzes the synthesis of *p*-coumaroyl CoA. *p*-coumaroyl CoA can then be used as an acyl donor by the BAHD (named based on the first four characterized enzymes of the family: BEAT, AHCT, HCBT, and DAT) family acyltransferase, hydroxycinnamoyltransferase (HCT), to synthesize *p*-coumaroyl shikimate for production of other monolignols or diverted to produce *p*-coumaraldehyde through reduction by cinnamoyl CoA reductase (CCR) and subsequently *p*-coumaryl alcohol (H-lignin) through catalysis by cinnamyl alcohol dehydrogenase (CAD). The alternative *p*-coumaroyl shikimate pathway leads to production of caffeoyl shikimate, caffeoyl CoA, ferulyoyl CoA and then coniferaldehyde through catalysis by HCT, CAFFEOYL CoA *O*-methyltransferase (CCoAOMT), and CCR respectively.

Coniferaldehyde can then either lead to the production of coniferyl alcohol (G-lignin) through dehydrogenation by CAD, or follow an alternative route to produce 5-hydroxyconiferaldehyde by F5H, then sinapaldehyde by CAFFEIC ACID *O*-methyltransferase (COMT) and finally sinapyl alcohol (S-lignin), again through catalyzing dehydrogenation by CAD (see Figure 2 from Bonawitz and Chapple, 2010; Figure 1 from Zhao and Dixon, 2011). The production of a lignin polymer from these H, G, and S lignin monomers may require the activity of cell wall peroxidases such as *AtPRXR9GE* (*PRXR9*) that use hydrogen peroxidase to generate monolignol phenoxy radicals allowing the spontaneous coupling of monolignols into polymers (Boerjan et al., 2003; Mele et al., 2003; Passardi et al., 2004).

BP, which functions to maintain cells in an indeterminate state, has been shown to play an important role in preventing premature lignification, a hallmark of irreversible cell differentiation (Mele et al., 2003; Zhao and Dixon, 2011). Loss-of-function *bp* mutants display ectopic lignification in the epidermal tissue and gaps in the vascular ring in addition to reduced size of the xylem elements (Douglas et al., 2002; Venglat et al., 2002; Mele et al., 2003; Smith and Hake, 2003). Overexpression of *BP* reduces and delays lignification with lignin deposition occurring only in the bundles and not in interfascicular cells as compared to wild-type stems (Mele et al., 2003). Transcripts of several genes including *4CL*, *C4H*, *PAL1* and *PRXR9* were increased in *bp* mutants with ectopic lignification and BP was shown to directly bind to the promoters of *COMT* and *CCoAOMT*, which are both involved in the production of G and S monolignols (Mele et al., 2003).

PNY also plays a role in secondary cell wall biosynthesis and patterning of stem vasculature. Loss-of-function *pny* mutants have a thick continuous vascular ring with reduced interfascicular space and additional vascular bundles. The vascular bundles in *pny* mutants are often missing in large xylem vessels and contain only xylary fibers. They also have more cambial cells and a larger more densely-packed cortex in comparison to wild-type (Smith and Hake, 2003). Combined mutations of *bp pny* display enhancement of the single mutant phenotypes. Vascular bundles in the double mutants are smaller and closely packed with phloem cells forming a continuous band inside the large cortex cells and with unligified xylem elements scattered around (Smith and Hake, 2003). Expression studies have shown that both BP and PNY regulate the expression of genes encoding cell-wall associated proteins (Mele et al., 2003; Etchells et al., 2012). *PNY* and *BP* are thought to regulate secondary cell wall differentiation with *REVOLUTA (REV)*, a gene associated with radial patterning and development of interfascicular fibres, xylem differentiation, and maintenance (Emery et al., 2003). Combined mutations of *bp pny rev* demonstrate a reduction in vascular tissues in contrast to an increase in *bp pny* alone suggesting in contrast to *BP* and *PNY*, *REV* functions to promote secondary growth. However, xylem cells are reduced in *bp pny rev* similar to those in *bp pny* alone suggesting *PNY*, *BP*, and *REV* function together in this process (Etchell et al., 2012). More research is required to show how *PNY* and *BP* regulate secondary cell wall biosynthesis.

1.5 BOP1/2 regulation of plant development and defense

BOP genes encode a conserved subclade of plant-specific transcriptional co-activators whose founding member is the defense regulator NONEXPRESSOR OF

PATHOGENESIS-RELATED GENES1 (NPR1) (Hepworth et al. 2005; Khan and Hepworth, 2013). Two protein interacting domain are conserved in all family members including an N-terminal BTB/POZ (Bric-a-Brac/POX virus and Zinc finger) domain that mediates dimerization and is required for transcriptional activation (Rochon et al., 2006). A second domain at the C-terminus consisting of two ankyrin repeats that interact with TGA (TGACG-motif binding) bZIP transcription factors is also conserved.

The Arabidopsis genome encodes six BTB-ankryin proteins. NPR1 was identified, based on loss-of-function mutants that were defective in SA-triggered plant immunity (Cae et al. 1994; Cao et al. 1997). Closely related family members, NPR2, NPR3, and NPR4 have related roles in plant defense (Zhang et al. 2006; Liu et al. 2004; Fu et al. 2012; Canet et al. 2010). Loss-of-function studies showed that BOP1/2 function primarily in plant development (Ha et al. 2003; 2004; Norberg et al. 2005; Hepworth et al. 2005; McKim et al. 2008). These roles are conserved in a variety of land plants including moss, tobacco, pea, and alfalfa. BOP activity in a variety of species controls promotion of reproductive meristem fate, leaf and floral patterning, and abscission through regulation of growth, determinacy, and cellular differentiation at lateral organ boundaries (Saleh et al. 2011; Gourlay et al. 2000; Yaxley et al. 2001; Wu et al. 2012).

1.5.1 Leaf patterning

BOP1/2 expression is primarily localized to lateral organ boundaries in the plant. Beginning during embryogenesis, *BOP1/2* are expressed in the axils of cotyledons where they contribute to repression of meristematic activity (Ha et al., 2004; Jun et al., 2010). In *stm* mutants, *BOP1* and *AS2* are misexpressed at the junction between the fused

cotyledons reflecting expansion of the lateral organ boundaries and loss of the meristem (Jun et al., 2010). Inactivation of *BOP1/2* in *stm* mutants causes the formation of ectopic shoot meristems from the fused cotyledonary petiole due to misexpression of *BP*. *BOP1* directly activates *AS2* (Jun et al., 2010) whose product forms a complex with *AS1* for the stable repression of *BP* and *KNAT2* through changes in chromatin structure (Guo et al., 2008; Lodha et al., 2013).

After germination, *BOP1/2* expression is observed in the boundaries of initiating leaf primordia and at the adaxial base of leaves which gives rise to petioles, another boundary region (Ha et al., 2004; Norberg et al., 2005). Loss-of-function *bop1 bop2* causes ectopic blade development on petioles in part due to misexpression of *KNOX* genes *STM*, *BP*, *KNAT2*, and *KNAT6* (Ha et al., 2003; Hepworth et al., 2005; Norberg et al., 2005; Ha et al., 2007; Ha et al., 2010; Xu, 2011). Jun et al. (2010) showed that lack of *AS2* expression correlated with ectopic outgrowths in *bop1 bop2* mutant leaves indicating that *BOP1/2* act through *AS2* to regulate petiole architecture. However, enhanced *KNOX* misexpression in *bop1 bop2 as2* triple mutants suggests an *AS2*-independent pathway as well (Ha et al., 2007; Xu, 2011). These data show how *BOP1/2* function indirectly via activation of lateral organ boundary genes to maintain stable repression of meristematic *KNOX* genes in leaves.

1.5.2 Flower development

Following the transition to reproductive development, *BOP1/2* expression is observed in initiating flower primordia. Expression shifts at an early stage to the floral meristem/bract boundary and subsequently appears in the sepal axils, and in abscission zones (AZ) at the

base of floral organs and the base of pedicels (Hepworth et al., 2005; Norberg et al., 2005; McKim et al., 2008; Xu et al., 2010). Loss-of-function *bop1 bop2* leads to loss of floral organ abscission due to lack of AZ differentiation. The double mutants also lack nectaries which develop adjacent to the AZ. The AZ at the base of floral organs is a boundary region consisting of several layers of condensed cells which are specialized to allow the separation of floral parts from the flower base (McKim et al., 2008; Wu et al., 2012a). These data show that BOP1/2 are required for the patterning of boundaries in flowers by promoting AZ anatomy and nectary formation.

During the reproductive phase of development, BOP1/2 are further required for proliferation and patterning of floral meristems, determinate axillary meristems that arise from leaf axils following the transition to flowering. Loss-of-function *bop1 bop2* results in partial loss of floral-meristem identity as evidenced by additional secondary (axillary) inflorescences, outgrowth of floral bracts, branched flowers, and the displacement of cauline leaves from the base of shoots (Norberg et al., 2005; Xu et al., 2010). Similar phenotypes are caused by mutation of *LFY* or *API*, key regulators of floral-meristem identity (Xu et al., 2010). BOP1/2 co-operate with *LFY* and *API* to initiate flowers. Triple mutants *bop1 bop2 ap1-1* show conversion of flowers to highly branched inflorescence-like shoots and *bop1 bop2 lfy* mutants displayed enlarged floral bracts, some without an axillary floral meristem, and floral branching (Norberg et al., 2005; Xu et al., 2010). There is some evidence to suggest that BOP1/2 promote *LFY* expression since inactivation of *PUCHI*, an AP2 transcription factor, in *bop1 bop2* leads to severe defects in *LFY* transcript accumulation in floral meristems compared to *puchi* alone (Karim et al., 2009). BOP1/2 and *LFY* function independently to promote *API*

expression (Xu et al., 2010). Preliminary evidence indicates that BOP1/2 bind directly to the *API* promoter via the TGA bZIP factor PERIANTHIA (PAN) to promote commitment to floral meristem fate but this has yet to be established biochemically (Xu et al., 2010). Once the floral meristem is initiated, BOP1/2, LFY, and AP1 activities converge to cause down-regulation of inflorescence meristem identity genes *AGL24* and *SOCI* to promote determinacy in the floral shoot (Liu et al., 2008; Xu et al., 2010). After this, BOP1/2 help to pattern the flower. Mutations in *bop1 bop2* enhance *lfy* and *apl* floral patterning in promotion of sepal and petal floral-organ identity (Xu et al., 2010). Flowers in *bop1 bop2* mutants are asymmetric due to outgrowth of the floral bract and the initiation of extra floral organs on the abaxial side of the floral meristem. Typically, the abaxial sepal is replaced by two wing-like petals that extend outwards. BOP1/2-PAN form a nuclear complex that likely controls meristematic activity on the abaxial side of the floral meristem to control floral organ number (Hepworth et al., 2005; Xu et al., 2010). These data show an important role for BOP1/2 in the floral meristem where they function in conjunction with LFY and AP1 to promote floral fate, meristem determinacy, and control floral-organ patterning.

1.5.3 Other species

Orthologs of BOP1/2 have been partially characterized in moss, alfalfa, pea and tobacco (Saleh et al., 2011; Couzigou et al., 2012; Wu et al., 2012a). The moss *Physcomitrella patens* contains three BOP orthologs indicating a role in early land plants (Saleh et al., 2011). Characterization showed that *Physcomitrella patens microRNA534a* (*Pp-MIR534a*) controls the timing of juvenile-to-adult gametophyte transition through negative regulation of *PpBOP1/2* (Saleh et al., 2011). Pp-miR34a-mediated cleavage of

PpBOP1/2 mRNA limits its abundance during juvenile development. During the transition to reproductive development, increased levels of cytokinin negatively regulate *Pp-miR534a* causing stabilization of *PpBOP1/2* transcripts, which promote formation of a reproductive bud meristem. This shows a conserved role for BOPs in cell differentiation during the reproductive phase (Hepworth et al., 2005; Norberg et al., 2005; Ha et al., 2007; McKim et al., 2008; Jun et al., 2010; Xu et al., 2010; Couzigou et al., 2012). It is possible that this ancient system of BOP regulation by miRNA is still present in Arabidopsis but no such relationship has yet been identified.

NODULE ROOT (NOOT) and *COCHLEATA (COCH)* genes are *BOP2* orthologs from *Medicago truncatula* (alfalfa) and *Pisum sativum* (pea) respectively. Legume BOPs play an important role in root nodule development. Loss-of-function *noot* and *coch* mutant show expanded meristematic regions in the nodule and nodule to root identity reversion suggesting a possible link between the *NOOT/COCH* genes and stem cell maintenance via a WUS-CLV regulatory loop (Couzigou et al., 2012). Furthermore, *noot* and *coch* mutants display aerial defects similar to Arabidopsis *bop1 bop2* mutants. Loss-of-function *bop1 bop2* lack stipules, which are organs at the base of the leaf that mark basal region of the leaf primordia (Ichihashi et al., 2011). Reduced or complete loss of stipules is also observed in *noot* and early nodes in *coch* mutants (Gourlay et al., 2000; Yaxley et al., 2001; Couzigou et al., 2012). Similar to the asymmetrical flowers observed in *bop1 bop2* mutants, *noot* flowers have additional organs (petals and stamens). In *coch* mutants, flowers are dorsalized. Arabidopsis *bop1 bop2* mutants display enlarged bracts and branched flowers which are also observed in *coch* mutants (Hepworth et al., 2005; Norberg et al., 2005; Xu et al., 2010; Couzigou et al., 2012).

NtBOP2 was identified as a BOP ortholog in *Nicotiana tabacum* (tobacco). NtBOP2 was shown to function in differentiation of the corolla abscission zone (AZ) by regulating longitudinal cell expansion, possibly through interaction with TGA transcription factors (Wu et al., 2012). NtBOP2 antisense plants and dominant negative *NtBOP2*-ox lines showed loss of floral-organ abscission similar to *bop1 bop2* mutants (McKim et al., 2008; Wu et al., 2012).

1.5.4 Plant defense

It was previously thought that BOP1/2 function exclusively in plant development while other members of the NPR1-like family functioned in plant defense but recent work by Canet et al. (2012) has revealed a role for BOP1/2 in disease resistance induced by methyl jasmonate (RIM). Loss-of-function *bop1 bop2* mutants do not show a RIM response (Canet et al., 2012). This suggests that BOP1/2 are responsive to methyl jasmonate. More detailed research is required to ascertain the role of BOP1/2 in defense.

1.5.5 Mechanism

Like NPR1, BOP1/2 function as transcriptional co-activators *in vivo* when recruited to promoter regions of target genes through interaction with DNA binding proteins. Since knowledge of how BOP1/2 may act as transcriptional co-activators is still unknown, NPR1 can be used as a model to understand the biochemical mechanism of BOP1/2 mode-of-action. NPR1 is a positive regulator of the plant defense response known as systematic acquired resistance (SAR). NPR1 in the cytoplasm is an inactive oligomeric complex held together by intermolecular disulfide bonds between conserved cysteines in and around the N-terminal BTB/POZ domain (Kinkema et al., 2000; Mou et al., 2003).

After accumulation of salicylic acid (SA) upon pathogen attack, NPR1 assembles a transactivating complex that requires its BTB/POZ domain and the oxidation of Cys521 and Cys529 in its C-terminal transactivation (TA) domain (Rochon et al., 2006; Boyle et al., 2009). Cys521/529 co-ordinate a copper ion that binds to SA (Wu et al., 2012b). When SA binds to NPR1, a conformational change exposes the TA domain to allow its binding to TGA2, and activation of target genes such as *PR-1* (Wu et al., 2012b). BOP1/2 lack the Cys521 and Cys529 in the C-terminus which may release them from SA-regulated subcellular localization but regulated nuclear transport in response to developmental signals is still a possibility. BOP1/2 binds to copper and BOP-GFP fusion proteins are found in both the cytoplasm and the nucleus similar to NPR1 (Mou et al., 2003; Hepworth et al., 2005; Wu et al., 2012b; Hepworth/Després labs, unpublished data).

Like NPR1, BOP1/2 lack a DNA binding domain and interact with TGA bZIP transcription factors as a means for recruitment to target genes (Hepworth et al., 2005; Xu et al., 2010; Jun et al., 2010). The Arabidopsis genomes encodes ten TGA transcription factors, most of which interact with BOP1/2 in yeast to various degrees (Jackoby et al., 2002; Hepworth et al., 2005). TGA-BOP interactions were also observed in tobacco via yeast two-hybrids, firefly luciferase complementation imaging, and *in vitro* pull-down assays (Wu et al., 2012b). Evidence for TGA-BOP interaction required for regulating of downstream targets was provided by Xu et al. (2010). This research showed that BOP1/2 interact with TGA8/PAN *in vivo* and that *bop1 bop2* and *pan-1* have similar defects in floral-meristem identity. ChIP assays showed enrichment of BOP1-GFP protein at two sites in the *API* promoter suggesting that BOP1/2 are recruited to this promoter by

binding to PAN (Xu et al., 2010). Biochemical studies on NPR1 provide clues regarding how BOP-TGA interactions might work. TGA2 oligomers bound to the promoter of *PR-1* and act as transcriptional repressors in resting cells. Upon binding to SA, NPR1 assembles a complex stabilizing a dimer form of TGA2. The BTB-POZ domain of NPR1 bound to TGA2 negates its repressor function and converts TGA2 from a repressor to an activator (Rochon et al., 2006; Boyle et al., 2009). BOP1/2 may function in a similar manner to modulate TGA transcription factor activity to promote the expression of downstream target genes.

1.6 Thesis rationale

Thus far, BOP characterization in land plants has focused on examination of its loss-of-function phenotypes in leaf and floral patterning, reproductive meristem development, and abscission. This thesis focuses on examination of BOP gain-of-function (*BOP-ox*) defects and the role of BOP1/2 in control of inflorescence architecture and flowering. *BOP-ox* plants display extremely shortened internodes and increased transcripts of *AS2* and related *LATERAL ORGAN BOUNDARY (LOB)* genes (Norberg et al., 2005; Ha et al., 2007). The inflorescence defects observed in *BOP-ox* plants recapitulate the defects observed in *bp pny* double mutants as well as in *ATH1* and *AS2* gain-of-function lines (Smith and Hake, 2003; Xu et al., 2003; Norberg et al., 2005; Ha et al., 2007; Proveniers et al., 2007; Gómez-Mena and Sablowski, 2008). Both BOP1/2 and *ATH1* gain-of-function lines are late-flowering. These data suggest close functional interactions between BOP1/2 and KNOX–BELL transcription factors. My thesis uses a molecular genetics approach to shed light on the relationship between BOP1/2 and KNOX-BELL

transcription factors and their mode-of-action in the IM and in inflorescences. The aim of my thesis was to test if:

1. Antagonistic interactions between BP-PNY and BOP1/2 in stems play a role in determining inflorescence architecture
2. BOP1/2 regulate inflorescence architecture in conjunction with lateral organ boundary genes *ATH1* and *KNAT6*.
3. Antagonistic interactions between STM-PNY/PNF and BOP1/2 in the IM regulate competence to flower.

To test these hypotheses, we used BOP1/2 gain-of-function lines as a way to shed light on KNOX-BELL function and to identify downstream targets in regulating flowering and inflorescence development.

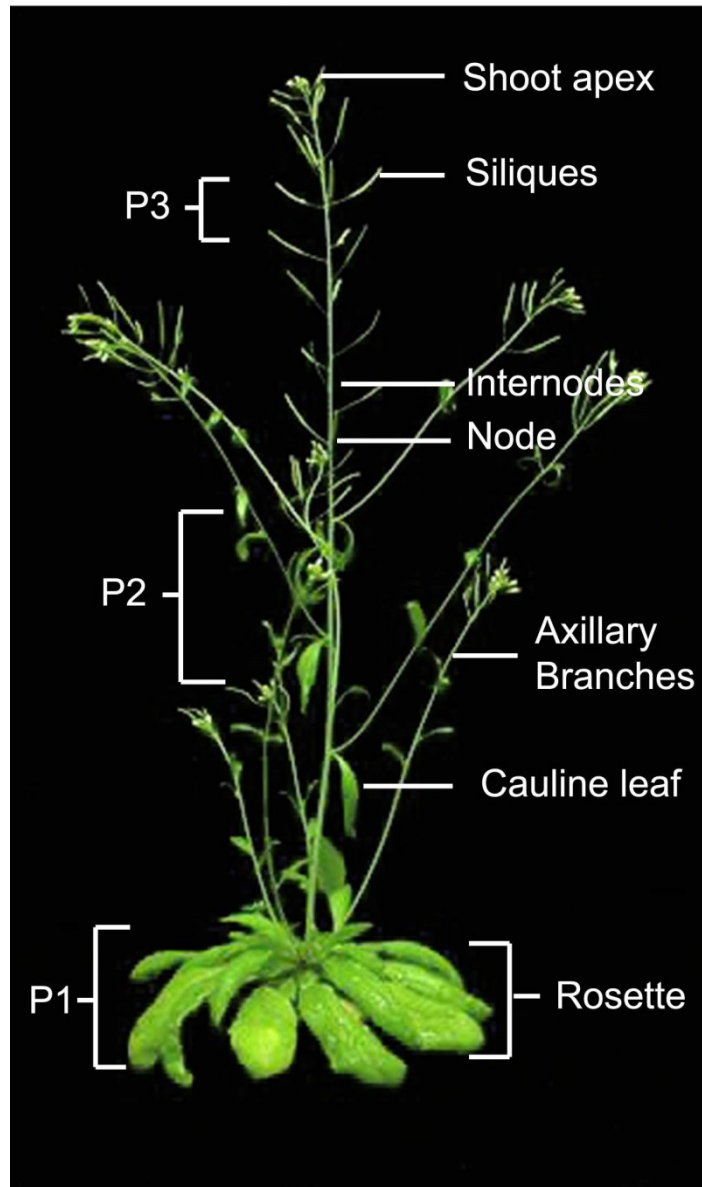


Figure 1.1 Architecture of the model plant *Arabidopsis thaliana*.

During vegetative development, the shoot apical meristem of *Arabidopsis* produces a basal rosette of leaves. At the transition to flowering, the meristem acquires inflorescence fate. This results in new patterns of aerial development. Axillary lateral branches (often called secondary inflorescences) and flowers separated by internodes are formed at the expense of leaves. Cauline leaves form at the base of axillary branches formed at early nodes in the inflorescences. At later nodes, flowers supported by pedicels are produced. Self-fertilization of flowers results in the production of fruits (siliques).

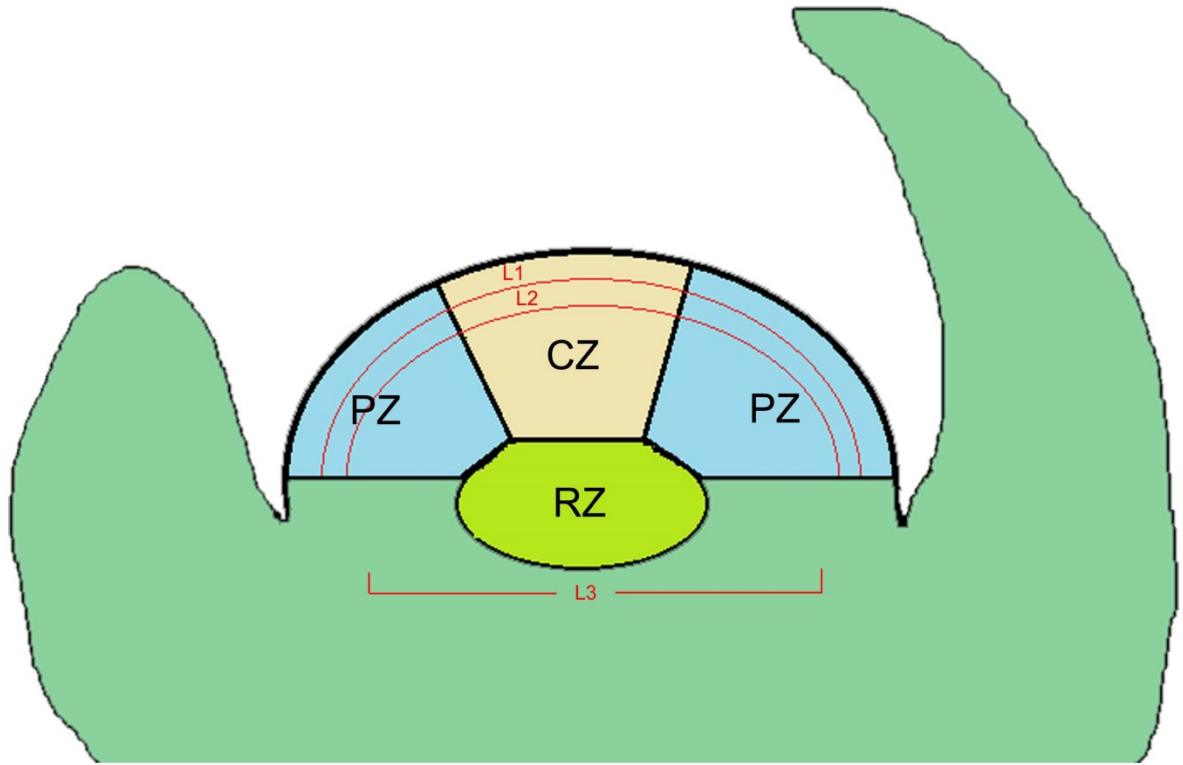


Figure 1.2 Organization of the SAM in *Arabidopsis thaliana*.

The shoot apical meristem (SAM) contains three domains: the central zone (CZ) containing undifferentiated stem cells flanked by the peripheral zone (PZ) on each side. The PZ consists of actively dividing cells that are competent to form lateral organ primordia in response to auxin-based signals. Division of cells in the rib zone (RZ) is responsible for the upward growth of the shoot with daughter cells incorporated into the stem below. The SAM is further divided into a tunica-carpus structure consisting of three cell layers. L1 and L2 epidermal and subepidermal cell layers of the tunica divide anticlinally. Cells in the underlying L3 corpus layer can divide in any plane contributing mainly to the stem (Figure adapted from Bäurle and Laux, 2003; Barton, 2010).

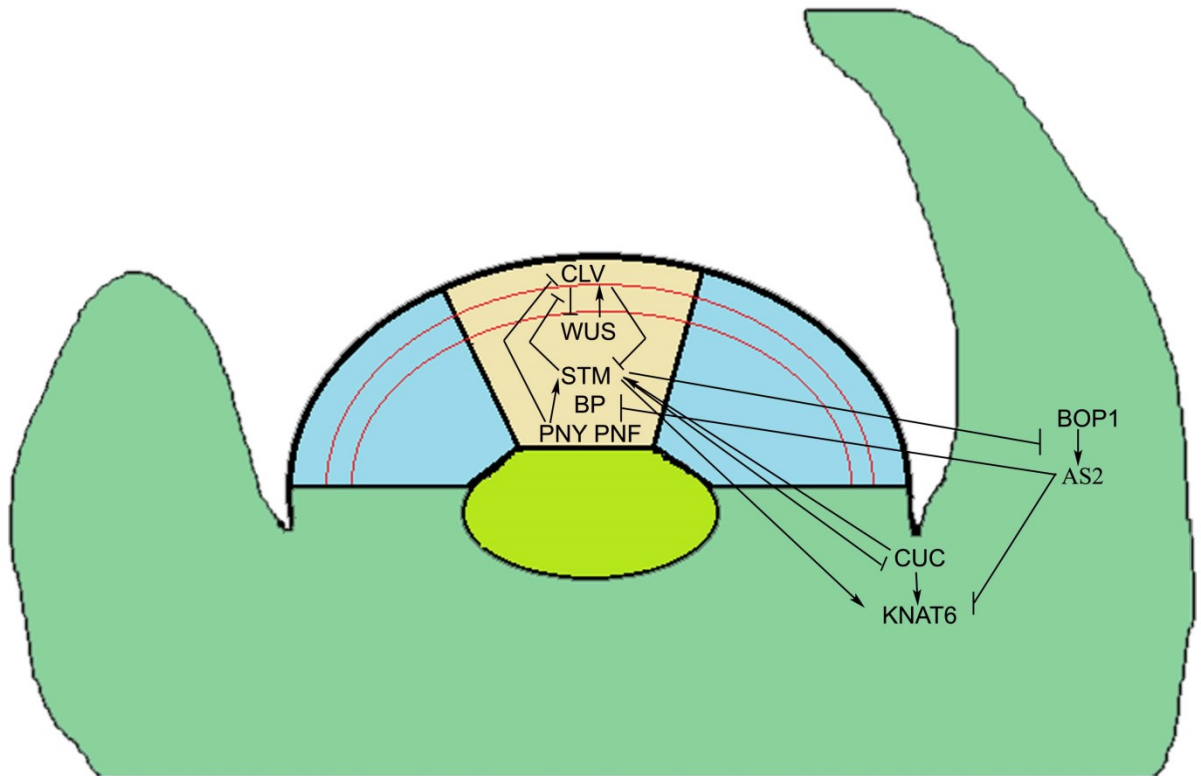


Figure 1.3 Genetic interactions in the SAM of *Arabidopsis thaliana*.

Complex genetic interactions between genes expressed in the SAM, boundaries, and lateral organ primordia control plant architecture during the vegetative phase. SHOOTMERISTEMLESS (*STM*) and CUP-SHAPED COTYLEDONS (*CUC*) negative feedback loop establishes the SAM. WUSHEL (*WUS*) and CLAVATA (*CLV*) feedback loop controls meristem size. *STM* initially restricts *BLADE-ON-PETIOLE* (*BOP1/2*) and *ASYMMETRIC LEAVES2* (*AS2*) to the initiating primordia. These genes in turn restrict the expression of *KNOX* genes [*STM* and *BREVIPEDICELLUS* (*BP*)] to the meristem. In the meristem, PENNYWISE and POUNDFOOLISH (*PNY/PNF*) form heterodimers with *KNOX* proteins. This heterodimerization is important for the nuclear localization of *STM* and potentially *BP*. ARABIDOPSIS THALIANA HOMEBOX GENE1 (*ATH1*) (not shown here) is expressed throughout the vegetative meristem. Domains are the same as in Figure 1.2

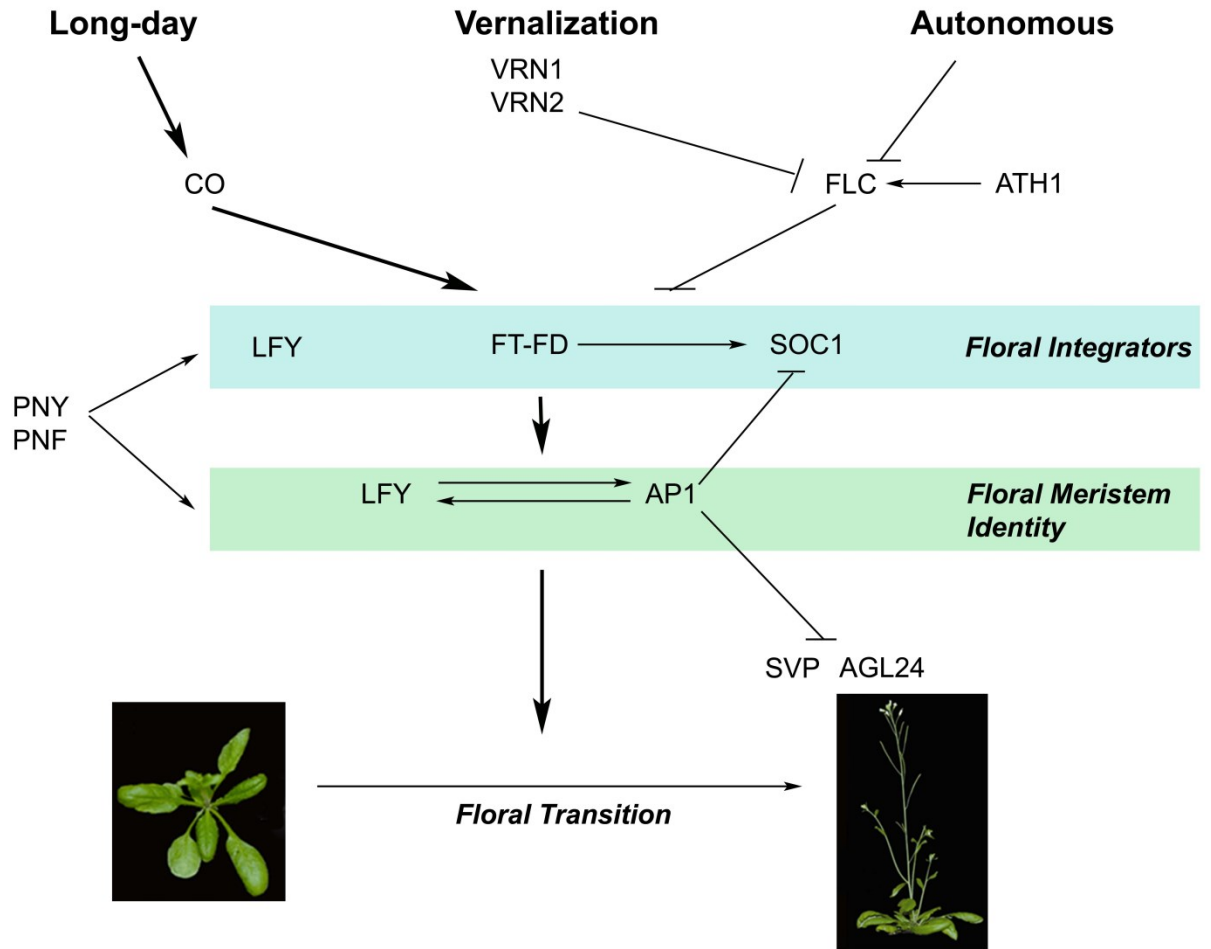


Figure 1.4 Genetic interactions regulating floral transition in *Arabidopsis thaliana*

Three main pathways for regulation of the floral transition are the long-day photoperiod, vernalization and autonomous pathways. The long day pathway promotes CONSTANS (CO) to stimulate flowering by upregulating floral integrators. The vernalization pathway promotes flowering through VERNALIZATION (VRN1/2)-based repression of FLOWERING LOCUS C (FLC), an inhibitor of floral integrators. Autonomous pathway also represses FLC to promote flowering. Floral integrators go on to promote floral meristem identity genes resulting in flower development.

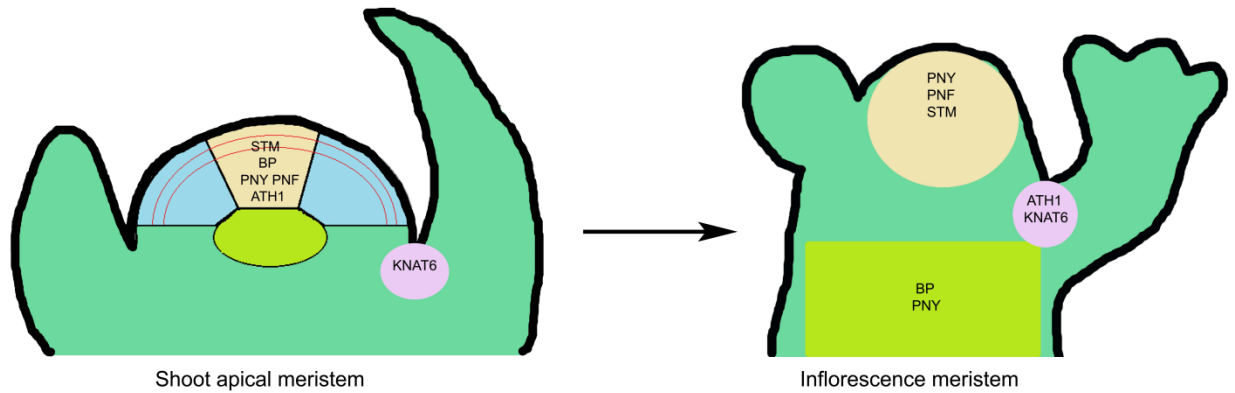


Figure 1.5 Reorganization of *TALE* homeobox genes upon transition to inflorescence meristem

At the transition to flowering, SAM acquires an IM fate accompanied by reorganization of *TALE* homeobox genes. *ATH1* dissipates from the meristem (SAM; cream) and becomes restricted to lateral organ boundaries in the stem (IM; purple). *BP* is also down-regulated in the meristem (SAM; cream) and now expressed in the stem (IM; green) along with expanded expression of *PNY* (IM; green) where they function to restrict *KNAT6* to the lateral organ boundary (IM; purple). *STM*, *PNY*, and *PNF* remain in the meristem where they confer stem cell fate and maintain indeterminacy (IM; cream).

CHAPTER 2

Antagonistic interaction of BLADE-ON-PETIOLE1 and 2 with BREVIPEDICELLUS and PENNYWISE regulates Arabidopsis inflorescence architecture

This chapter is presented essentially as published in Khan et al. (2012) Plant Physiology
158: 946-60.

Madiha Khan, Mingli Xu, Jhadeswar Murmu, Paul Tabb, Yuanyuan Liu, Kathryn Storey,
Sarah M. McKim, Carl J. Douglas, and Shelley R. Hepworth

2.1 Abstract

The transition to flowering in many plant species, including *Arabidopsis thaliana*, is marked by the elongation of internodes to make an inflorescence upon which lateral branches and flowers are arranged in a characteristic pattern. Inflorescence patterning relies in part on the activities of two three-amino-acid loop-extension homeodomain transcription factors: BREVIPEDICELLUS (BP) and PENNYWISE (PNY) whose interacting products also promote meristem function. We examine here the genetic interactions between BP-PNY whose expression is up-regulated in stems at the floral transition, and the lateral organ boundary genes *BLADE-ON-PETIOLE1* (*BOP1*) and *BOP2*, whose expression is restricted to pedicel axils. Our data show that *bp* and *pny* inflorescence defects are caused by *BOP1/2* gain of function in stems and pedicels. Compatible with this, inactivation of *BOP1/2* rescues these defects. *BOP* expression domains are differentially enlarged in *bp* and *pny* mutants, corresponding to the distinctive patterns of growth restriction in these mutants leading to compacted internodes and clustered or downward-oriented fruits. Our data indicate that *BOP1/2* are positive regulators of *KNOTTED1-LIKE FROM ARABIDOPSIS THALIANA6* expression and that growth restriction in *BOP1/2* gain-of-function plants requires *KNOTTED1-LIKE FROM ARABIDOPSIS THALIANA6*. Antagonism between *BOP1/2* and BP is explained in part by their reciprocal regulation of gene expression, as evidenced by the identification of lignin biosynthetic genes that are repressed by BP and activated by *BOP1/2* in stems. These data reveal *BOP1/2* gain of function as the basis of *bp* and *pny* inflorescence defects and reveal how antagonism between *BOP1/2* and BP-PNY contributes to inflorescence patterning in a model plant species.

2.2 Introduction

Flowering plants display a remarkable variety of inflorescence architectures selected to optimally display flowers for pollination and seed dispersal. Formation of the aerial parts of a plant is controlled by the shoot apical meristem (SAM), a cluster of pluripotent stem cells located at the apex of the primary shoot. The SAM produces a series of reiterative modules known as phytomers to generate the aerial parts of the plant. Each phytomer comprises an internode (stem) subtending a node, which is a leaf associated with a potential axillary meristem (Steeves and Sussex, 1989). Elaboration of the different parts of a module (leaves, internodes, and axillary meristems) varies according to the phase of development and between species to generate architectural diversity (Sussex and Kerk, 2001)

Arabidopsis (*Arabidopsis thaliana*) has distinct vegetative and reproductive phases. During vegetative development, the SAM generates leaf primordia on its flanks; both internode and axillary meristem formation are inhibited, resulting in a compact rosette of leaves. At the end of the vegetative phase, endogenous and environmental cues promote the transition to flowering. The SAM responds to floral inductive signals by acquiring inflorescence meristem (IM) fate. During reproductive development, internodes elongate and axillary meristems proliferate at the expense of leaves to generate lateral branches and flowers in a regular spiral pattern on the inflorescence (Bowman and Eshed, 2000; Fletcher, 2002; Barton, 2010). While the pathways that promote floral fate of axillary meristems and repress leaf development are well studied, less is known about the formation and patterning of internodes.

Internode patterning is a key determinant of inflorescence architecture, with variations in the length and pattern of internode elongation contributing to diversity in inflorescence height and organization of secondary branches and flowers on the primary stem. Formation of internodes is associated with the proliferation and elongation of cells in the region underlying the central zone of the meristem, termed the rib zone (Steeves and Sussex, 1989; Fletcher, 2002). Following their elongation, internodes are gradually fortified through the differentiation of interfascicular fibers with secondary thickened cell walls, which provides mechanical support (Nieminen et al., 2004; Ehltting et al., 2005).

Internode patterning is dependent in part on the overlapping activities of two three-amino-acid loop extension homeodomain transcription factors: the class I KNOTTED1-like homeobox (KNOX) protein BREVIPEDICELLUS (BP; formerly KNOTTED1-LIKE FROM ARABIDOPSIS THALIANA1 [KNAT1]) and the BEL1-like (BELL) protein PENNYWISE (PNY; also called BELLRINGER, REPLUMLESS, and VAMAANA) whose interacting products also promote meristem maintenance (Douglas et al., 2002; Venglat et al., 2002; Byrne et al., 2003; Smith and Hake, 2003; Bhatt et al., 2004; Rutjens et al., 2009; for review, see Hamant and Pautot, 2010). Mutations in *BP* cause short internodes and downward-pointing pedicels (Douglas et al., 2002; Venglat et al., 2002) whereas mutations in *PNY* cause irregular internode elongation, resulting in clusters of lateral organs (branches and flowers) spaced along the inflorescence stem (Byrne et al., 2003; Smith and Hake, 2003). In *bp pny* double mutants internodes are shorter than in either single mutant, signifying that BP and PNY have only partly overlapping roles in internode elongation and patterning (Smith and Hake, 2003). In both mutants, defects in vascular differentiation also occur, resulting in changes in how lignin

is deposited in stems (Douglas et al., 2002; Mele et al., 2003; Smith and Hake, 2003). Previous genetic studies have shown that two class I KNOX genes, *KNAT2* and *KNAT6*, are misexpressed in *bp* and *pny* mutant stems and pedicels. Inactivation of these genes, primarily *KNAT6*, rescues *bp* and *pny* defects in inflorescence architecture (Ragni et al., 2008) however this is the extent of our current knowledge.

Here, we examine genetic interactions between BP-PNY and BLADE-ON-PETIOLE1 (BOP1) and BOP2, two BTB-ankryin transcriptional coregulators that are expressed in lateral organ boundaries (Ha et al., 2004; Hepworth et al., 2005). *BOP1/2* expression is limited to the pedicel axil in inflorescence stems where their function is to promote the formation of a vestigial abscission zone (McKim et al., 2008). *BOP1/2* are indirect transcriptional repressors of *BP* in leaves (Ha et al., 2007; Jun et al., 2010) but their genetic interactions with BP, and its partner PNY, during reproductive development have yet to be examined. We show here that BP and PNY are transcriptional repressors of *BOP1/2*, preventing expression in stems and pedicels. Consistent with this, inactivation of the *BOP* genes rescues *bp* and *pny* inflorescence defects. We further show that *BOP1/2* exert their activity in part through the boundary gene *KNAT6*, which functions in the same genetic pathway. Finally, we show that *bp* and *pny* inflorescence defects are mimicked by *BOP1/2* gain of function. To explain this, we provide evidence that the reciprocal functions of BP and *BOP1/2* in the inflorescence are likely a consequence of their antagonistic regulation of downstream target genes, such as those involved in lignin biosynthesis that are repressed by BP and activated by *BOP1/2* in stems. These data redefine *bp* and *pny* phenotypes as the consequence of *BOP1/2* gain of function, shedding

light on how interactions between BP-PNY and BOP1/2 influence inflorescence architecture in a model plant species.

2.3 Materials and methods

2.3.1 Plant material and growth conditions

Plants were grown in growth chambers on agar plates and/or in soil at 21°C in 24 h light (100 $\mu\text{mol m}^{-2}\text{s}^{-1}$). Wild-type was the Columbia-0 (Col-0) ecotype of *Arabidopsis* unless stated otherwise. The double mutant *bop1-3 bop2-1* has been described previously (Hepworth et al., 2005). Mutant alleles of *as2-1* (CS3117), *ppy-40126* (SALK_40126), *knat2-5* (SALK_099837), and *knat6-2* (SALK_054482) were obtained from the *Arabidopsis* Biological Resource Center and have been described previously (Bryne et al., 2000; Iwakawa et al., 2002; Smith and Hake, 2003; Belles-Boix et al., 2006). Mutant alleles of *bp-1* and *bp-2* (introgressed into Col-0) were provided by Raju Datla (Venglat et al., 2002). The strong *35S:BOP2* line and activation-tagged overexpression line *bop1-6D* were kindly provided by O. Nilsson (Norberg et al., 2005). The reporter lines *KNAT2:GUS* (C24 ecotype) and *KNAT6:GUS* (WS ecotype) were gifts from Veronique Pautot (Dockx et al., 1995; Belles-Boix et al., 2006). The reporter line *BLR:GUS* (here called *PNY:GUS*) was provided by Mary Byrne (Byrne et al., 2003). The reporter line *BOP2:GUS* is described elsewhere (Xu et al., 2010). All mutant combinations were constructed by crossing and confirmed by PCR genotyping where possible.

2.3.2 Primers and genotyping

Primers used for genotyping, plasmid construction, and transcript analysis are listed in Supplemental Table S2.1. The strategy for genotyping *bop1-3*, *bop2-1*, *ppy-0126*, *knat2-5*, and *knat6-2* Salk T-DNA insertion mutants was as described (www.signal.salk.edu). For genotyping *bp-2*, primers bp-2dCAPS-F1 and bp-2dCAPs-R1 were used to amplify products from wild-type and *bp-2* genomic DNA. The product from Col wild type is slightly larger than the corresponding product from *bp-2*, allowing their resolution on a 3.5% agarose gel.

2.3.3 Construction of 35S:BOP1, 35S:BOP2, and tCUP4:BOP1 transgenic lines

To create pBAR/35S:BOP1/2 constructs, a fragment containing one copy of the viral 35S promoter was excised from p35S:BOP2 (Norberg et al., 2005) by digestion with *EcoR1* and *BamHI* and cloned into the corresponding site of pBAR1 (a gift from the Dangl Lab, University of North Carolina) to create the intermediate plasmid pBAR/35S. Primer pairs B1-1/B1-2 and B2-1/B2-2 incorporating *BamHI* restriction sites were used to amplify *BOP1* and *BOP2* coding sequences respectively from cloned cDNA templates. The resulting PCR products were digested with *BamHI* and ligated into the corresponding site in pBAR to generate pBAR/35S-BOP1 and pBAR/35S-BOP2. The *EntCUP4* promoter is an alternative constitutive promoter (Malik et al., 2002). To create ptCUP4:BOP1, a DNA fragment containing the *BOP1* coding sequence was amplified by PCR from cloned cDNA template using *EcoR1*-BOP1-F1 and BOP1-RR as the primers. The resulting fragment was digested with *EcoRI* and *BamHI* and ligated into the corresponding sites of pBAR1 to generate the intermediate plasmid pBAR1/BOP1. A 0.5-kb DNA fragment

containing the EntCUP4 promoter was then amplified by PCR using the EntCUP4-nos-GUS plasmid as template and *Eco*R1-tCUP-F1 and *Eco*R1-tCUP-R1 as the primers. The resulting fragment was digested with *Eco*R1 and ligated into the corresponding sites of pBAR/BOP1 to create ptCUP4:BOP1. Wild-type plants were transformed by floral dipping (Clough and Bent, 1998) using the *Agrobacterium* strain C58C1 pGV101 pMP90 (Koncz and Schell, 1986). Basta[®]-resistant transformants were selected on soil using the herbicide Finale (AgrEvo, Winnipeg, Canada). Phenotypes were scored in the T1 generation.

2.3.4 Phenotypic analysis of inflorescence structure

Quantitative analyses of twenty-four 6-week-old plants per genotype were performed as described (Ragni et al., 2008). Phyllotaxy measurements were performed using the device and method previously described (Peaucelle et al., 2007). The divergence angle between the insertion points of two successive floral pedicels along the main inflorescence was measured. This measurement is independent of the orientation of pedicel outgrowth. Fifteen divergence angles between the 1st and 16th siliques (counting acropetally) of each inflorescence were measured according to the orientation that resulted in the smallest average divergence angle. Angle of pedicel orientation was determined using a protractor to measure the angle of pedicel attachment relative to the stem. Orientation was measured for the first eleven siliques of each inflorescence (counting acropetally).

2.3.5 *In situ* hybridization and localization of GUS activity

Tissues were fixed and analyzed for GUS activity essentially as described by Sieburth and Meyerowitz (1997). Tissues were stained for 2-18 hours at 37°C and cleared

overnight with 70% ethanol prior to imaging. Alternatively, stained tissues were embedded in Paraplast Plus (Sigma, St. Louis, MO) from which 10 μm sections were cut using a microtome, affixed to glass slides, and dewaxed with tert-butanol and xylene prior to imaging. *In situ* hybridizations were performed as previously described (Xu et al., 2010). Primers used to create anti-sense probes for *BP* and *KNAT6* were as listed in Supplemental Table S2.1.

2.3.6 Scanning electron microscopy (SEM)

Samples were prepared for SEM as described previously (Hepworth et al., 2005). Images were collected using a Vega-II XMU Variable Pressure SEM (Tescan USA, Cranberry Township, PA).

2.3.7 Lignin staining

Tissue sections (25 μm) were cut from paraffin-embedded mature green siliques to analyze replum patterning or from elongated internodes located between the third and fourth siliques on the primary stem to analyze stem patterning. Sections were affixed to glass slides by overnight incubation at 42°C. Tissues were dewaxed and dehydrated prior to treatment with 2% phloroglucinol (in 95% ethanol) followed by 6N HCl for colour development. For the analysis of lignin at the base of stems, cross-sections were hand-cut with a razor blade from the base of 32-day-old flowering plants and placed in 3 ml of phloroglucinol staining solution. After 5 minutes, 5 drops of concentrated HCl were added. Two minutes were allowed for colour development and images were immediately collected.

2.3.8 qRT-PCR

Total RNA was isolated from leaves, pedicels, internodes, or the base of bolting stems (bottom 2.5-cm of 32-day-old flowering plants) using Trizol[®] reagent (Invitrogen, Carlsbad, CA). cDNA was generated using 1 μ g of total RNA as the template and Superscript III RT (Invitrogen, Carlsbad, CA) as the polymerase. qPCR was performed in triplicate using 2 μ l of 10-fold diluted cDNA as the template in reactions containing SYBR[®] Green and IQ Supermix (BioRad, Hercules, CA) with a Rotor-Gene 6000 thermocycler (Qiagen, Alameda, CA). Annealing conditions were optimized for each primer pair and data quality was verified by melting curve analysis. Relative transcript levels were calculated as described (Murmu et al., 2010). Values were normalized to *GAPC* and then to the wild-type control. For Figure 9G only, cDNA was generated using 2 μ g of total RNA as the template and diluted 20-fold prior to use. *ACTIN2* was used as a normalization control and reactions were performed in triplicate using an annealing temperature of 55°C. All experiments were repeated at least twice with independently isolated RNA with similar results obtained. Gene-specific primers for the analysis of lignin genes were as listed in Supplemental Table S2.

2.3.9 Accession numbers

Sequence data for genes described in this article can be found in the GenBank/EMBL data libraries under the accession numbers: At2g41370 (BOP1), At3g57130 (BOP2), At1g70510 (KNAT2), At1g23380 (KNAT6), At4g08150 (BP), At5g02030 (PNY), At3g04120 (GAPC), At2g37040 (PAL1), At2g30490 (C4H1), At1g51680 (4CL1),

At2g40890 (C3H1), At4g34050 (CCoMT1), At4g34230 (CAD5), At3g21770 (AtPRXR9GE), At3g18780 (ACT2).

2.4 Results

2.4.1 Expression of *BOP1* and *BOP2* in lateral-organ boundaries

Previous analysis of *BOP* expression by *in situ* hybridization or through use of *BOP1:GUS* or *BOP2:GUS* reporter genes is consistent in showing that the *BOP* genes are expressed in lateral-organ boundaries formed during embryonic, vegetative, and reproductive development (Ha et al., 2004; Hepworth et al., 2005; Norberg et al., 2005; McKim et al., 2008; Xu et al., 2010). We have consolidated these data (Fig. 2.1). Using a *BOP2:GUS* reporter gene, expression was verified at the base of cotyledons in mature embryos (Fig. 2.1A; Ha et al., 2004). During postembryonic vegetative development, *BOP2* expression was first associated with the boundary at stage 2 of leaf development, when primordia first appear as morphologically distinct from the SAM (Fig. 2.1, B and C, arrow indicates stage 2 leaf). As leaves expand, expression associates with the adaxial base of leaves, which gives rise to the petiole (Fig. 2.1, B and C; Norberg et al., 2005). Expression is also observed in the axil of pedicels (Fig. 2.1, D and E; McKim et al., 2008) and in the valve margins of fruit (Fig. 2.1F). Importantly, *BOP1/2* expression is excluded from the IM and the replum of fruits, representing structures with meristematic function. While analysis of loss-of-function *bop1 bop2* mutants has revealed that *BOP1/2* transcriptionally repress meristematic genes in leaves (Ha et al., 2007) and floral primordia (Xu et al., 2010) relatively little is known about how *BOP1/2* gain of function perturbs plant architecture.

2.4.2 A spectrum of inflorescence architecture defects caused by *BOP1/2* gain of function

Previous phenotypic analysis of *BOP1* or *BOP2* overexpression in plants has drawn attention to *bp* and *ppy*-like defects in inflorescence architecture, either short plants with floral pedicels pointing downward (Ha et al., 2007) or short bushy plants with irregular internodes (Norberg et al., 2005). Comparison of the strong activation-tagged *bop1-6D* line to *bp ppy* double mutants revealed remarkably similar inflorescence architectures (Fig. 2.2, A–C), suggesting that BOP1/2 might antagonize both activities. This also suggested that BOP1/2 gain of function might elicit a spectrum of inflorescence defects. To examine this further, we generated transgenic plants overexpressing *BOP1* or *BOP2* in Columbia-0 (Col-0) and Landsberg *erecta* (*Ler*) backgrounds and scored for defects in inflorescence architecture (Fig. 2.2, D–I; Table 2.1). This analysis showed that in *Ler* plants, downward-pointing siliques was the prevalent phenotype (up to 45% of transformants) whereas in Col-0 plants, clustered siliques was the prevalent phenotype (up to 20% of transformants). Compatible with this, the *erecta* mutation enhances the phenotypic severity of *bp* mutants (Douglas et al., 2002). Taken together, these findings suggest that BOP gain of function has variable effects on inflorescence architecture conditioned in part by ecotype. These defects may result from the antagonism of BP and/or PNY expression or activity. To examine this further, we tested the effect of *bop1 bop2* loss of function on expression of *bp* and *ppy* mutant phenotypes in a Col background.

2.4.3 Inactivation of BOP1/2 partially rescues the *bp* phenotype

To first examine *BOP1/2* interactions with *BP*, we generated *bop1 bop2 bp-1* and *bop1 bop2 bp-2* triple mutants and analyzed their phenotypes relative to wild-type and parental controls. *bp* mutants are characterized by short internodes, reduced apical dominance, and downward-pointing siliques (Douglas et al., 2002; Venglat et al., 2002). This analysis showed that inactivation of the *BOP* genes largely rescues *bp* inflorescence defects (Fig. 2.3, A–D; Supplemental Fig. S2.1) similar to inactivation of *KNAT2* and *KNAT6* (Ragni et al., 2008). Quantitative phenotypic analyses were performed on 24 plants per genotype, by measuring the average height, internode length, and number of rosette paraclades for wild type and mutants (Fig. 2.4, A–D). These analyses confirmed that *bop1 bop2* loss of function counteracted the short stature of *bp-1* and *bp-2* plants (Fig. 2.4A) and partially restored apical dominance in *bp-1* mutants (Fig. 2.4B). Whereas *bp-1* mutants have a significant number of short internodes in the 1- to 5-mm range, the distribution in *bop1 bop2 bp-1* triple mutants was similar to wild type (Fig. 2.4C). Whereas *bp-1* pedicels point downward at an average angle of 84.9° relative to the primary stem, the average angle in *bop1 bop2 bp-1* triple mutants was 47.7°, similar to wild type (Fig. 2.4D). Also, the average pedicel angle in *bop1 bop2* double mutants was steeper than wild type (34.7° versus 50.3°), showing that *BOP1/2* regulate pedicel orientation as well as abscission zone formation at the stem-pedicel junction (Fig. 2.4D; Supplemental Fig. S2.2; McKim et al., 2008). No rescue occurred in *bp-2 bop1* or *bp-2 bop2* double mutants (data not shown), indicating that *BOP1* and *BOP2* have redundant functions.

2.4.4 Inactivation of *BOP1/2* completely rescues the *pnv* phenotype

Given that BP and PNY coregulate internode patterning, we next examined the interaction of *BOP1/2* with *PNY* by generating *bop1 bop2 pny* triple mutants. *pnv* mutants are characterized by clusters of siliques due to irregular internode elongation, defects in phyllotaxy, reduced apical dominance, and replumless fruits (Byrne et al., 2003; Roeder et al., 2003; Smith and Hake, 2003; Bhatt et al., 2004). Inactivation of the *BOP* genes also rescued *pnv* inflorescence defects (Fig. 2.3, A, E, and F). Quantitative phenotypic analyses were performed on 24 plants per genotype to further monitor this rescue, by measuring the average height, internode length, and number of rosette paraclades for wild type and mutants. These analyses confirmed that loss-of-function *bop1 bop2* restored the stature of *pnv* plants and the number of rosette paraclades to wild type (Fig. 2.5, A and B). Whereas *pnv* mutants have a significant number of internodes in the 1- to 5-mm range, the distribution in *bop1 bop2 pny* triple mutants was similar to wild type (Fig. 2.5C). To quantify rescue of phyllotactic patterning in *bop1 bop2 pny* triple mutants, we measured divergence angles between successive floral pedicels on the primary stem (Fig. 2.5D; see Peaucelle et al., 2007). Whereas the distribution of divergence angles in *pnv* was largely random (mean of 175°), the distribution in *bop1 bop2 pny* triple mutants was similar to wild type (mean of 142° versus 141°). Surprisingly, partial loss of *BOP* function was sufficient to rescue the *pnv* phenotype since *pnv bop1* and *pnv bop2* mutant inflorescences also resembled wild type (data not shown).

A final defining characteristic in *pnv* mutants is a replumless fruit (Roeder et al., 2003). Scanning electron microscopy (SEM) showed that inactivation of *BOP1/2* also rescues replum formation in *pnv* fruits (Supplemental Fig. S2.3, A–D), similar to inactivation of

KNAT6 and consistent with coexpression of *BOP1/2* and *KNAT6* in valve margins (Fig. 1F; Supplemental Fig. S2.4; Ragni et al., 2008). We further examined the pattern of lignin deposition in fruit cross sections (Supplemental Fig. S2.3, E–H). In *pnv* mutants, lignin (pink color) was detected throughout the junction between the valves, reflecting lack of the replum. In *bop1 bop2* and *bop1 bop2 pnv* triple mutants, lignin formed only at the valve margins as in wild type. Collectively, these data demonstrate complete rescue of *pnv* defects, supporting the model that BOP1/2 antagonize BP and PNY activities in the inflorescence. These data further suggest that BOP1/2 and KNAT6 control similar developmental processes, based on their similar interactions with BP and PNY and their overlapping expression patterns in lateral organ boundaries Ragni et al., 2008; see also Fig. 2.1; Supplemental Fig. S2.4).

2.4.5 *BOP1/2* expression domains are expanded in *bp* and *pnv* mutants

Ragni et al. (2008) showed that BP and PNY prevent *KNAT2* and *KNAT6* expression in stems and pedicels and that loss-of-function *knat6* (and *knat2 knat6*) rescues *bp* and *pnv* defects. This prompted us to examine if *BOP1/2* expression domains are likewise expanded in *bp* and *pnv* mutants, using the *BOP2:GUS* reporter gene (Fig. 2.6, A–O). In *bp* mutants, *BOP2* expression was expanded in stems and pedicels, particularly below nodes. Expression on the abaxial side of nodes is consistent with localized growth restriction, causing pedicels to point downward. Staining was also seen in stripes of abnormal epidermal tissue that extend below the node and become ectopically lignified in mature *bp* stems (Fig. 2.6, F–I; Venglat et al., 2002; Mele et al., 2003). Stem cross sections from just below the node confirmed *BOP2* misexpression in the stem cortex beneath the epidermis and in phloem regions associated with the primary vascular bundle

(Fig. 2.6J). In *pnv* mutants, *BOP2* expression was also expanded in stems and pedicels above and below nodes, compatible with growth impairment, causing irregular internodes and silique clustering (Fig. 2.6, K–N). Stem cross sections near *pnv* nodes confirmed *BOP2* misexpression throughout the stem cortex (Fig. 2.6O). *BOP1:GUS* expression in *bp* and *pnv* mutants showed a similar pattern (Supplemental Fig. S2.5). In summary, the misexpression patterns of *BOP1/2* differ in *bp* and *pnv* mutants, bearing resemblance to the distinct inflorescence defects that characterize these mutants.

2.4.6 BOP1/2 promote *KNAT6* expression

Given that *BOP1/2* and *KNAT6* are both required for *bp* and *pnv* phenotypes and *BOP1/2* gain of function produces *bp*- and *pnv*-like phenotypes, we compared *KNAT6:GUS* expression in various *BOP* gain-of-function lines: *bp*, *pnv*, and *35S:BOP2* or *bop1-6D*. Misexpression of *KNAT6:GUS* in stems was confirmed for all genotypes (Fig. 2.7, A–D). However, the reporter gene was not expressed in boundaries of the IM, indicating that some of its control sequences were missing (data not shown). We therefore used *in situ* hybridization to further examine *KNAT6* expression in the inflorescence apex and stem (Fig. 2.7, E–T). In the *bp* mutant, *KNAT6* transcript was misexpressed in the stem cortex and vascular tissue (Fig. 2.7, J and N) and beneath the node in a stripe pattern (Fig. 2.7R) similar to misexpression of *BOP2* (Fig. 2.6, I and J). In the *pnv* mutant, *KNAT6* was misexpressed in the vascular tissue of elongated stems similar to *bop1-6D* mutants (Fig. 2.7, K, L, O, P, S, and T). Both mutants formed extra vascular bundles, resulting in a dense vascular ring with little interfascicular space (Fig. 2.7, O and P; Smith and Hake, 2003). *KNAT6* transcript levels were also monitored in internodes and pedicels by quantitative reverse transcription (qRT)-PCR. These data confirmed 2- to 3-fold higher

levels of *KNAT6* transcript in *bp-2*, *pny*, and *bop1-6D* plants relative to wild type and *bop1 bop2* controls (Fig. 2.7U). Higher levels of *KNAT6* transcript are consistent with an expanded domain of *KNAT6* expression in *bop1-6D/35S:BOP2* stems. We therefore concluded that BOP1/2 promote *KNAT6* expression. Consistent with this, *KNAT6* transcript levels were slightly lower in *bop1 bop2 bp* and *bop1 bop2 pny* internodes and pedicels relative to *bp-2* and *pny* single mutants (Fig. 2.7U). No similar up-regulation was observed for *KNAT2* in *bop1-6D* plants (data not shown).

2.4.7 BOP1/2 exert their function through KNAT6

Given that BOP1/2 promote *KNAT6* expression, we reasoned that BOP1/2 may exert all or part of their function through *KNAT6*. To examine this, we tested the effect of *knat6* loss of function on the phenotype of a strong *35S:BOP2* gain-of-function line with short compact inflorescences (Norberg et al., 2005). In this experiment, plants that were homozygous for the *35S:BOP2* transgene were crossed to wild type or to lines homozygous for *knat2*, *knat6*, or *knat2 knat6* mutations. The phenotypes of progeny were scored in the F1 generation. To rule out transgene silencing, we took the additional step of confirming *BOP2* overexpression in F1 populations (Supplemental Fig. S2.6). These experiments revealed that partial *knat6* loss of function (i.e. *knat6/+* or *knat2/+ knat6/+*) was sufficient to restore internode elongation in *35S:BOP2* plants (Fig. 2.8, A and C–E). In contrast, no rescue occurred in control crosses to wild type or *knat2* alone (Fig. 2.8, A, B, and E). Compatible with this, mutations in *knat2* alone do not rescue *bp* or *pny* inflorescence defects (Ragni et al., 2008). These data indicate that BOP1/2 exert much of their function through *KNAT6*. Interestingly however, *35S:KNAT6* plants are not short and mimic *35S:BP* plants with lobed leaves (Supplemental Fig. S2.7A; see also Lincoln

et al., 1994; Dean et al., 2004), indicating that the functions of BP and KNAT6 are redundant when BOP1/2 is not coexpressed. Thus, both BOP1/2 and KNAT6 are required to exert changes in inflorescence architecture.

2.4.8 BOP1/2 and BP/PNY are antagonistic regulators of stem lignification

We next sought to determine how BOP1/2 gain of function antagonizes BP and PNY activities in the stem. We initially considered that BOP1/2 might function through ASYMMETRIC LEAVES2 (AS2) to inhibit BP and/or PNY expression in stems. BOP1/2 indirectly repress BP in leaves by promoting AS2 expression, whose product is a direct repressor of BP transcription (Guo et al., 2008; Jun et al., 2010). However, inactivation of AS2 failed to rescue the short stature of *35S:BOP2* plants (Ha et al., 2007) or *bp* and *pny* inflorescence defects (Supplemental Fig. S2.7, B and C). Moreover, no decrease in BP or PNY expression was detected in the stem of BOP1/2 loss- or gain-of-function mutants (Supplemental Fig. S2.8). These data indicate that BOP1/2 control of stem architecture is largely independent of AS2 and transcriptional repression of BP. We therefore examined the model that BOP1/2 function downstream of BP-PNY and have reciprocal functions in the stem based on their compartmentalized expression domains in the inflorescence.

To examine this, we turned to work showing that BP is a negative regulator of lignin deposition in stems (Mele et al., 2003). In the primary inflorescence stem, formation of secondary cell walls is tightly regulated over developmental time (Ehlting et al., 2005). Cross sections were cut from the base of wild-type and mutant primary stems at the same developmental age and stained with phloroglucinol, which detects lignin deposition, a hallmark of secondary walls in vessel and fiber cells in the inflorescence stem. As

expected, complex patterning changes were seen in *bp* mutants. Phloem fibers overlying primary vascular bundles were prematurely lignified. In addition, gaps were observed in the ring of interfascicular fiber cells with lignin abnormally deposited in the epidermis and cortex of these gaps. This pattern correlates with the position of abnormally differentiated stripes of tissue in *bp* stems that originate below nodes and extend basipetally (Fig. 2.9, A–C; Douglas et al., 2002; Venglat et al., 2002; Mele et al., 2003). Loss-of-function *bop1 bop2* partially rescued *bp* defects, resulting in a pattern similar to wild type (Fig. 2.9, A, C, and D). Ectopic stem lignification also occurs in *pny* stems, albeit in a different pattern than for *bp*, which may reflect differences in where or when *BOP1/2* are misexpressed. In *pny* stems, vascular bundles were more crowded than in wild type, resulting in a dense vascular ring (Fig. 2.7O; Supplemental Fig. S2.9; Smith and Hake, 2003). Loss-of-function *bop1 bop2* also rescued *pny* defects, resulting in a pattern similar to wild type (Supplemental Fig. S2.9, A, E, and G). Importantly, stem cross sections from *35S:BOP2* and *bop1-6D* plants showed expanded patterns of lignification, similar to *bp pny* double mutants (Fig. 2.9E; Supplemental Fig. S2.9; Smith and Hake, 2003). In *BOP1/2* overexpressing lines, the vascular ring was dense (similar to *pny* mutants) and phloem fiber cells overlying primary vascular bundles were prematurely lignified (similar to *bp* mutants). However, there were no gaps in the vascular ring, presumably due to uniformity in *BOP1/2* misexpression. In *bop1-6D* mutants, parts of the pith were lignified, never observed in wild-type stem development. Thus, *BOP1/2* gain of function induces lignified phloem and interfascicular fibers in a pattern reminiscent of the secondary growth that occurs in trees (Fig. 2.9E; Supplemental Fig. S2.9; Nieminen et al., 2004; Baucher et al., 2007). These data support the model

BOP1/2 function downstream of BP-PNY in the stem and have a reciprocal function associated with lignin biosynthesis.

2.4.9 BOP1/2 activate genes repressed by BP

Microarray and electrophoretic mobility shift assay experiments have previously identified lignin biosynthetic genes that are directly repressed by *BP* in stems (Mele et al., 2003). Direct targets of PNY have not been identified to our knowledge. Therefore, qRT-PCR was used to examine whether lignin biosynthetic gene transcripts are reciprocally regulated by BP and BOP1/2 in inflorescence stems (Fig. 2.9G). This approach confirmed up-regulation of all four genes previously identified by Mele et al. (2003) as up-regulated in mature *bp-2* stems (*Phe ammonia lyase1* [*PAL1*]; *cinnamate 4-hydroxylase1* [*C4H1*]; *4-coumarate CoA ligase1* [*4CL1*]; and *PRXR9GE*, a class III peroxidase) as well as several additional genes (*C3H1*; *caffeoyl CoA 3-Omethyltransferase1* [*CCoMT1*]; *cinnamyl alcohol dehydrogenase5* [*CAD5*]) in the lignin biosynthetic pathway (for review, see Boerjan et al., 2003). Mutation of *bop1 bop2* in *bp-2* restored all but one of these gene transcripts to near wild-type levels, supporting the observed promotive effect of BOP1/2 on lignin deposition in stems. Four of the above genes were also up-regulated in *bop1-6D* stems (*C4H1*, *C3H1*, *CAD5*, and *PRXR9GE*), suggesting that BOP1/2 directly or indirectly promotes the expression of genes in the lignin biosynthetic pathway. Similar results were obtained using internode tissue (data not shown). As reported by Mele et al. (2003), the class III peroxidase gene *PRXR9GE* showed the greatest fold-change (15- to 20-fold) over wild type in both *bp-2* and *bop1-6D* stems, suggesting that polymerization of monolignol subunits may be a key regulatory point in the developmental control of secondary wall formation. Collectively,

these data support the model that BOP1/2 and BP have reciprocal functions in the stem and show how antagonistic interactions between BOP1/2 and BP-PNY are important for patterning of cell-type differentiation in stems as well as inflorescence architecture.

2.5 Discussion

Internodes are elongated at the transition to flowering as a result of expanded rib meristem activity in the IM (Steeves and Sussex, 1989; Fletcher, 2002). The meristem expression of *BP* diminishes with the floral transition and becomes restricted to the cortex of the inflorescence stem and pedicel, where its activity together with PNY promotes internode elongation and vascular patterning (Lincoln et al., 1994; Douglas et al., 2002; Venglat et al., 2002; Smith and Hake, 2003). In this article, we used a genetics approach to examine how interactions between BP- PNY and the lateral organ boundary regulators BOP1/2 govern Arabidopsis inflorescence architecture. Our data show that a spectrum of *bp*- and *pny*-like defects in inflorescence architecture are caused by *BOP1/2* gain of function. Our key findings are that BP and PNY restrict *BOP1/2* expression to the pedicel axil together with *KNAT6* to prevent their misexpression in stems and pedicels, which causes altered growth patterns in *bp* and *pny* inflorescences. Our data also indicate that BOP1/2 promote *KNAT6* expression and that both activities are required to inhibit internode elongation in stems (Fig. 2.10). Our analysis of gain-of-function mutants demonstrates that BOP1/2 function downstream of BP-PNY in a reciprocal manner, accelerating the final steps of stem differentiation in opposition to BP.

2.5.1 BOP1/2 differentially regulate KNOX activity in leaves and inflorescences

Previous work has established that BOP1/2 in leaves function together with AS1/2 to maintain repression of the class I KNOX genes *BP*, *KNAT2*, and *KNAT6* during leaf development (Ori et al., 2000; Semiarti et al., 2001; Ha et al., 2003, 2007; Jun et al., 2010). In this context, BOP1/2 indirectly represses *BP* transcription by promoting *AS2* expression in leaf petioles (Jun et al., 2010). Genetic assays show that BOP1/2 also repress *BP* through an AS2-independent pathway that is as-yet undefined (Ha et al., 2007; data not shown). Our data reveals an opposite regulatory pattern in inflorescences with BP and PNY functioning as transcriptional repressors of *BOP1/2* and *KNAT6*. Co-misexpression of *BOP1/2* and *KNAT6* permits their opposing function downstream of BP-PNY to restrict growth and promote premature differentiation of the stem. These data are compatible with BOP1/2 gain-of-function studies in moss. In this species, stabilization of *BOP1/2* transcripts causes premature gametophore differentiation (Saleh et al., 2011).

2.5.2 Misexpression of *BOP1/2* restricts growth to create variations in inflorescence architecture

Variations in inflorescence architecture are extensive among flowering plants, with the length and pattern of internode elongation and pedicel angle acting as key variables in the display of flowers (Steeves and Sussex, 1989; Sussex and Kerk, 2001). Short internodes and pedicels like those in *bp* mutants are reminiscent of species with spike-type inflorescences where internodes between successive flowers are short (Bell and Bryan, 2008). Conversely, long internodes separating whorls of flowers on the stem, like those in

pnv mutants, are reminiscent of species with verticillate type inflorescences (Bell and Bryan, 2008). Our data show that a spectrum of inflorescence architectures ranging from short internodes, to downward-pointing pedicels, to clusters of flowers may be produced by differentially regulating the pattern and degree of BOP gain of function in stems. In *bp* mutants, ectopic *BOP1/2* expression on the abaxial side of nodes leads to growth restriction and downward-pointing pedicels. *BOP1/2* are also misexpressed in the stem cortical tissue where BP-PNY normally function, thereby inhibiting internode elongation and causing cells to differentiate prematurely. In *pnv* mutants, *BOP1/2* are strongly misexpressed in the pedicels and stem cortex of young internodes, leading to irregular elongation of internodes and the clustering of flowers in whorls. These defects are phenocopied to various degrees by ectopically expressing *BOP1/2* under the control of single or multiple 35S Cauliflower mosaic virus (CaMV) enhancers, indicating that *BOP1/2* function downstream of BP-PNY in an antagonistic manner. However, *BOP1/2* gain of function does not reduce *BP* or *PNY* transcript levels in the stem (Supplemental Fig. S8), indicating that *BOP1/2* likely oppose BP-PNY function post-transcriptionally.

2.5.3 BOP1/2 and KNAT6 function in the same genetic pathway

Our genetic assays and expression data show that misexpression of *BOP1/2* is the cause of inflorescence patterning defects in *bp* and *pnv* mutants. For reasons that are unclear, inactivation of *BOP1/2* partially suppresses *bp* defects but completely suppresses *pnv* defects. This difference may be related to the slightly different roles that *bp* and *pnv* play in internode development (Hake and Smith, 2003; Peaucelle et al., 2011). These data extend the work of Ragni et al. (2008) who showed an identical pattern of rescue for *bp* and *pnv* defects by inactivation of *KNAT6* (and to a lesser extent *KNAT2*), genes that are

misexpressed in an overlapping domain with *BOP1/2* in *bp* and *pnv* stems (Figs. 6 and 7). These studies place *BOP1/2* and *KNAT6* in the same genetic pathway controlling inflorescence architecture. Compatible with this, *BOP1/2* gain of function promotes *KNAT6* expression. However, both activities are required to restrict internode elongation since inactivation of *KNAT6* restores internode elongation in *35S:BOP2* plants and *35S:KNAT6* internodes are not short (Fig. 2.8; Supplemental Fig. S2.7; Dean et al., 2004). Despite several attempts with *35S:BOP1-GR* transgenic plants and chromatin immunoprecipitation assays, we have yet to determine if *BOP1/2* directly regulate *KNAT6*. Given that *BP* and *KNAT6* are highly related proteins with the same gain-of-function phenotype (Lincoln et al., 1994; Chuck et al., 1996; Dean et al., 2004) they may regulate some of the same genes. However, *KNAT6* with *BOP1/2* function in opposition to *BP*. A physical complex between *BOP1/2* and *KNAT6* was not detected in yeast (*Saccharomyces cerevisiae*; data not shown). We therefore favor a model in which *BOP1/2* bind independently to the same promoters as *KNAT6* or induce the expression of a *KNAT6* cofactor to exert their effect.

In fruits, *BOP1/2* and *KNAT6* likewise function in the same genetic pathway as evidenced by rescue of replum formation in *pnv* mutants by either *bop1 bop2* or *knat6* loss of function (Ragni et al., 2008; this study). *BOP1/2* and *KNAT6* may also share a role in floral-organ abscission based on recent evidence that *IDA*- dependent signaling inhibits *BP* activity, allowing *KNAT2* and *KNAT6* to promote abscission (McKim et al., 2008; Shi et al., 2011). Thus, antagonism between *BP-PNY* and a genetic pathway involving *BOP1/2* and *KNAT6* is likely to be a conserved module in plant development.

2.5.4 ARABIDOPSIS THALIANA HOMEODOMAIN GENE1 is a potential KNAT6 cofactor

The BELL homeodomain protein encoded by *ARABIDOPSIS THALIANA HOMEODOMAIN GENE1* (*ATH1*) is another potential member of the *BOP1/2* and *KNAT6* genetic pathway that will be important to investigate. KNOX homeodomain proteins like *KNAT6* perform many of their functions as heterodimers with BELL proteins (e.g. Byrne et al., 2003; Bhatt et al., 2004; Kanrar et al., 2006; Rutjens et al., 2009). These partnerships can influence protein-protein interactions, nuclear localization of the KNOX partner, and/or binding-site selection (Smith and Hake, 2003; Hackbusch et al., 2005; Cole et al., 2006; Rutjens et al., 2009). Interestingly, loss-of-function *ath1-1* rescues *pn1* inflorescence defects (like *bop1 bop2* and *knat6*) whereas *ATH1* gain of function causes short internodes (Gómez-Mena and Sablowski, 2008; Rutjens et al., 2009). Given that *ATH1* transcripts are highly up-regulated in *bop1-6D* internodes (data not shown), an *ATH1-KNAT6* complex may restrict stem growth. Short internodes are typical of defects in gibberellic acid (GA) biosynthesis (Achard and Genschik, 2009; Schwechheimer and Willige, 2009) of which *BP* is a repressor (Hay et al., 2002). However, *GA 20-oxidase* transcript levels in *35S:BOP2* and *bop1-6D* stems are not significantly different from wild type (data not shown) and spray treatment of *35S:BOP2* plants with GA did not restore internode elongation (data not shown), making it uncertain if defects in GA biosynthesis or catabolism are at play.

2.5.5 BP and BOP1/2 antagonistically regulate secondary cell wall biosynthesis

Lignin biosynthesis is one of the major components of secondary cell wall formation, essential for water transport and the structural support of plants. In Arabidopsis, abundant interfascicular fibers with secondarily thickened cell walls develop in the primary stem as the inflorescence matures (Nieminen et al., 2004; Ehrling et al., 2005). In *bp* mutants, lignin deposition in interfascicular fibers and phloem occurs prematurely, showing that part of the function of BP is to delay terminal cell differentiation, potentially until internode elongation is complete (Mele et al., 2003). However, these defects are alleviated by *bop1 bop2* mutation, showing that BOP1/2 promotes terminal cell fate and is a developmental regulator of lignin formation. Although *BOP1/2* are not normally expressed in Arabidopsis stems, boundaries such as the valve margin of fruits and the base of floral organs or leaves following abscission are lignified in aid of cell separation and scar fortification, respectively (Sexton, 1976; Lewis et al., 2006; Lee et al., 2008b). Interestingly, publically available poplar (*Populus* spp.) microarray data indicates that two potential *BOP* orthologs are highly expressed in xylem (<http://www.bar.utoronto.ca>), which suggests a conserved role for BOP1/2 in promoting secondary growth in trees.

Mele et al. (2003) identified four lignin biosynthetic genes whose expression was up-regulated in *bp-9* stems. Our study confirmed up-regulation of these genes (*PAL1*, *C4H1*, *4CL1*, *PRXR9GE*) as well as several others (*C3H1*, *CAD5*, *HCT*) in *bp-2* and *bop1-6D* stems and internodes. Given that BP binds directly to the promoters of lignin genes (Mele et al., 2003) it will be interesting to confirm biochemically whether BOP1/2 and BP directly regulate a common set of genes to exert their antagonistic functions. Of the lignin genes surveyed, the class III cell wall peroxidase transcript *PRXR9GE* shows the most

dramatic up-regulation in *bp-2* and *bop1-6D* lines (15-fold or more) relative to wild-type control plants. Class III peroxidases are one of several classes of cell wall enzymes that use hydrogen peroxide as an oxidant to generate monolignol phenoxy radicals, thus allowing the spontaneous coupling of monolignols into their polymer form (Boerjan et al., 2003; Passardi et al., 2004). Peroxidase activity is low in seedlings and increases with age in the aerial parts of the plant (Mele et al., 2003; Cosio and Dunand, 2010). Thus, the final step of lignin formation may be a key point of developmental control, making the transcriptional regulation of *PRXR9GE* an interesting case study.

In conclusion, our data establish BOP1/2 gain of function as the basis of *bp* and *pny* inflorescence defects. Our study shows that ectopic BOP1/2 activity in stems both restricts growth and promotes terminal cell differentiation, dramatically altering inflorescence architecture. Future studies will establish the molecular basis of antagonism between BP-PNY and BOP1/2. Ultimately, this work will provide important insight into how changes in the interplay between KNOX-BELL factors in the meristem and BOP1/2 in lateral organ boundaries drives species variation in inflorescence architecture.

Table 2.1 Summary of inflorescence defects in plants overexpressing *BOP1* or *BOP2*

Transgene	Ecotype	Plants with Downward-Oriented Siliques (%)	Plants with Clustered Siliques (%)	Total No. of Transformants
<i>35S:BOP1</i>	Col	0.0	20.6	175
<i>35S:BOP2</i>	Col	0.0	10.0	80
<i>tCUP:BOP1</i>	Col	0.0	61.1	18
<i>35S:BOP1</i>	Ler	44.5	22.0	164
<i>35S:BOP2</i>	Ler	27.6	20.4	196

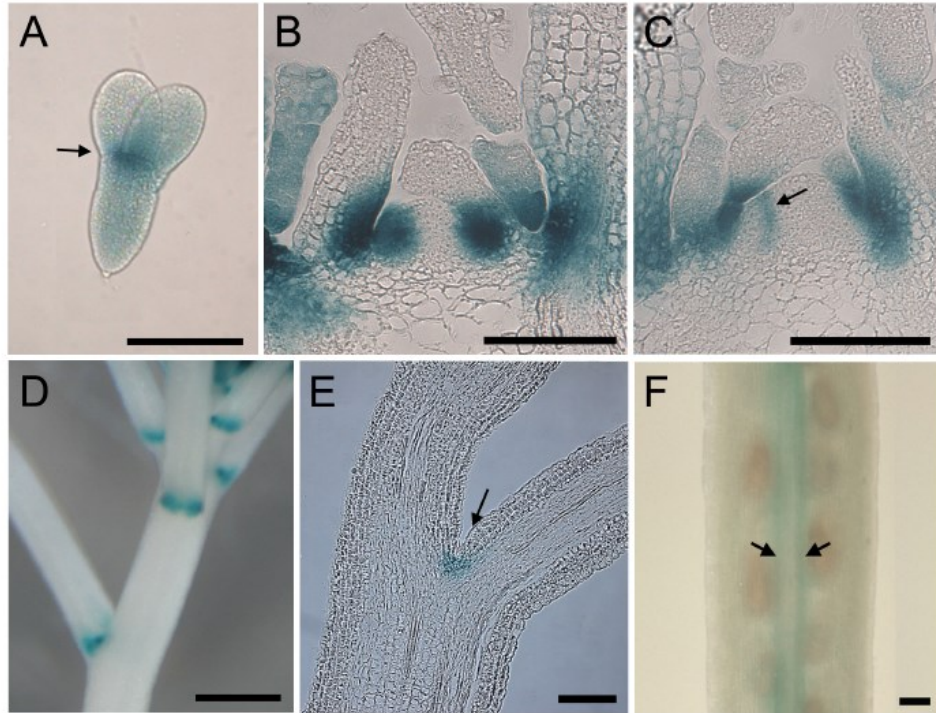


Figure 2.1 *BOP2:GUS* expression pattern in boundaries

(A) Mature embryo; expression at base of cotyledons (arrow).

(B-C) Shoot apex of a short-day-grown seedling, longitudinal section; expression begins in stage 1 leaf primordia and localizes to the boundary of stage 2 leaves (arrow). As primordia expand, *BOP2* expression associates with the adaxial base of leaves, which elongate to form the petiole.

(D) Inflorescence; horse-shoe pattern of expression in the axils of floral pedicels.

(E) Pedicel, longitudinal section; expression in the axil (arrow).

(F) Silique; expression in the valve margins (arrows).

Scale bars, 0.1 mm except D, 0.5 mm.

Figure 2.2 BOP1 gain-of-function causes bp- and pny-like defects in inflorescence architecture

Representative inflorescences are shown for:

(A) Col WT.

(B) *bp-2 pny* double mutant.

(C) *bop1-6D*; an activation-tagged *BOP1* overexpression line (with four 35S CaMV enhancers). Compact internodes similar to *bp-2 pny*.

(D) Col WT.

(E) *pny* mutant.

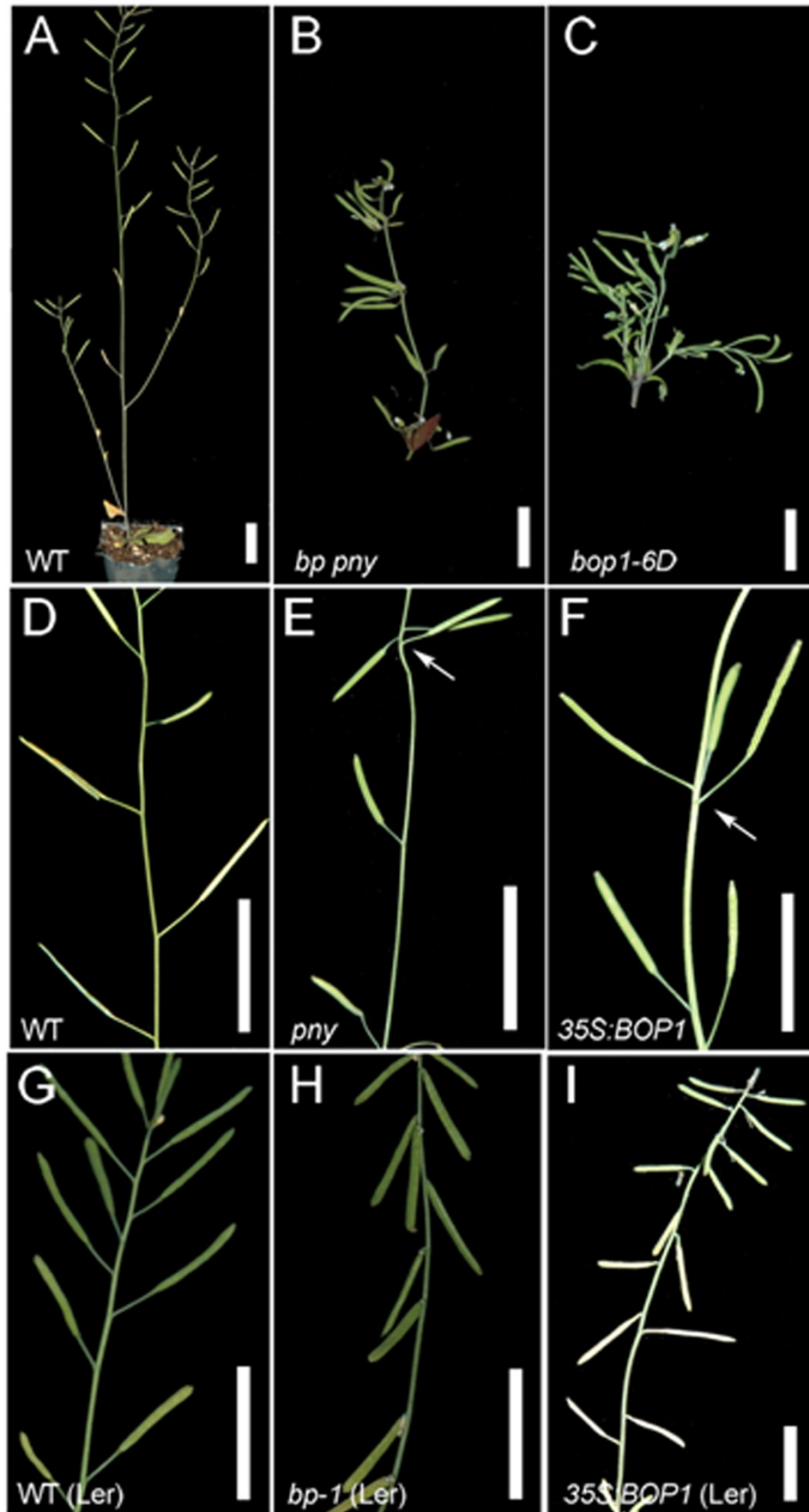
(F) *35S:BOP1* transformant in Col (one 35S CaMV enhancer) with clustered siliques as in *pny*.

(G) Ler WT.

(H) *bp-1* in Ler.

(I) *35S:BOP1* transformant in Ler; downward-pointing siliques as in *bp-1*.

Scale bars, 1 cm.



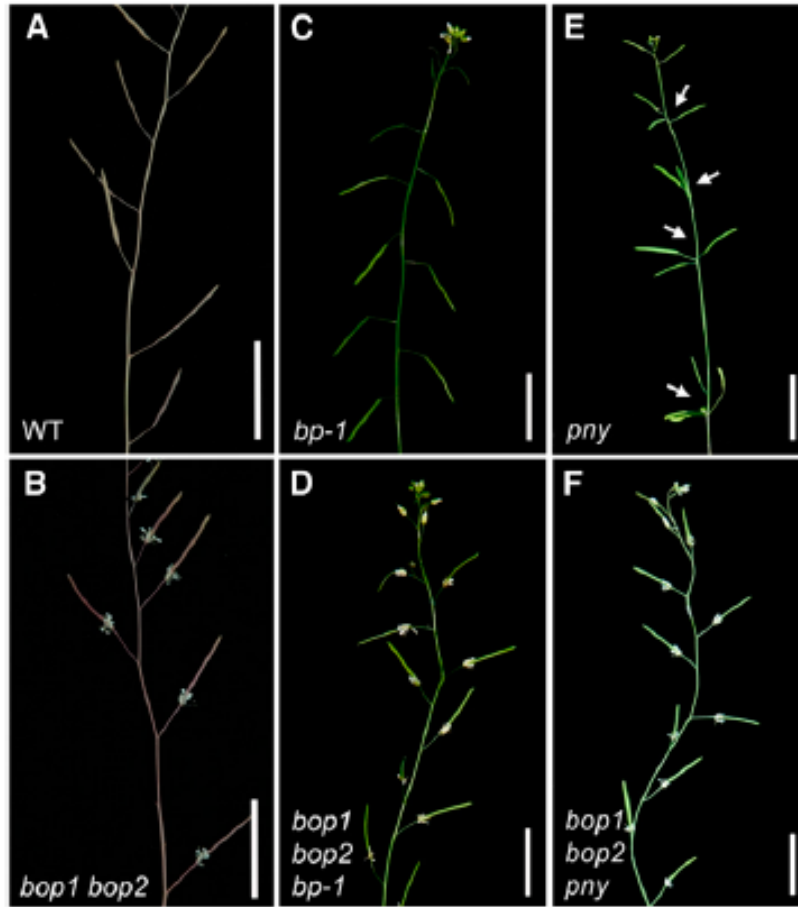


Figure 2.3 Phenotypic suppression of *bp* and *pny* inflorescence defects by *bop1 bop2*

(A) WT control.

(B) *bop1 bop2* mutant.

(C) *bp-1* mutant; downward-pointing siliques.

(D) *bop1 bop2 bp-1* mutant; partial rescue of *bp-1* phenotype.

(E) *pny* mutant; clustered siliques (arrows).

(F) *bop1 bop2 pny* mutant; similar to WT.

Scale bars, 2 cm.

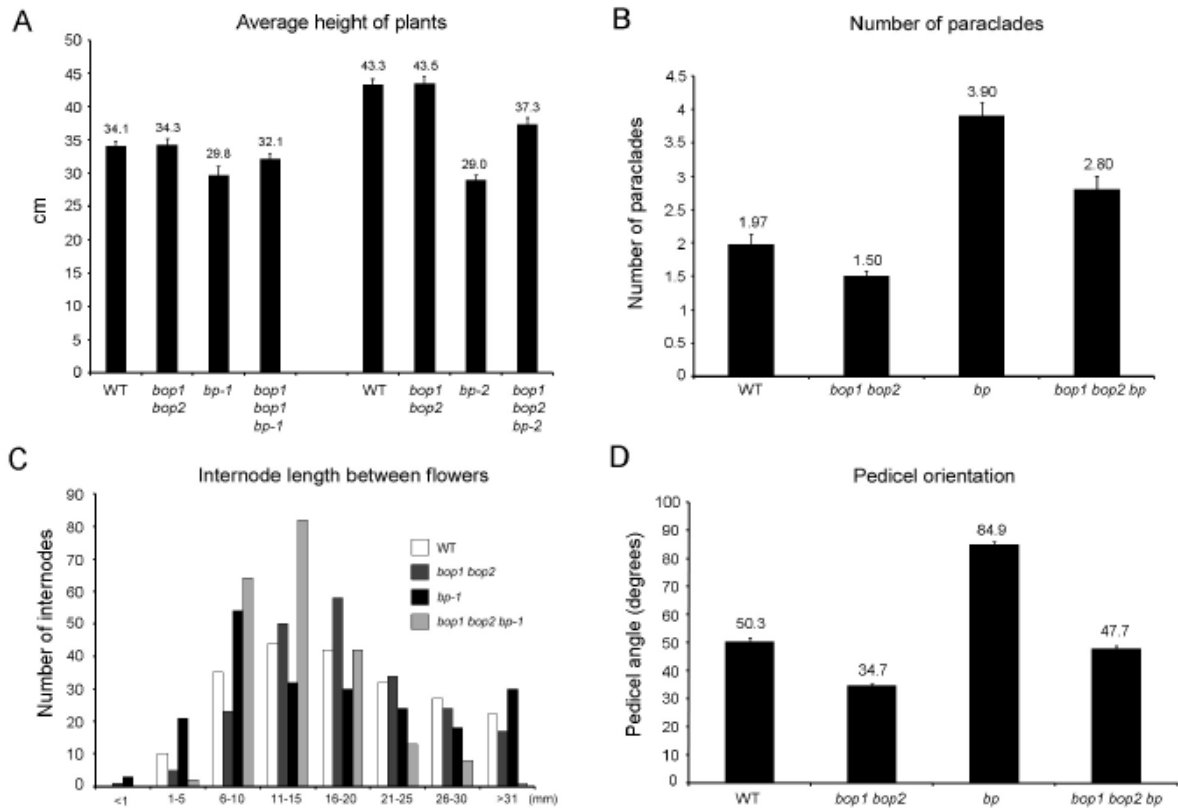


Figure 2.4 Quantitative analysis of *bp* phenotypic rescues of *bop1 bop2*

At least 24 plants for the indicated genotypes were analyzed.

(A) Average inflorescence height; inactivation of *BOPI/2* partially rescues the short stature of *bp-1* and *bp-2* mutants.

(B) Average number of paraclades; inactivation of *BOPI/2* partially restores apical dominance in *bp-1* mutants.

(C) Distribution of internode lengths between successive siliques on the primary inflorescence. Internodes between the 1st and 11th siliques (counting acropetally) were measured. Distribution of internode lengths in *bop1 bop2 bp-1* triple mutants is similar to WT.

(D) Average orientation of pedicels; inactivation of *BOPI/2* restores normal pedicel orientation to *bp-1* mutants.

Error bars, SE.

Figure 2.5 Quantitative analysis of *pny* phenotypic rescue by *bop1 bop2*

At least 24 plants for the indicated genotypes were analyzed.

(A) Average height of primary inflorescence; inactivation of *BOP1/2* rescues short stature of *pny* mutants.

(B) Average number of rosette paraclades; inactivation of *BOP1/2* restores apical dominance in *pny* mutants.

(C) Distribution of internode lengths between successive siliques on the primary inflorescence. Internodes between the 1st and 11th siliques (counting acropetally) were measured. The distribution of siliques in *bop1 bop2 pny* mutants was similar to wildtype.

(D) Distribution of divergence angles between siliques on the primary inflorescence. At least 10 successive angles between the 1st and 24th siliques (counting acropetally) were measured for $n \geq 14$ plants per genotype. The class containing the theoretical angle of 137° is indicated by a vertical line. Average angle, Avg. In *pny* plants, distribution is uniform across all classes but in *bop1 bop2 pny* plants, the distribution is similar to wildtype.

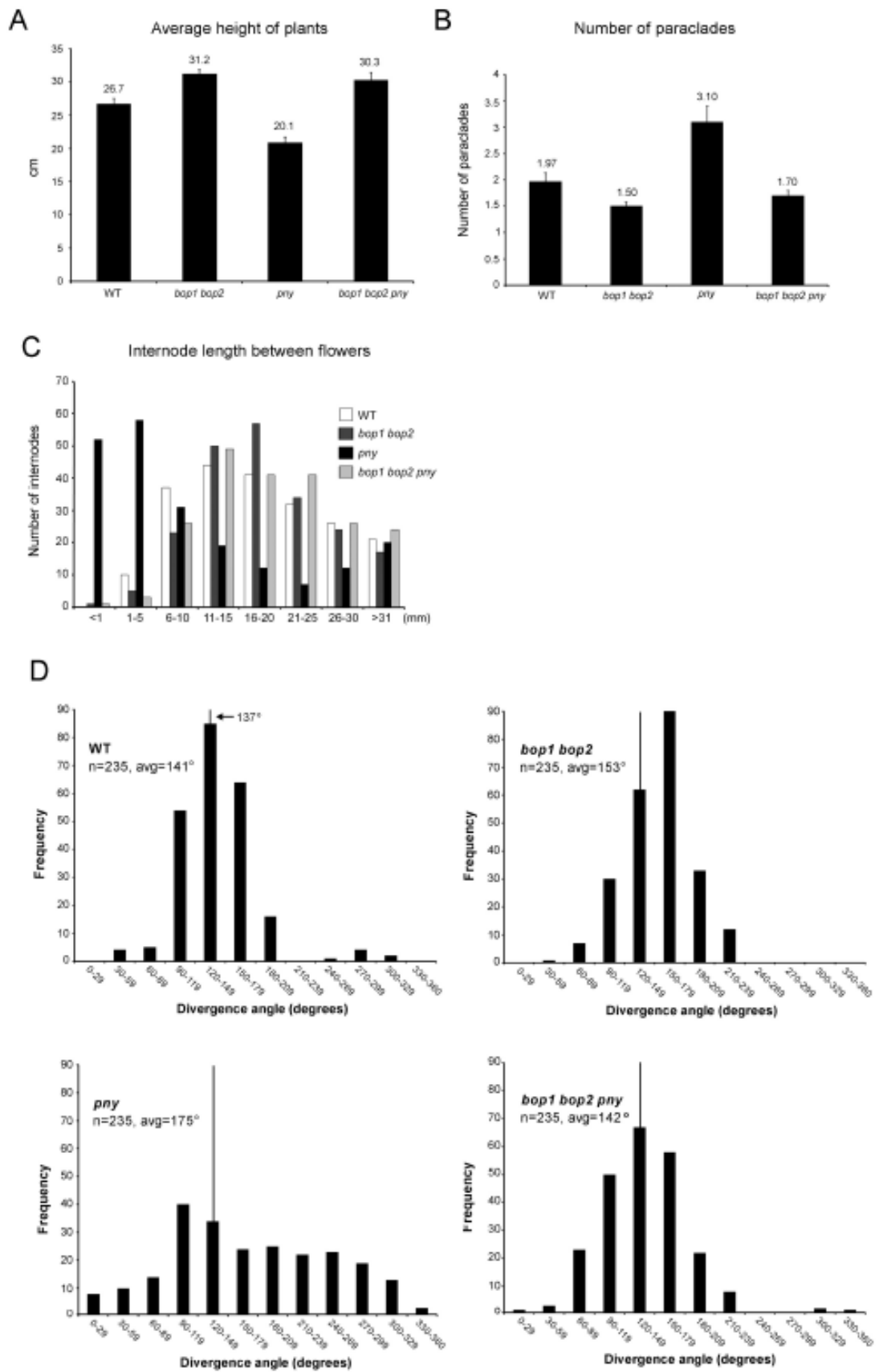


Figure 2.6 *BOP2:GUS* expression in wildtype, *bp*, and *pny* inflorescences

(A to E) Wild type.

(A and B) Expression restricted to stem-pedicel axil.

(C) Apex; no expression in the IM, internodes, or pedicels.

(D) Node.

(E) Stem;

Line in (D) shows plane of cross-section.

(F to J) *bp-2* mutant.

(F to G) Expression expands beyond nodes, thin stripes of tissue extending basipetally below nodes stain strongly (arrow).

(H) Apex; misexpression on the abaxial side of nodes (arrows) and in pedicels.

(I) Node; misexpression on the abaxial side of the node (arrows).

(J) Stem; stripe of expression below node.

Line in (I) shows plane of cross-section. Arrow, cortical cells; arrowhead, phloem.

(K to O) *pny* mutant.

(K to L) Expression expands above and below nodes.

(M) Apex; staining strongest near the apex and in pedicels.

(N) Node; diffuse expression above and below the node (arrows).

(O) Stem; misexpression in stem cortex (arrow).

Line in (N) shows plane of cross-section.

Scale bars, 1 mm except 100 μ m for C to E, H to J, M to O.

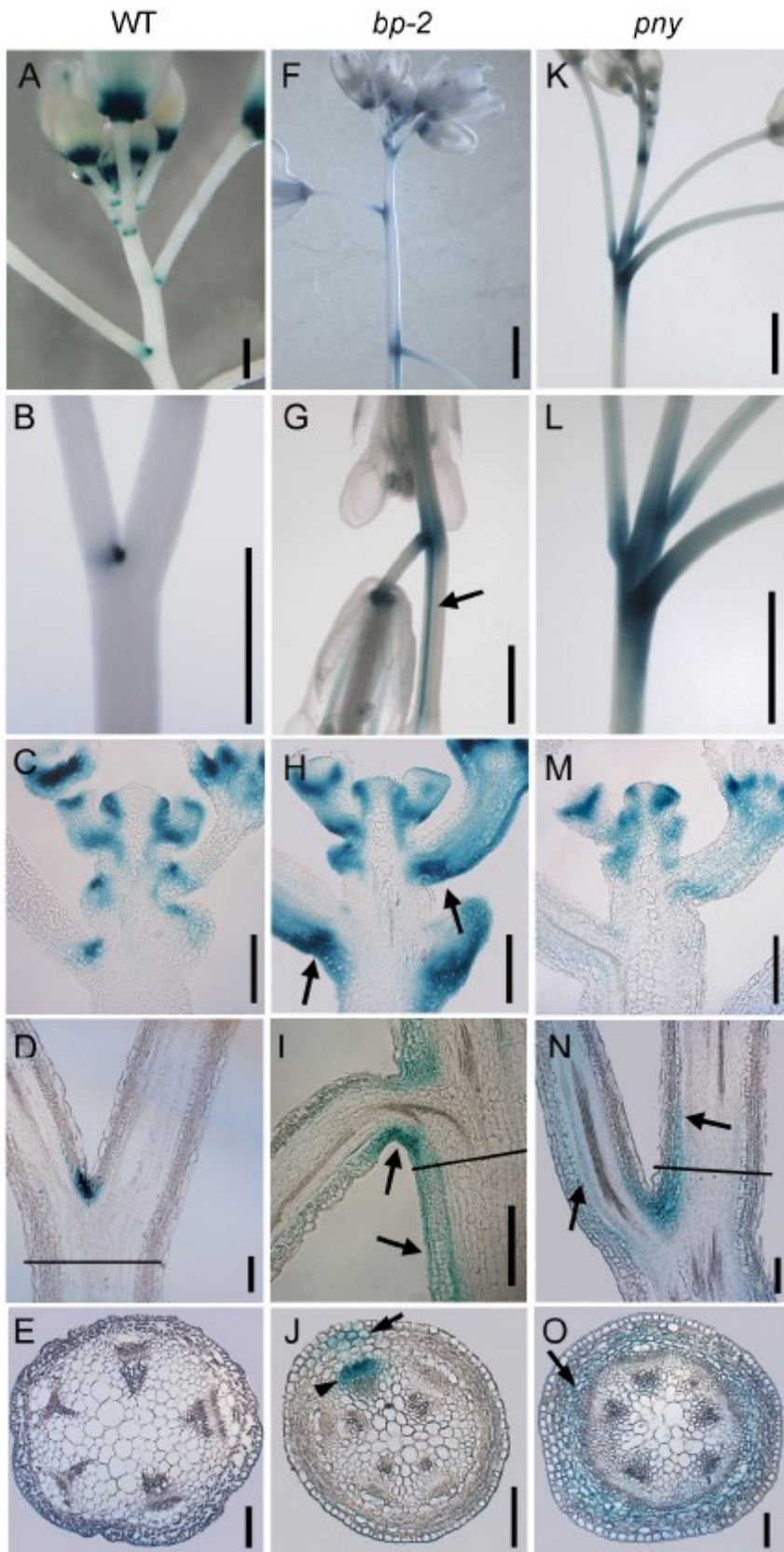


Figure 2.7 *KNAT6* expression in wild type, *bp-2*, *pny*, and *BOP* gain-of-function mutants

(A to D) *KNAT6:GUS* expression.

Inflorescences shown for:

(A) Wild type.

(B) *bp-2*.

(C) *pny*.

(D) *35S:BOP2*.

Expression localized to the pedicel axil in wild type (A) but upregulated in stems and pedicels of mutants (B to D).

(E to T) *KNAT6* mRNA detected using *in situ* hybridization.

Inflorescence apices shown for:

(E) Wild type.

(F) *bp-2*.

(G) *pny*.

(H) *bop1-6D*.

Transcript is correctly localized to the IM-floral meristem boundary except in *bop1-6D* (H) where expression is throughout the adaxial area of floral meristems.

Stem longitudinal sections shown for:

(I) Wild type.

(J) *bp-2*.

(K) *pny*.

(L) *bop1-6D*.

Transcript is upregulated in the cortex of mutant stems (J to L). In (K) and (L), the vascular cambium area shows strong expression.

Stem cross-sections shown for:

(M) Wild type.

(N) *bp-2*. Expression is strongest in the cortex and vascular bundles (arrowheads).

(O) *pny*. Irregular vascular bundles; vascular cambium area shows the strongest expression (arrowhead).

(P) *bop1-6D*; strong expression in vascular bundles (arrowhead).

Magnified stem cross-sections shown for:

(Q) Wild type.

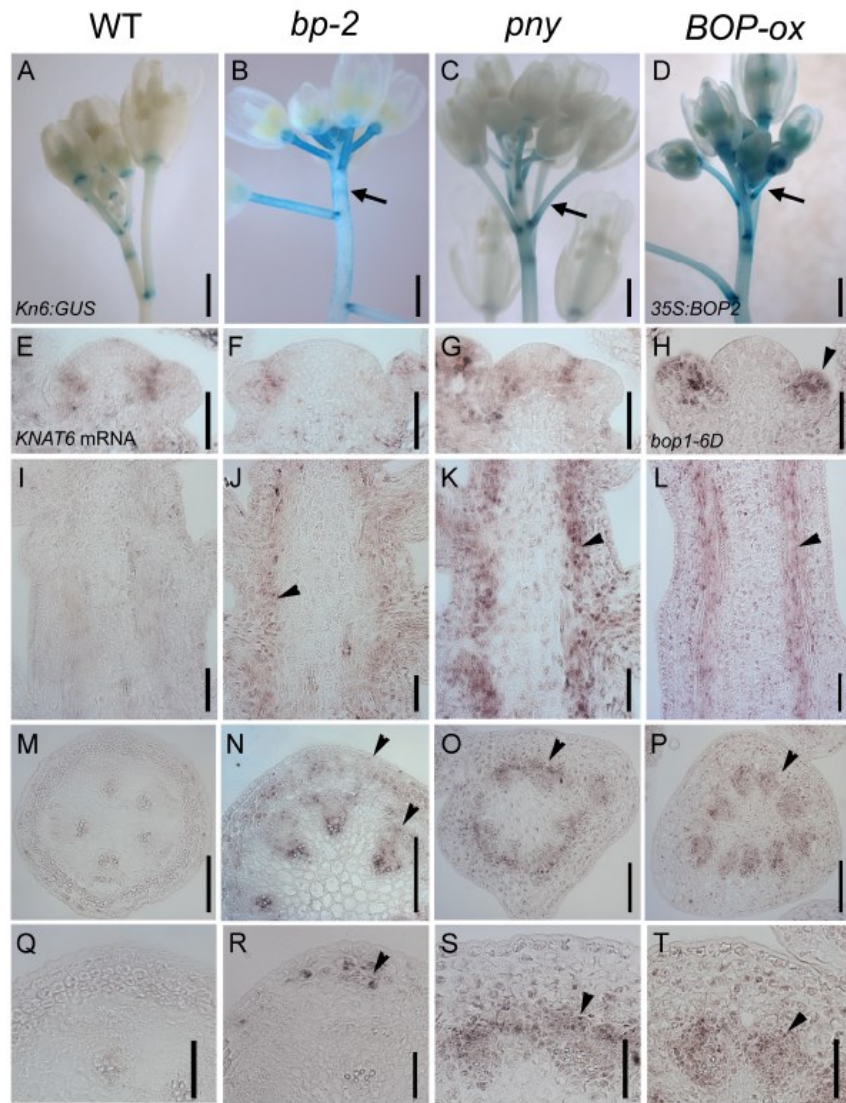
(R) *bp-2*. Stripe of expression in cortex below node (arrowhead).

(S) *ppy*; expression strongest in stripe of cells near vascular cambium (arrowhead).

(T) *bop1-6D*; expression in vascular bundles.

(U) qRT-PCR analysis of relative *KNAT6* transcript levels wild type and mutant internodes and pedicels. Asterisks, significantly different from wild type (Student's t-tests, $p < 0.0001$; except *ppy*, $p < 0.001$).

Scale bars, 50 mm except 0.5 mm for A to D and 100 mm for M to P.



U

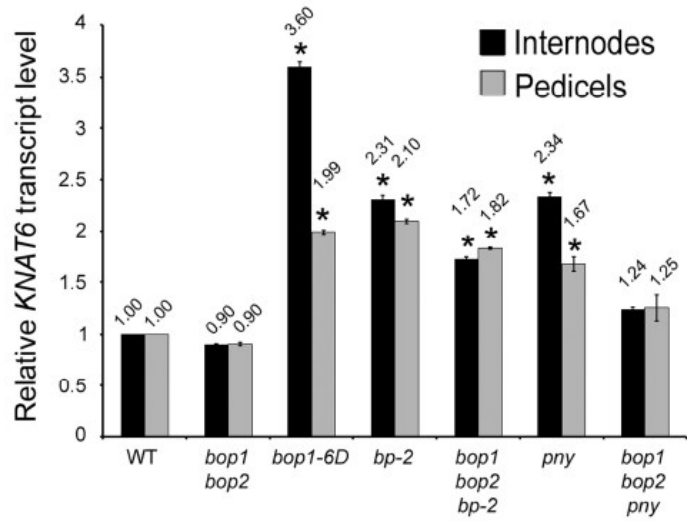


Figure 2.8 Inactivation of *KNAT6* rescues compact internodes caused by *BOP2* gain-of-function

Plants homozygous for a *35S:BOP2* transgene were crossed to wild type control plants or to plants homozygous for mutations in *knat2*, *knat6*, or *knat2 knat6*. The inflorescences of representative F1 plants are shown.

(A) *35S:BOP2/+ Col.*

(B) *35S:BOP2/+ knat2/+.*

(C) *35S:BOP2/+ knat6/+.*

(D) *35S:BOP2/+ knat2/+ knat6/+.*

(E) Quantitative analysis of inflorescence height in populations of F1 plants for the genotypes indicated.

Scale bars, 2 cm.

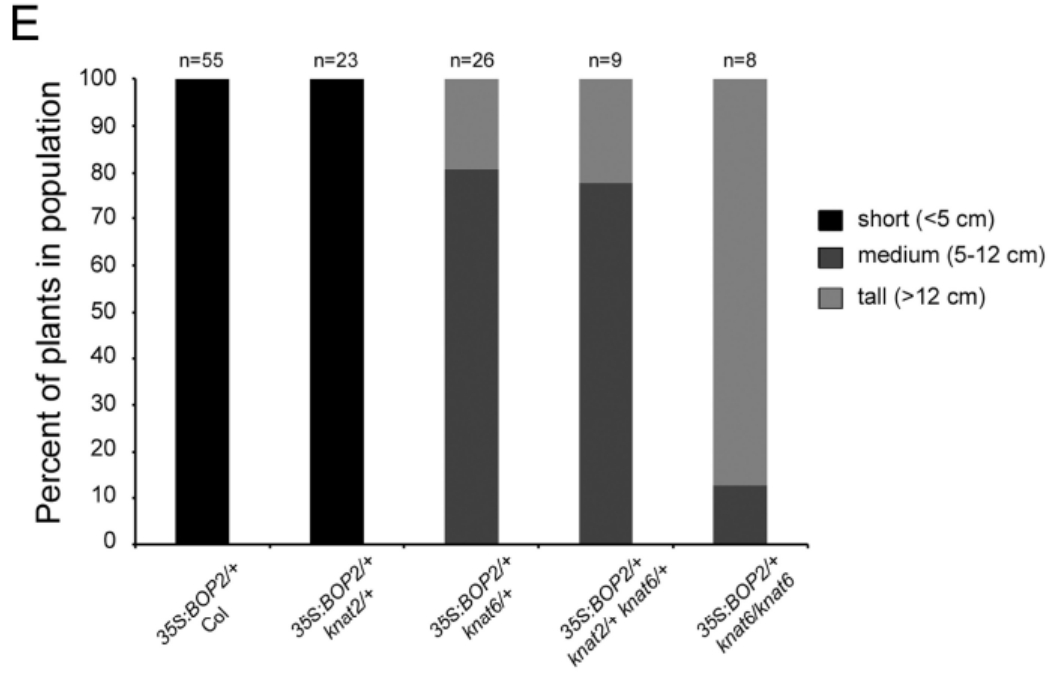
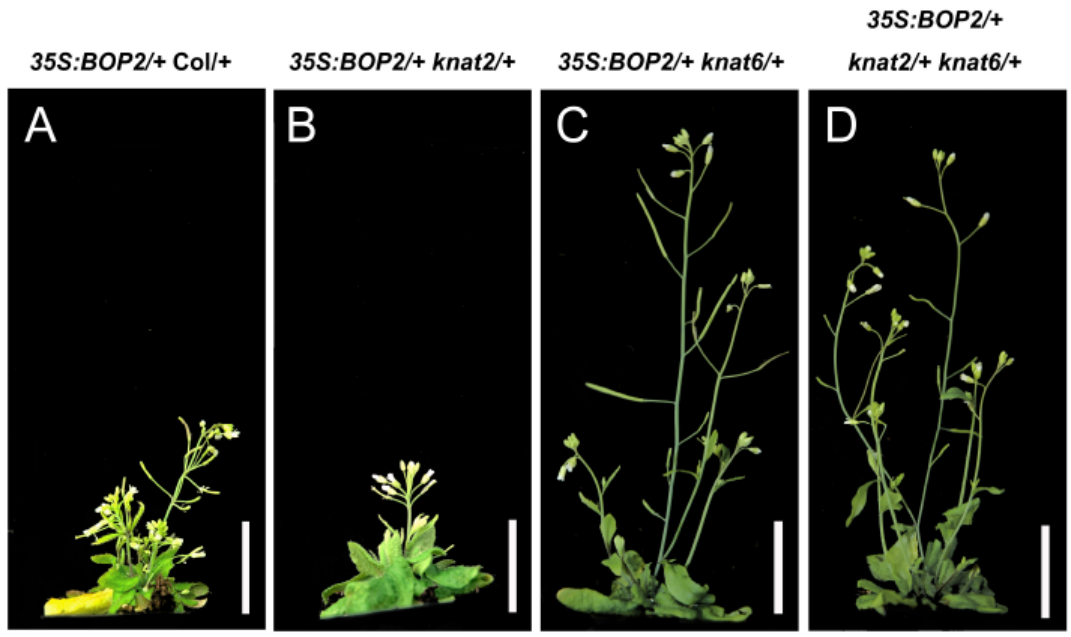


Figure 2.9 Lignification pattern and lignin biosynthesis gene expression in wild-type and mutant stems

(A to F) Cross sections from the base of fully elongated stems were stained with phloroglucinol-HCl to reveal lignin.

Representative sections are shown for:

(A) Wild type;

(B) *bop1 bop2*.

(C) *bp-2*; gaps in the vascular ring (arrows) are associated with stripes of ectopically lignified epidermal/cortical tissue. Arrowheads, Premature lignification of phloem fiber cells in primary vascular bundles.

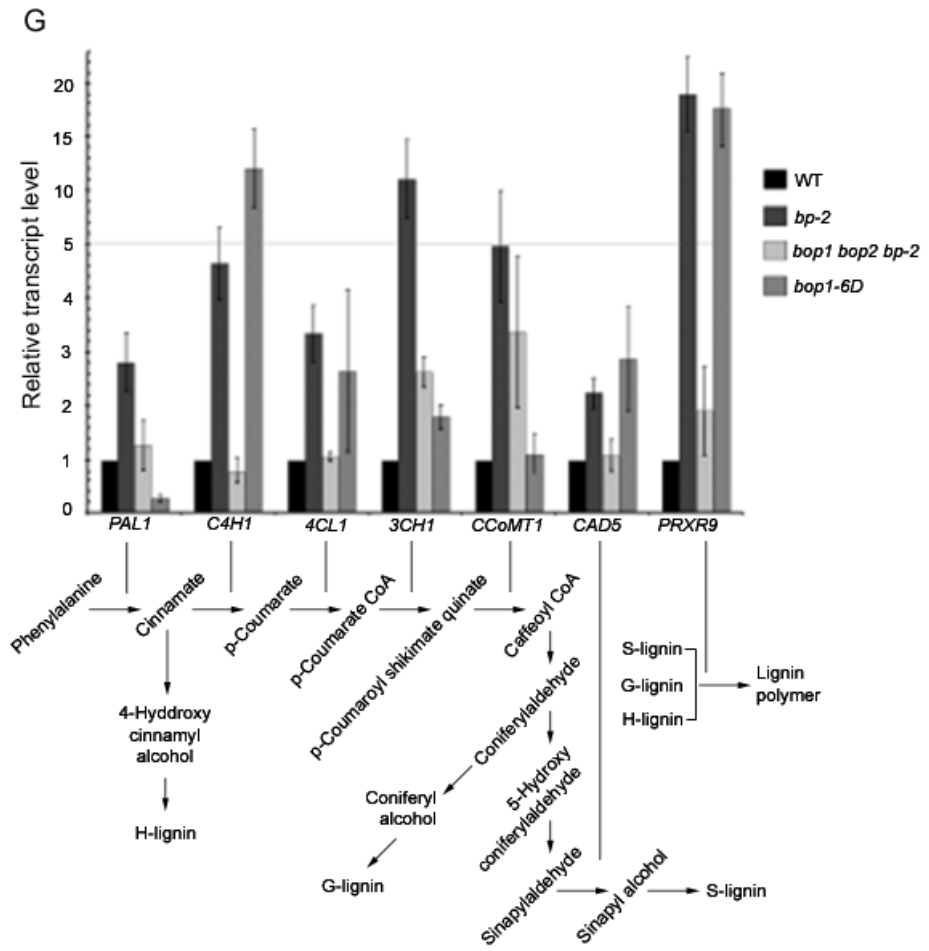
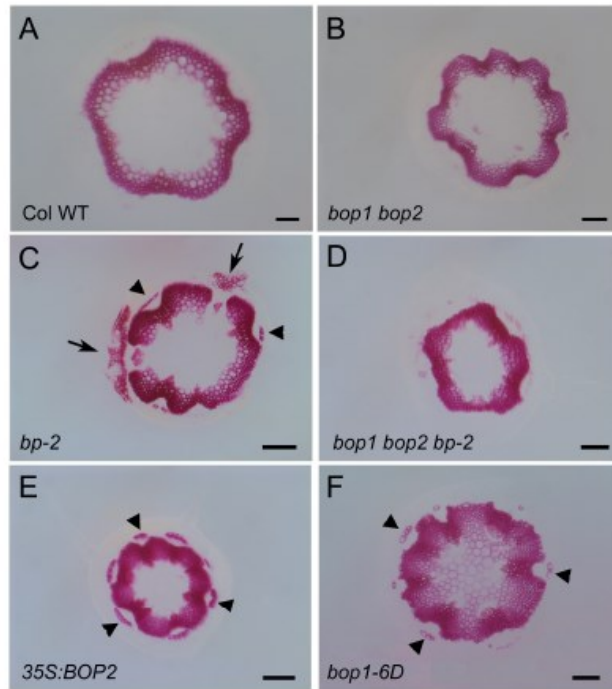
(D) *bop1 bop2 bp-2*; similar to wild type.

(E) *35S:BOP2*; dense vascular ring compared to wild type. Arrowheads, Premature lignification of phloem fiber cells, similar to *bp-2* mutants.

(F) *bop1-6D*; similar to *35S:BOP2* but pith is also lignified.

Scale bars, 100 μ m.

(G) qRT-PCR analysis of lignin biosynthesis genes in stem tissue (same stage as above). Error bars, SE of three biological replicates. Position of genes in the lignin biosynthetic pathway is depicted below (adapted from Mele et al., 2003; Zhou et al., 2009).



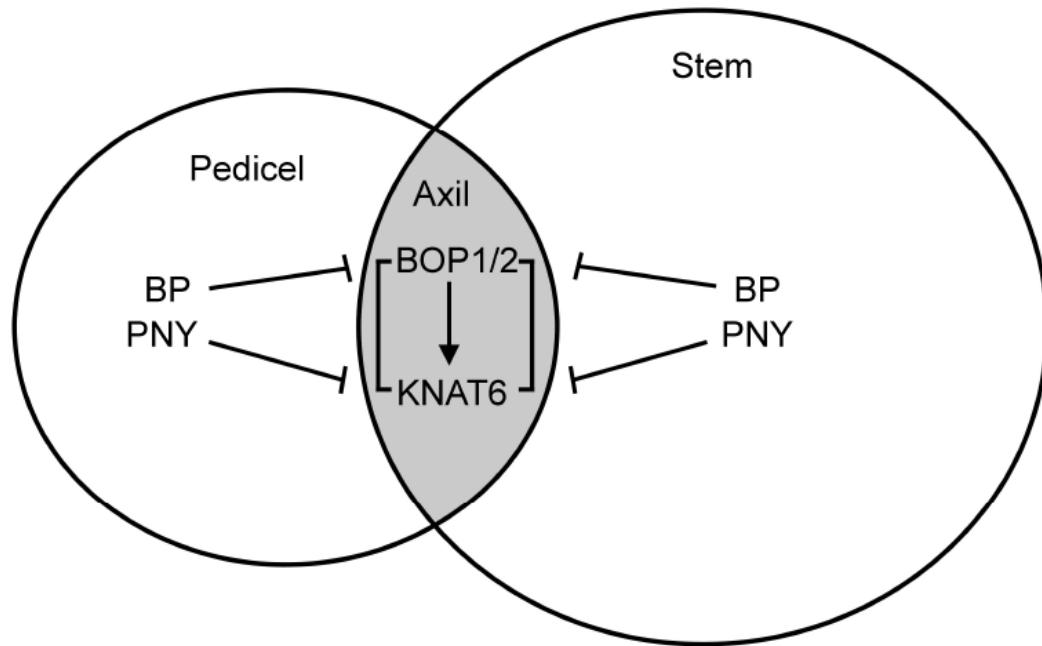


Figure 2.10 Summary of genetic interactions between BP-PNY, BOP1/2, and KNAT6 in the inflorescence

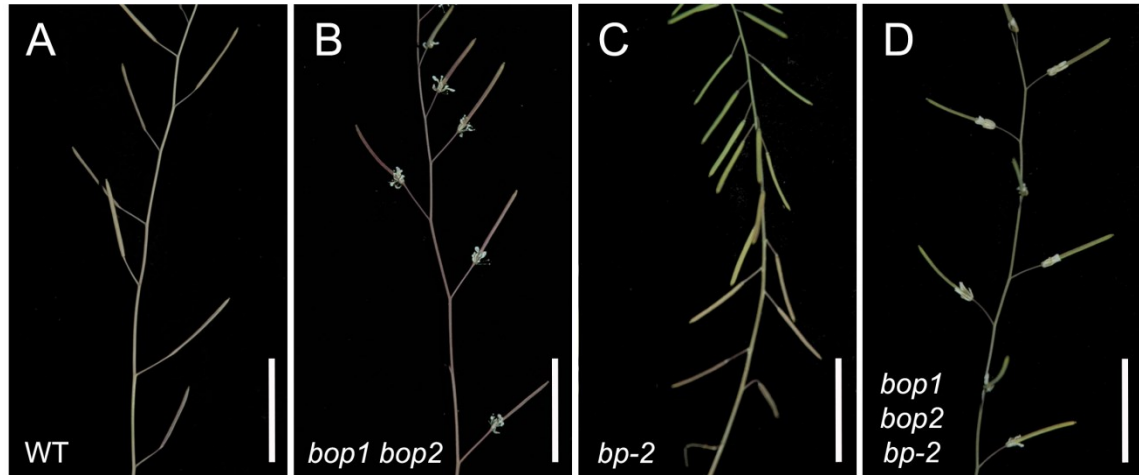
BP and PNY in the stem and pedicels are transcriptional repressors of *BOP1/2* and *KNAT6*, limiting their expression to the pedicel axil. *BOP1/2* gain-of-function mutants phenocopy *bp* and *pny* mutants because *BOP1/2* function downstream of BP-PNY in an antagonistic manner. *BOP1/2* are positive regulators of *KNAT6* expression that depend in part on *KNAT6* activity to exert changes in inflorescence architecture.

Table S2.1. List of general primers

Description	Primer	Sequence 5' – 3'	Reference
Genotyping			
<i>bop1-3</i>	4H Salk RP	CGTACCCTTTGATTTTAGTATGCTG	Hepworth et al. 2005
	4H Salk LP	GCACAATCTTTGACTTCATCACC	
<i>bop2-1</i>	5H Salk RP	CCCTTTTATAATCAGCATCAAGA	Hepworth et al. 2005
	5H Salk LP	TCGACGCCGAAGTAACGAGAG	
<i>bp-2</i>	bp-2dCAPs-F1	ACCCTCCTACAAGCTTACTTGGACTGCCA	Venglat et al. 2002
	bp-2dCAPs-R1	GGAGGCAGAGACAGACGGTGTGACCGCT	
<i>ppy-40126</i>	PNY Salk_40126 RP	TTGGAATTGGAGACAAAATGTGTTA	Smith and Hake, 2003
	PNY Salk_40126 LP	GGAACCAAGTTCAAACCTCGAATCCA	
<i>knat2-5</i>	KN2 Salk_099837 RP	CAAAAGGTGATCTCGCTGCTTTTCGT	Belles-Boix et al. 2006
	KN2 Salk_099837 LP	AATCTCTAGCGCAAAAGTTTTTGCT	
<i>knat6-2</i>	KN6 Salk_054482 F2	CTTACTTCAAGCTTACATCGATTGC	Belles-Boix et al. 2006
	KN6 Salk_054482 LP	TGCTTTCTGATCACTTCAAAAAGCCT	
Overexpression			
<i>35S:BOP1</i>	B1-1	AAAGGATCCGAAATCAACAAAGGAGCTATGAGC	Norberg et al. 2005
	B1-2	AAAGGATCCAAAAAGACCTAGAAATGGTGGTGG	
<i>35S:BOP2</i>	B2-1	TAGGGATCCTAGAGAATCCAAGAACCATGAA	Norberg et al. 2005
	B2-2	TAGGGATCCAGAGACCAATATAGA	
<i>tCUP4:BOP1</i>	EcoR1-BOP1-F1	ATCGAATTCATGAGCAATACTTTGGAAGAA	This study
	BOP1-RR	GCTGGATCCCTAGAAAT GGTGGTGGTGGT	This study
	EcoR1-tCUP-F1	ATCGAATTCATCTTCTGCAAGCATCTCTAT	
	EcoR1-tCUP-R2	ATCGAATT CCCGGTGGGTTTTGAGGT	
In situ			
<i>BP</i>	BP-LF	T7 polymerase binding site is <u>underlined</u> ATGGAAGAATACCAGCATGACAAC	This study
	BP-T7-RR	<u>CATAATACGACTCACTATAGGCCTTCTGACTC</u> AGAAGGATATG	
<i>KNAT6</i>	KNAT6-F3 (in situ)	ATGGATGGAATGTACAATTTCATTC	This study
	KNAT6-T7-R1	<u>CATAATACGACTCACTATAGGTCATTCCTCGGTA</u> AAGAATGAT	
qPCR			
<i>BP</i>	KNAT1-F1 HAY qPCR	CCATTCAGGAAGCAATGGAGTT	Hay et al. 2006
	KNAT1-R1 HAY qPCR	ACTTTCCCATCAGGATTGTTGA	
<i>KNAT6</i>	KNAT6- F2	CTTACTTCAAGCTTACATCGATTGC	This study
	KNAT6-R1	CGCAGTACGTTTCCATAAAATTCATC	
<i>PNY</i>	BLR-F1	TAATGTGGGTCGTGGGATTTACACC	This study
	BLR-R2	ACCTCTTGAAACCTCGTCGAGCAT	
<i>GAPC</i>	GAPC-P1	TCGACTCGAGAAAGCTGCTA	This study
	GAPC-P2	GATCAAGTCGACCACACGG	

Table S2.2. List of primers for qPCR analysis of lignin genes

Gene ID	Gene name	Primer	Sequence 5'-3'
At2g37040	<i>PAL1</i>	PAL1-L PAL1-R	AAGATTGGAGCTTTCGAGGA TCTGTTCCAAGCTCTCCCT
At2g30490	<i>C4H</i>	C4H-L C4H-R	ACTGGCTTCAAGTCGGAGAT ACACGACGTTTCTCGTTCTG
At1g51680	<i>4CL</i>	4CL1-L 4CL1-R	TCAACCCGGTGAGATTTGTA TCGTCATCGATCAATCCAAT
At2g40890	<i>C3H1</i>	C3H1-L C3H1-R	GTTGGACTTGACCGGATCTT ATTAGAGGCGTTGGAGGATG
At4g34050	<i>CCoMT1</i>	CCoMT1-L CCoMT1-R	CTCAGGGAAGTGACAGCAAA GTGGCGAGAAGAGAGTAGCC
At4g34230	<i>CAD5</i>	CAD5-L CAD5-R	TTGGCTGATTCGTTGGATTA ATCACTTCTCCCAAGCAT
At3g21770	<i>PRXR9GE</i>	PRXR9GE-F1 PRXR9-qPCR-R	CGCAAGAGCTGTCCAAACGCAGAG CCGTCACATCCCCTAACGAAGCAAT
At3g18780	<i>ACT2</i>	ACT2 F ACT2 R	GTTGGGATGAACCAGAAGGA GAACCACCGATCCAGACACT



Supplemental Figure 2.1 Phenotypic suppression of *bp-2* inflorescence defects by *bop1 bop2*

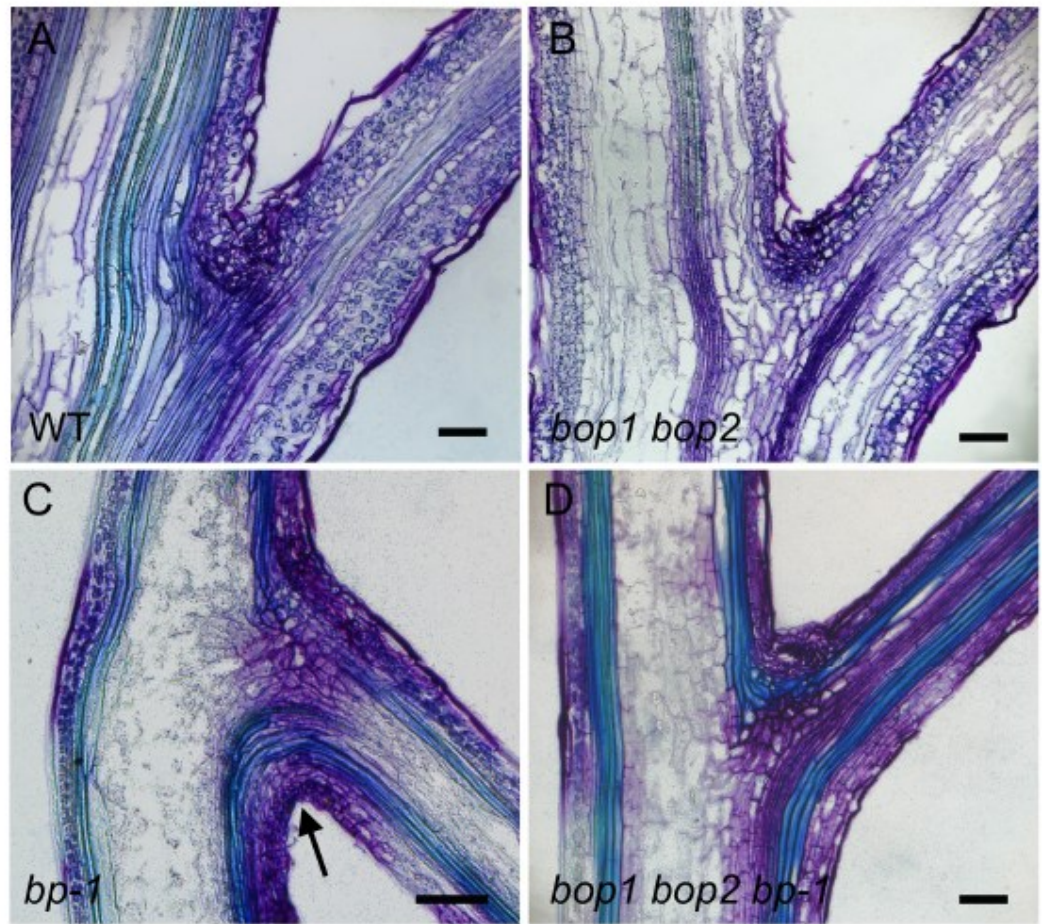
(A) Wild type control.

(B) *bop1 bop2* mutant.

(C) *bp-2* mutant with downward-pointing silicles.

(D) *bop1 bop2 bp-2* mutant; inactivation of *BOP1/2* partially rescues the *bp* phenotype.

Scale bars, 2 cm.



Supplemental Figure 2.2 Comparison of stem-pedicle junctions in wild type and mutants

Stem longitudinal sections were stained with toluidine blue.

(A) Wild type control.

(B) *bop1 bop2* mutant.

(C) *bp-1* mutant; growth restriction on the abaxial side bends the pedicle downward (arrow).

(D) *bop1 bop2 bp-1* mutant; similar to wild type.

Scale bars, 100 μ m.

Supplemental Figure 2.3 Loss-of-function *bop1 bop2* restore replum formation in *pny* mutants

SEM images showing the replum region of stage 17 fruits for the genotypes indicated.

Arrowheads denote the valve margins in:

(A) Wild type.

(B) *bop1 bop2* mutant.

(C) *pny* mutant; replum between valve margins is absent.

(D) *bop1 bop2 pny* mutant; replum is restored. Transverse sections of WT and mutant fruits showing the replum stained with phloroglucinol-HCl to detect lignin (pink colour).

Arrowheads denote the valve margins in:

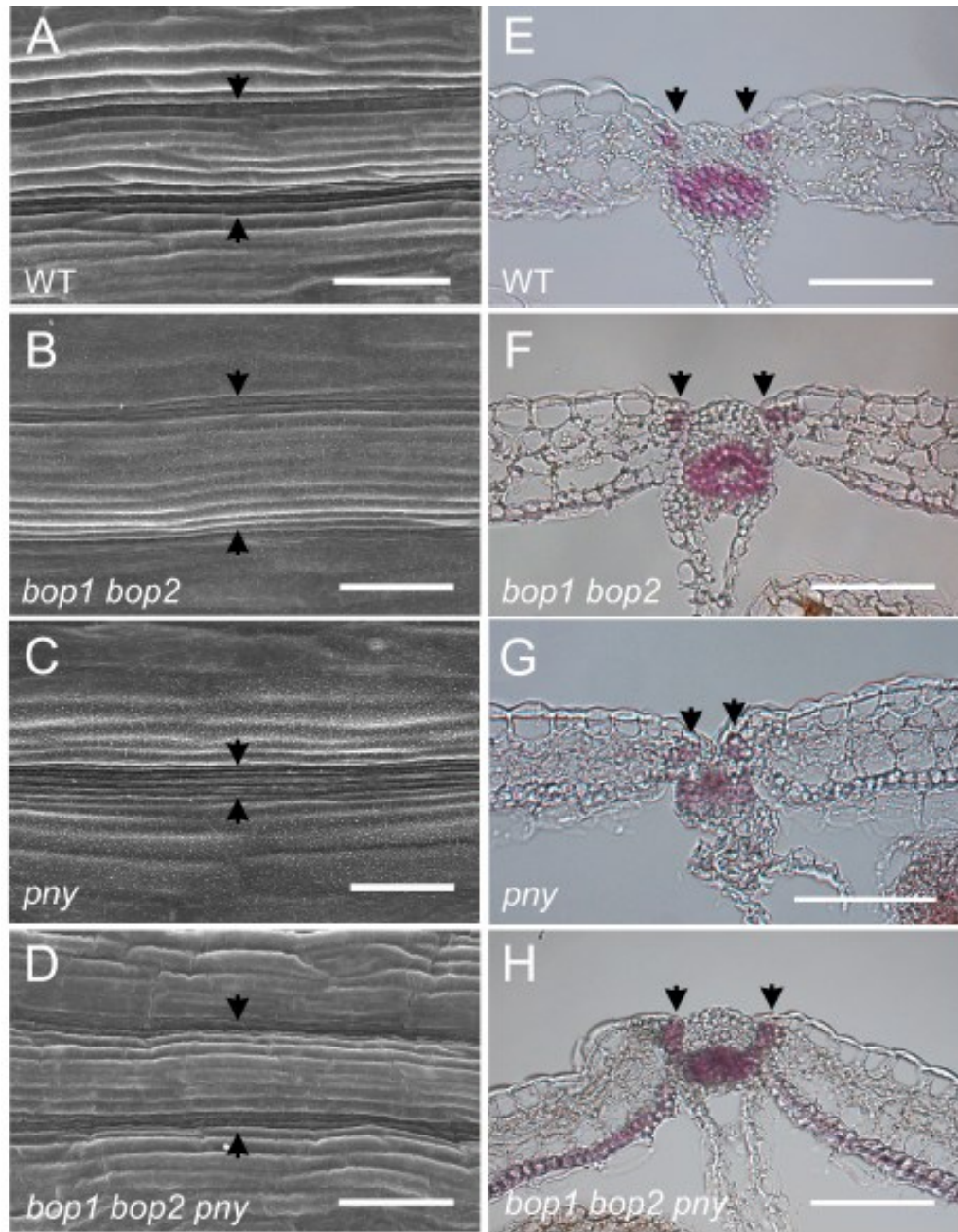
(E) Wild type.

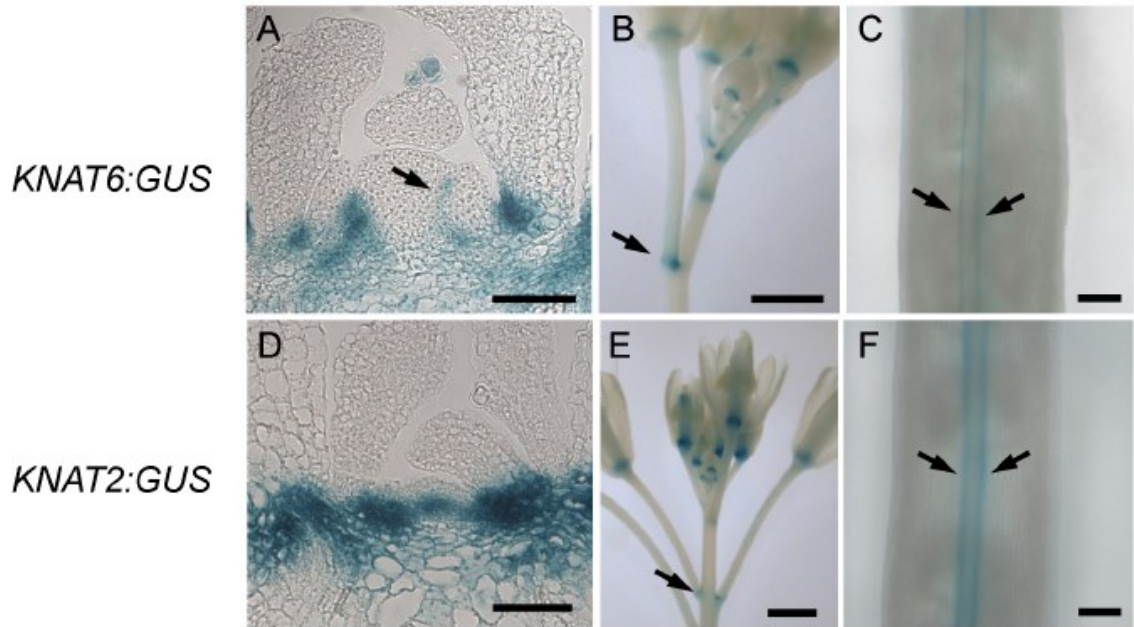
(F) *bop1 bop2* mutant.

(G) *pny* mutant; valve margins are closely spaced due to a diminished replum.

(H) *bop1 bop2 pny*; mutant; replum is restored.

Scale bars, 50 μm in A to D, 100 μm in E to H.





Supplemental Figure 2.4 *KNAT6:GUS* and *KNAT2:GUS* expression patterns in WT plants

KNAT6:GUS expression is shown in:

(A) Vegetative apex of short-day grown seedling; arrow denotes boundary between stage 2 leaf and the SAM.

(B) Inflorescence; arrow denotes expression in the stem-pedicel axil.

(C) Fruit; arrows denote valve margins.

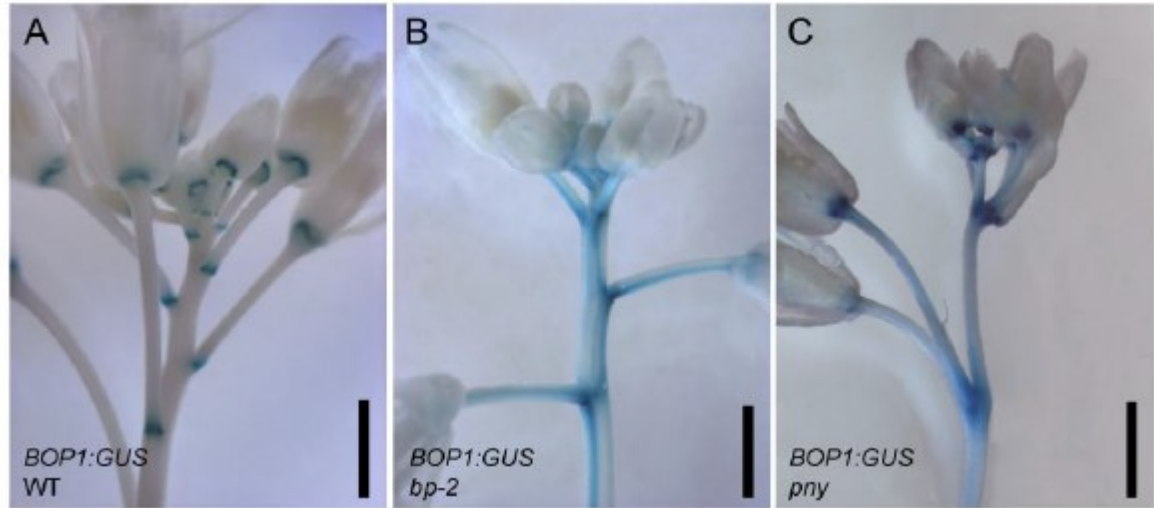
KNAT2:GUS expression is shown in

(D) Vegetative apex of short-day grown seedlings; expression is in the meristem rib zone and at the base of leaves.

(E) Inflorescence, arrow denotes expression in the stem-pedicel axil.

(F) Fruits, arrows denote valve margins.

Scale bars, 0.5 mm; except 50 μ m in A and D.



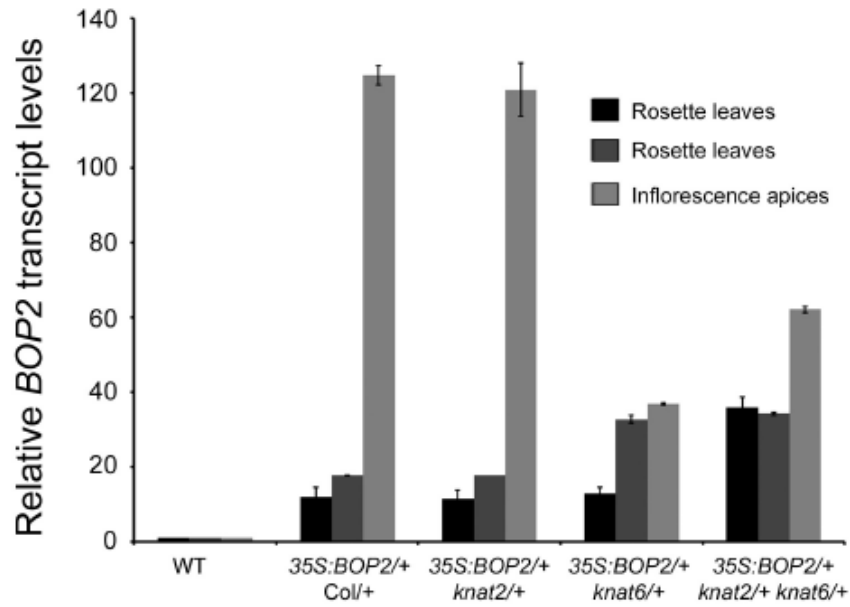
Supplemental Figure 2.5 *BOP1:GUS* expression pattern in WT, *bp-2*, and *pny* inflorescences

(A) Wild type control.

(B) *bp-2* mutant.

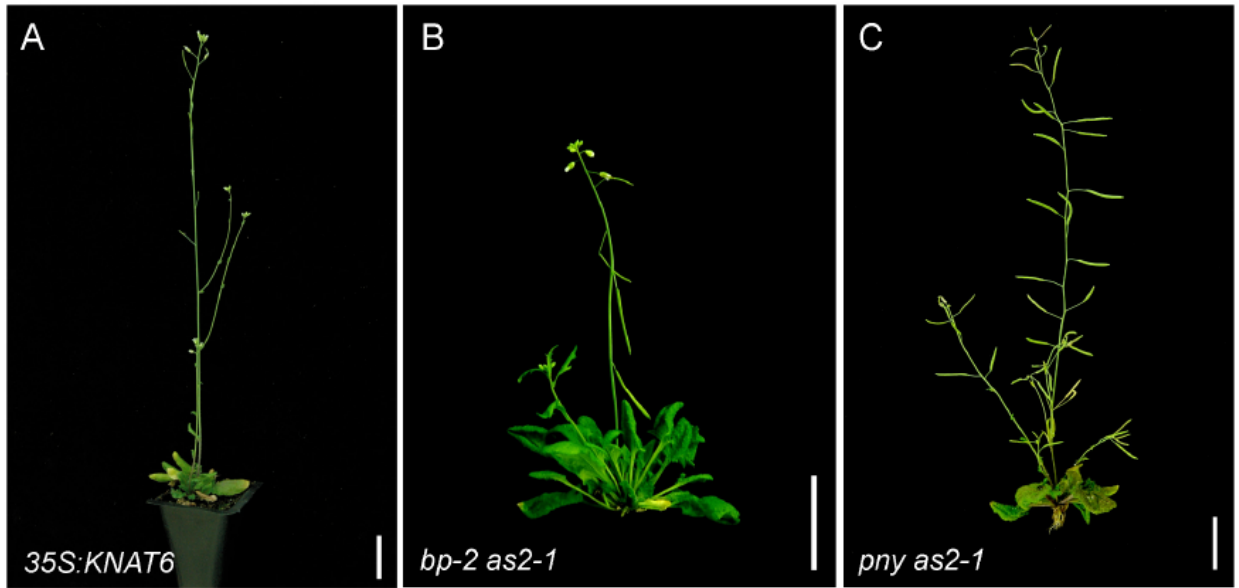
(C) *pny* mutant.

Scale bars, 1 mm.



Supplemental Figure 2.6 Quantitative analysis of *BOP2* transcript in *35S:BOP2* lines crossed to wild type and mutants

Tissue was from leaves or inflorescence apices harvested from a pool of 5-8 plants for the genotypes indicated. All pools containing the *35S:BOP2* transgene contain dramatically higher levels of *BOP2* transcript relative to wild type control plants.



Supplemental Figure 2.7 Inflorescence phenotype of *35S:KNAT6* transgenic plants and the double mutants *bp as2-1* and *pny as2-1*

Representative plants are shown for:

(A) *35S:KNAT6*. No effect on internode elongation.

(B) *bp-2 as2-1*.

(C) *pny as2-1*. Loss-of-function *as2* fails to rescue *bp* and *pny* inflorescence defects.

Scale bars, 2 cm.

Supplemental Figure 2.8 Comparison of *BP* and *PNY* expression levels in wild type, *bop1 bop2*, and *bop1-6D* in primary stems

BP transcript monitored by *in situ* hybridization in:

(A) Wild type.

(B) *bop1 bop2*.

(C) *bop1-6D*. *BP* transcript accumulation is similar in all three genotypes.

PNY:GUS expression is shown in:

(D) Wild type.

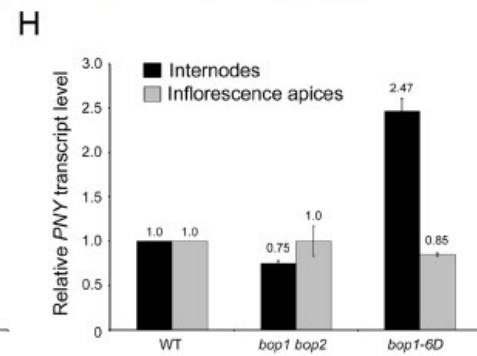
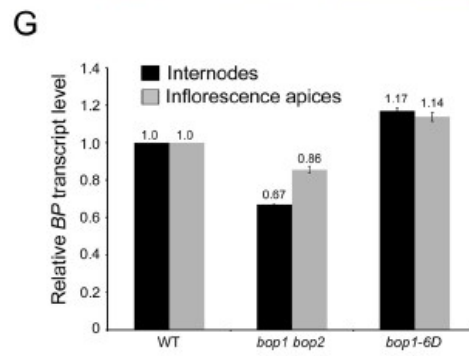
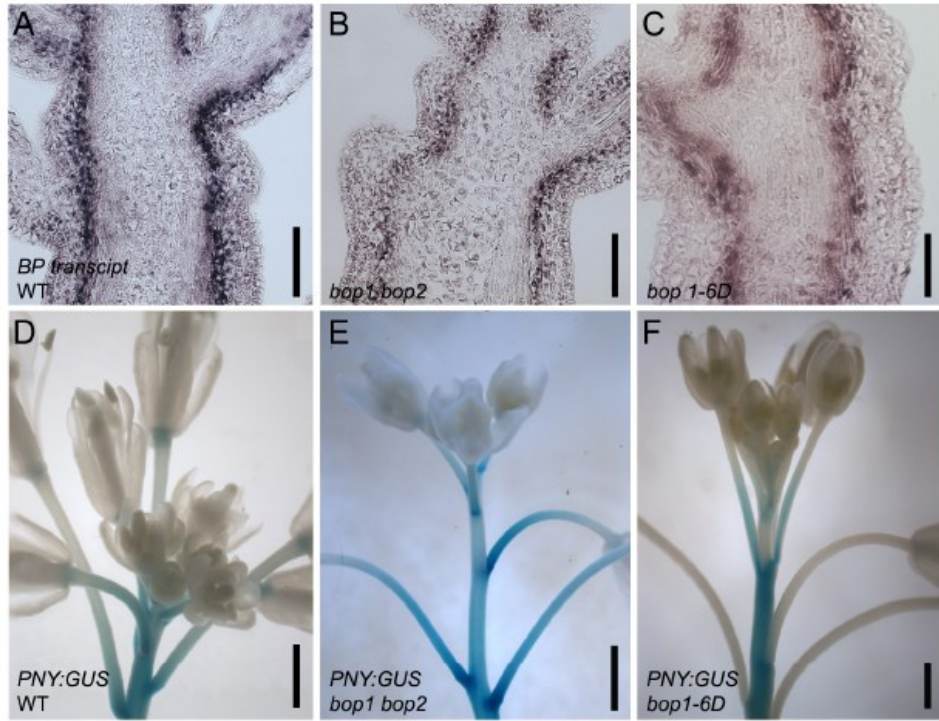
(E) *bop1 bop2*.

(F) *bop1-6D*. *PNY:GUS* expression is similar in all three genotypes.

(F) Quantitative analysis of relative *BP* transcript levels in wild type, *bop1 bop2*, and *bop1-6D* internodes and apices. *BP* transcript levels are similar in all three genotypes.

(G) Quantitative analysis of relative *PNY* transcript levels in wild type, *bop1 bop2*, and *bop1-6D* internodes and apices. *PNY* transcript levels are similar in all three genotypes except higher in *bop1-6D* apices.

Error bars, SE. Scale bars, 50 μ m in A to C; 1 mm in D to F.



Supplemental Figure 2.9 Analysis of stem lignification pattern in WT and mutants with *pny*

Mature internodes from between the 3rd and 4th silique on the primary stem were embedded in paraffin and sectioned using a microtome (as described by Smith and Hake, 2003). Panels on the left were stained with toluidine blue; primary and secondary cell walls stain dark blue. Panels on the right were stained with phloroglucinol-HCl; lignin stains pink.

(A-B) Wild type.

(C-D) *bop1 bop2* mutant.

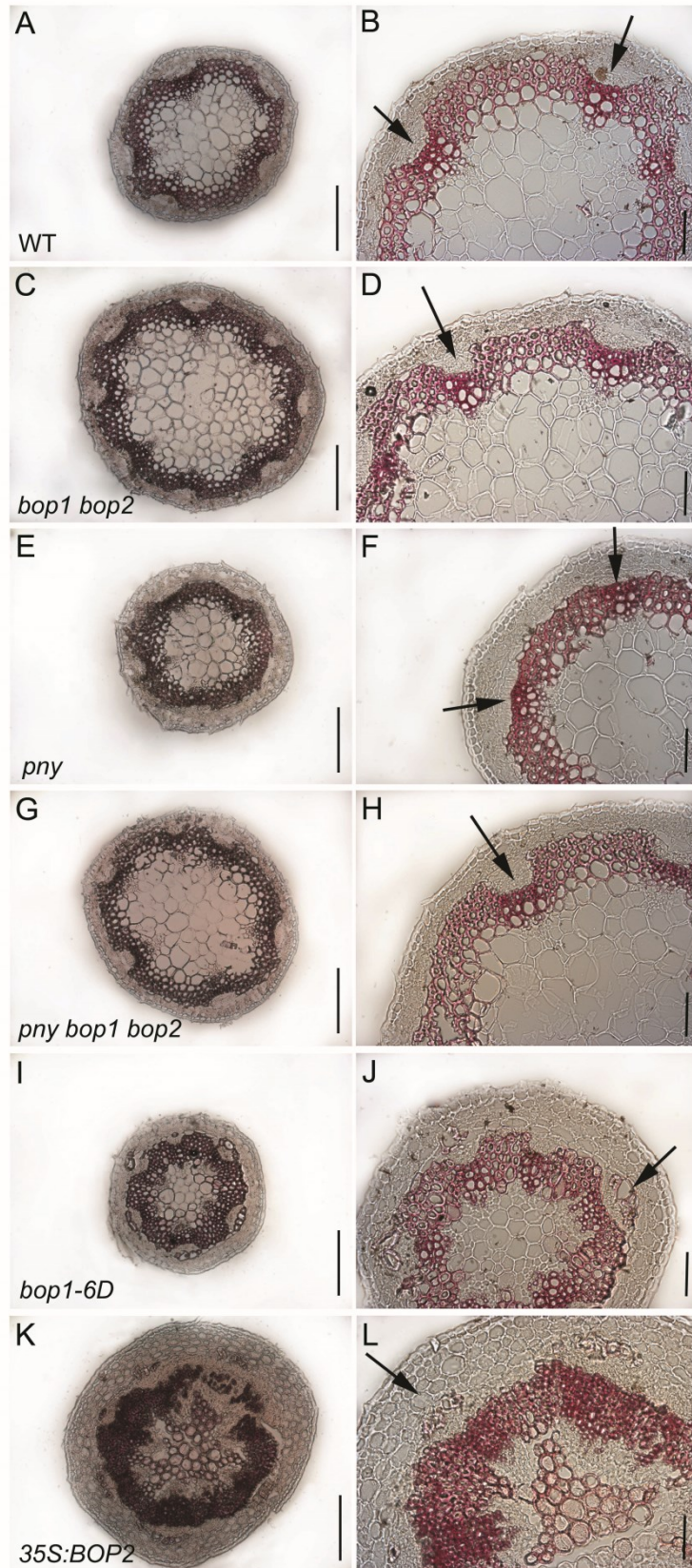
(E-F) *pny* mutant; a continuous vascular ring with little interfascicular space.

(G-H) *bop1 bop2 pny* mutant; similar to wild type and *bop1 bop2*.

(I-J) *bop1-6D*; a continuous vascular ring similar to *pny*. Lignification of phloem fibres is advanced.

(K-L) *35S:BOP2*; extensive secondary growth has occurred. Lignification of phloem fibres is advanced; pith is ectopically lignified. Arrows, primary vascular bundles.

Scale bars, 0.25 mm (left panels); 100 μ m (right panels).



CHAPTER 3

BLADE-ON-PETIOLE1* and *2* regulate *Arabidopsis* inflorescence architecture in conjunction with homeobox genes *KNAT6* and *ATH1

This chapter is presented essentially as published in Khan et al. (2012) *Plant Signaling and Behavior* **7**: 788-92.

Madiha Khan, Paul Tabb, and Shelley R. Hepworth

3.1 Abstract

Inflorescence architecture varies widely among flowering plants, serving to optimize the display of flowers for reproductive success. In *Arabidopsis* (*Arabidopsis thaliana*), internode elongation begins at the floral transition, generating a regular spiral arrangement of upwardly-oriented flowers on the primary stem. Post-elongation, differentiation of lignified interfascicular fibers in the stem provides mechanical support. Correct inflorescence patterning requires two interacting homeodomain transcription factors: the KNOTTED1-like protein BREVIPEDICELLUS (BP) and its BEL1-like interaction partner PENNYWISE (PNY). Mutations in *BP* and *PNY* cause short internodes, irregular spacing and/or orientation of lateral organs, and altered lignin deposition in stems. Recently, we showed that these defects are caused by the misexpression of lateral organ boundary genes, *BLADE-ON-PETIOLE1* (*BOP1*) and *BOP2*, which function downstream of BP-PNY in an antagonistic fashion. *BOP1/2* gain-of-function in stems promotes expression of the boundary gene *KNOTTED1-LIKE FROM ARABIDOPSIS THALIANA6* (*KNAT6*) and shown here, *ARABIDOPSIS THALIANA HOMEBOX GENE1* (*ATH1*), providing *KNAT6* with a BEL1-like co-factor. Our further analyses show that defects caused by *BOP1/2* gain-of-function require both *KNAT6* and *ATH1*. These data reveal how *BOP1/2*-dependent activation of a boundary module in stems exerts changes in inflorescence architecture.

3.2 Introduction

Inflorescence architecture is remarkably diverse between plant species, serving to optimize the arrangement of flowers for successful pollination and seed set (Robert Wyatt, 1982). Timing, length, and pattern of internode elongation together with pedicel angle are key parameters in the organization of lateral branches and flowers on the primary stem. In the model plant, *Arabidopsis* (*Arabidopsis thaliana*), elongation of internodes begins at the transition to flowering and is associated with proliferation of cells in the rib meristem (Steeves and Sussex, 1989; Vaughan, 1954). Post-elongation, internodes are fortified through the differentiation of interfascicular fibers with secondary cell walls (Nieminen et al., 2004; Ehling et al., 2005).

Two three-amino-acid loop-extension (TALE) homeodomain transcription factors: the class I KNOTTED1-like homeodomain (KNOX) protein BREVIPEDICELLUS (BP) and its interaction partner, the BEL1-like (BELL) protein PENNYWISE (PNY) play significant roles in meristem maintenance and internode patterning (Douglas et al., 2002; Venglat et al., 2002; Bryne et al., 2003; Smith and Hake, 2003; Bhatt et al., 2004; Rutjens et al., 2009). Mutations in *BP* cause short internodes, downward-pointing pedicels, and reduced apical dominance whereas mutations in *PNY* cause altered phyllotaxy and irregular internode elongation leading to clusters of flowers on the primary stem, and reduced apical dominance (Douglas et al., 2002; Venglat et al., 2002; Byrne et al., 2003; Smith and Hake, 2003). Both mutants exhibit changes in vascular patterning, indicated by altered lignin deposition in stems (Douglas et al., 2002; Venglat et al., 2002; Mele et al., 2003). Stem patterning defects in *bp pny* double mutants are enhanced, indicating that BP and PNY play related but distinct roles in internode development (Smith and Hake,

2003). For example, whereas BP is a negative regulator of lignin biosynthetic genes required for differentiation of interfascicular fibers, PNY promotes internode elongation and lateral organ initiation by spatially regulating the expression of *PECTIN METHYLESTERASE5*, which is associated with loosening of the plant cell wall (Mele et al., 2003; Paucelle et al., 2011; Khan et al., 2012b).

In a recent paper, we showed that *bp* and *pnv* inflorescence defects are caused by stem and pedicel misexpression of the lateral organ boundary genes *BLADE-ON-PETIOLE1* (*BOP1*) and *BOP2* (Khan et al., 2012b). *BOP1/2* encode BTB/POZ and ankyrin domain containing transcriptional co-activators with redundant functions (Hepworth et al., 2005; Jun et al., 2010). Loss-of-function *bop1 bop2* rescues *bp* and *pnv* inflorescence defects and *BOP1/2* gain-of-function mimics *bp* and *pnv* inflorescence defects. We showed that *BOP1/2* function downstream of BP-PNY in an antagonistic manner, acting as positive regulators of the KNOX boundary gene *KNAT6*, whose ectopic activity is required, but not sufficient, to induce changes in inflorescence architecture. We speculated that *KNAT6* requires a co-factor, provided directly or indirectly by *BOP1/2*, to exert its activity (Khan et al., 2012b).

We show here that *BOP1/2* activity induces expression of the BELL homeobox gene *ARABIDOPSIS THALIANA HOMEBOX GENE1* (*ATH1*), whose transcripts are likewise upregulated in *bp* and *pnv* internodes contributing to defects in pedicel orientation and internode patterning. *KNAT6* forms a heterodimer with *ATH1* (Rutjens et al., 2009; Li et al., 2012). Collectively, our work shows that both products are required by *BOP1/2* to exert changes in inflorescence architecture. Thus, *BOP1/2* gain-of-function in stems may promote the formation of a *KNAT6-ATH1* complex that antagonizes BP-PNY

activity. Our findings shed light on how interplay between KNOX-BELL complexes associated with meristem and boundary compartments governs inflorescence architecture in a model plant species.

3.3 Results and discussion

3.3.1 BOP1/2 promote *ATH1* expression

The BELL homeobox gene *ATH1* is strongly expressed in vegetative apices prior to the floral transition where its product heterodimerizes with class I KNOX proteins (SHOOTMERISTEMLESS and BP) to promote maintenance of the vegetative meristem (Gómez-Mena et al., 2008; Rutjens et al., 2009; Li et al., 2012). *ATH1* is also expressed in basal and lateral organ boundaries where its activity inhibits growth and controls patterning (Gómez-Mena et al., 2008; Rutjens et al., 2009). *35S:ATH1* plants have short internodes similar to *35S:BOP2* plants, (Gómez-Mena et al., 2008; Rutjens et al., 2009) prompting us to test if BOP1/2 induce *ATH1* expression to exert changes in inflorescence architecture. Analysis of *ATH1* transcript using quantitative RT-PCR (qRT-PCR) in wild-type (WT) and mutant internodes showed a significant increase in *bp-2* (10.6-fold) and *ppy-40126* (89.7-fold) internodes relative to WT control plants suggesting that BP and PNY repress *ATH1* expression (Fig. 3.1). Transcripts were also elevated in BOP1/2 gain-of-function lines, *35S:BOP2* and *bop1-6D* (20.1-fold and 24.3-fold, respectively), suggesting that BOP1/2 induce *ATH1* expression. Thus, BP and PNY are transcriptional repressors of several boundary genes, including *BOP1/2*, (Khan et al., 2012b) *KNAT6*, (Ragni et al., 2008) and *ATH1*, whose products define a potentially linear genetic pathway.

3.3.2 Inactivation of *ATH1* rescues *pny* and partially rescues *bp* inflorescence defects

To determine if *ATH1* misexpression in *bp* and *pny* internodes exerts changes in inflorescence patterning along with *BOP1/2* and *KNAT6*, we tested if inactivation of *ATH1* suppresses *bp* and/or *pny* mutant phenotypes (Ragni et al., 2008; Khan et al., 2012b). Double mutants *bp-2 ath1-3* and *pny-40126 ath1-3* were generated by crossing and the resulting inflorescence phenotypes were examined (Fig. 3.2). Inactivation of *ATH1* dramatically rescued *pny* inflorescence defects but rescue of *bp* defects was less obvious (Fig. 3.2A-F; see also Li et al., 2012). To better assess *ath1-3* rescue of *pny* inflorescence defects, we performed quantitative phenotypic analyses on 20 plants per genotype. Average plant height, rosette paraclade number, and internode lengths in *ath1-3 pny* double mutants were similar to WT control plants (Fig. 3.2G-I) as seen for *bop1 bop2* and *knat2 knat6* rescue of *pny* defects (Ragni et al., 2008; Khan et al., 2012b). The *ath1-3* mutation also suppressed *pny-57747* (see Smith and Hake, 2003) silique clustering defects (data not shown; similar to Rutjens et al., 2009). Measurement of pedicel angles showed that inactivation of *ATH1* partially rescues *bp* pedicel orientation, but less efficiently than inactivation of *KNAT6* (Fig. 3.2J; Ragni et al., 2008). Thus, misexpression of *ATH1* contributes unequally to *bp* and *pny* defects. This complexity is unsurprising. First, *ATH1* transcripts accumulate to higher levels in *pny* vs. *bp* internodes (Fig. 3.1). Second, *ATH1* has the potential to form functionally distinct complexes with several KNOX proteins, including BP, *KNAT2* and *KNAT6*, whose transcripts are differentially expressed in *bp* and *pny* stems (Ragni et al., 2008; Rutjens et al., 2009; Li et al., 2012). Overall, the data show that inactivation of *ATH1* suppresses *bp-2* and *pny* inflorescence defects, similar to inactivation of *BOP1/2* (Khan et al., 2012b) and *KNAT6*

(Ragni et al., 2008). These data support the model that BOP1/2 function in conjunction with KNAT6 and ATH1 to antagonize BP and PNY activities.

3.3.3 BOP1/2 require ATH1 activity to exert changes in inflorescence architecture

To test if misexpression of *ATH1* contributes to restricted internode elongation in *35S:BOP2* transgenic plants, we examined the effect of *ath1-3* loss-of-function on the phenotype of a strong *35S:BOP2* line with short compact internodes (Khan et al., 2012b). Plants homozygous for a *35S:BOP2* transgene (see Norberg et al., 2005) were crossed to WT control plants or *ath1-3* homozygous mutants. The phenotypes of F1 progeny were examined, revealing that partial *ath1-3* loss-of-function (*ath1-3/+*) was sufficient to restore internode elongation in *35S:BOP2* plants (Fig. 3.3). The average height of *35S:BOP2/+ Col/+* control plants was 3.33 ± 0.23 cm vs. 19.14 ± 0.72 cm for *35S:BOP2/+ ath1-3/+* plants (n = 24). Thus, BOP1/2 require both KNAT6 (Khan et al., 2012b) and ATH1 to exert changes in inflorescence architecture.

3.3.4 Roles for KNAT6 and ATH1 in secondary stem development

Post-elongation, differentiation of vessel and fiber cells with secondary thickened cell walls strengthens the stem (Nieminen et al., 2004; Ehling et al., 2005). In *bp-2* mutants, the vascular ring contains gaps where lignin is abnormally deposited in the epidermal and cortical layers, and phloem fibers overlying the primary vascular bundles are prematurely lignified (Fig. 3.4A and B; see Mele et al., 2003; Khan et al., 2012b). Loss-of-function *bop1 bop2* partially rescues *bp* lignin defects, resulting in a pattern more similar to WT (Khan et al., 2012b). To test if KNAT6 and ATH1 contribute to *bp-2* lignin defects caused by *BOP1/2* misexpression, cross-sections were cut from the base of fully

elongated stems and stained with phloroglucinol-HCl (Fig. 3.4). While *knat2* mutation alone had no significant effect on *bp-2* stem patterning (Fig. 3.4, A-C), *ath1-3* and *knat6* mutations partially rescued *bp-2* defects by closing the gaps in the vascular ring, but evidence of epidermal lignification remained (Fig. 3.4, A, B, D and E). Loss-of-function *knat6* together with *knat2* significantly rescued *bp-2* stem patterning defects, similar to that seen in *bop1 bop2 bp-2* triple mutants (Fig. 3.4, A, B and F; see Khan et al., 2012b). These data confirm that both KNAT6 and ATH1 contribute to lignin defects in *bp-2* stems, which are caused by BOP1/2 gain-of-function.

3.3.5 BOP1/2 are positive regulators of a KNAT6-ATH1 boundary module

Internode elongation in many flowering plant species begins at the transition to flowering as a result of increased rib meristem activity in response to floral inductive signals (Vaughan, 1955; Bernier, 1988; Steeves and Sussex, 1989) Our data support the model that BP and PNY promote internode elongation by inhibiting expression of the lateral organ boundary genes, *BOP1/2*, *ATH1* and *KNAT6* in stems (see also Ragni et al., 2008). *BOP1/2* in stems induces the expression of *KNAT6* (Khan et al., 2012b) and its potential co-factor *ATH1*, permitting the formation of a complex that potentially antagonizes BP and PNY activities (Fig. 3.5; see also Rutjens et al., 2009; Li et al., 2012). While it is yet unclear if *BOP1/2* are direct transcriptional regulators of *KNAT6* or *ATH1*, these genes are likely to form a module whose functional interactions are conserved in development, at the meristem-leaf boundary during vegetative development, at floral abscission zones, and at the valve margin-replum interface in developing fruits (Rast and Simon, 2008; Girin et al., 2009; Shi et al., 2011). Future experiments will address these issues.

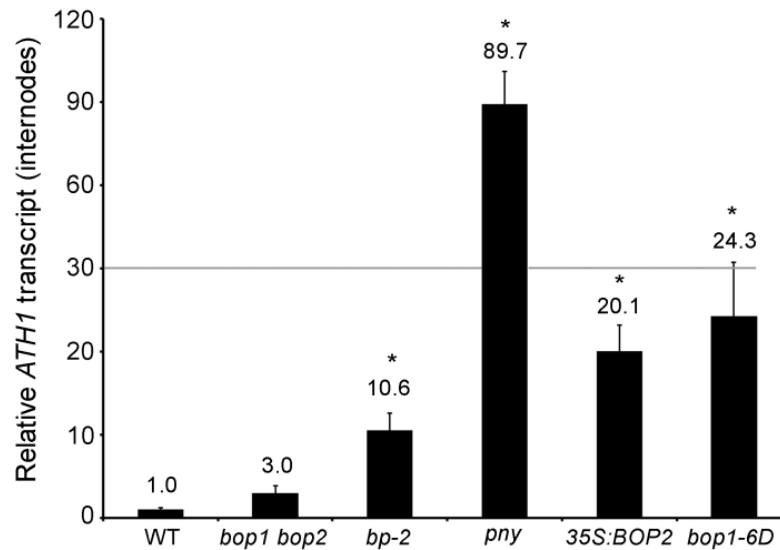


Figure 3.1 qRT-PCR analysis of relative *ATH1* transcript levels in internodes of WT, *bp-2*, *pny*, and BOP1/2 gain-of-function lines: *35S:BOP2* and *bop1-6D*

Plant lines, growth conditions, and experimental conditions were as previously described (Khan et al., 2012b). WT was the Columbia-0 (Col-0) ecotype of *Arabidopsis*. Gene-specific primers for *ATH1* were: *ATH1*-qPCR-F1 (5'-ATACTCGCTCGATTATTCATCTCGA) and *ATH*-R1 (5'-ATCGATCATCCAACCATTGGAAGAAG). Asterisks, significantly different from WT (Student's t-tests, p , 0.0001 for all). Error bars, s.e.m.

Figure 3.2 Phenotypic suppression of *pny-40126* and *bp-2* inflorescence defects by *ath1-3* loss-of-function

The *ath1-3* allele (Gómez-Mena and Sablowski, 2008) was obtained from the Arabidopsis Biological Resource Center (ABRC). Mutant combinations were constructed by crossing and confirmed by PCR genotyping as described (Khan et al., 2012a; Gómez-Mena and Sablowski, 2008). Inflorescences of five-week-old representative plants are shown for:

(A) WT.

(B) *ath1-3*.

(C) *bp-2*.

(D) *bp-2 ath1-3*.

(E) *pny*; arrow denotes cluster of siliques.

(F) *pny ath1-3*.

(G-I) Quantitative analyses of *pny* phenotypic rescue by *ath1-3*. Seven-week-old plants were analyzed as previously described (Khan et al., 2012b).

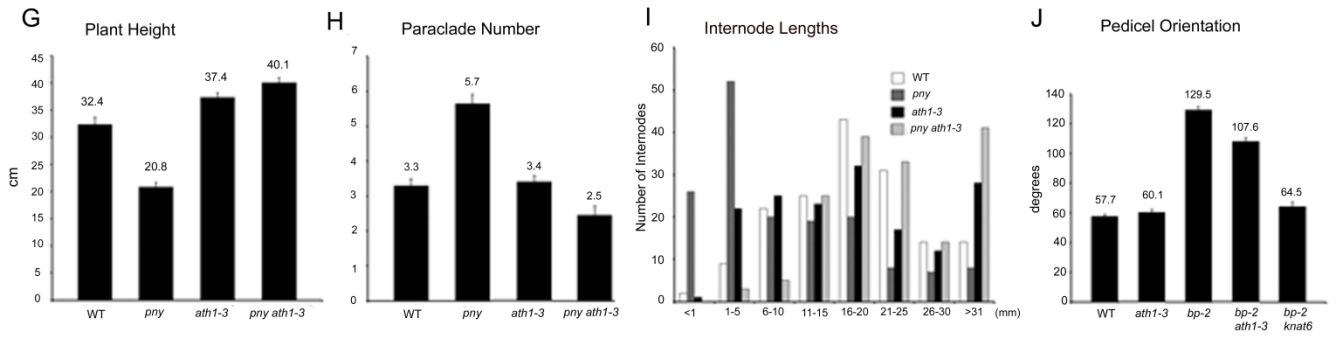
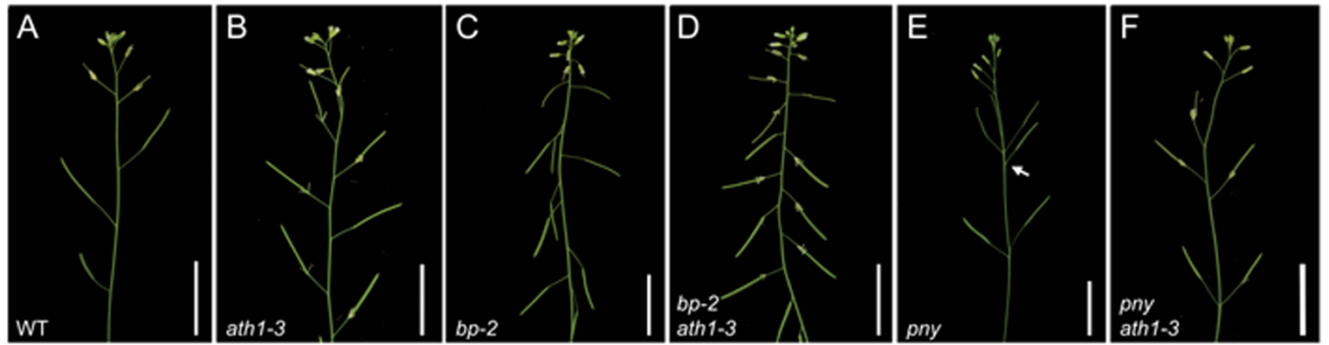
(G) Average plant height.

(H) Average number of paraclades.

(I) Distribution of internode lengths; internodes were measured between the first and 11th siliques on the primary stem (counting acropetally).

(J) Pedicel orientation; angles were measured with a protractor (n = 55).

Scale bars, 2 cm.



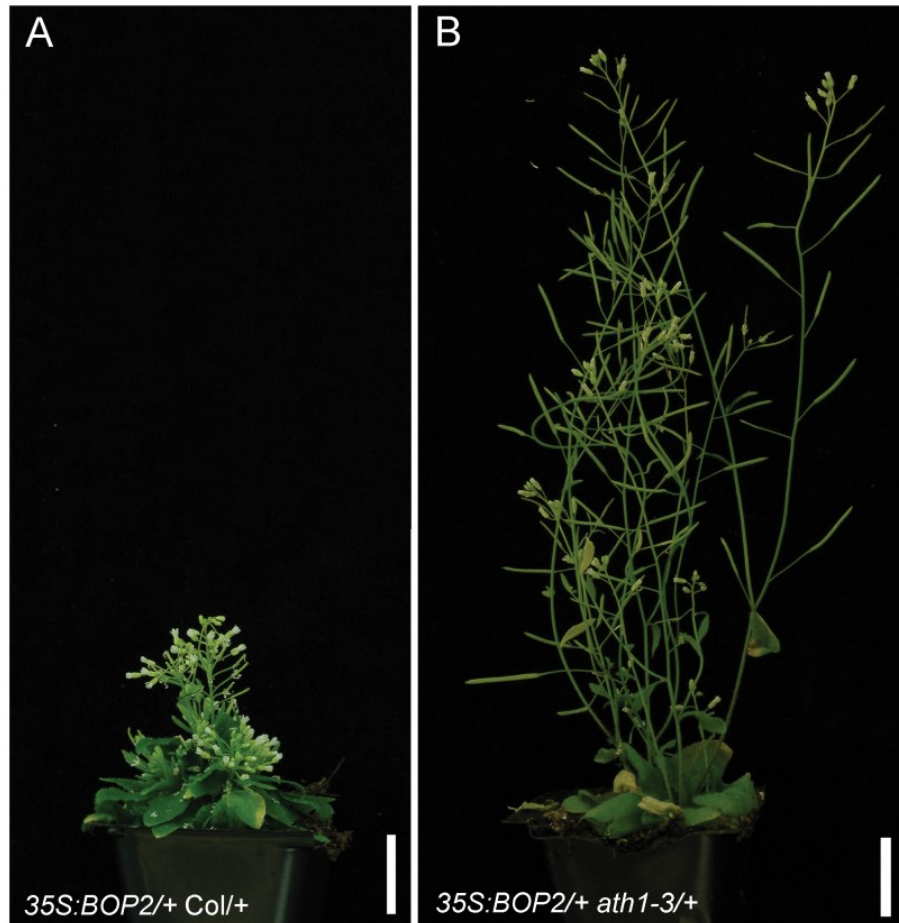


Figure 3.3 Inactivation of *ATH1* rescues compact internodes in *BOP2* gain-of-function plants

Plants homozygous for a *35S:BOP2* transgene were crossed to WT control plants or *ath1-3* homozygous mutants. Representative F1 plants are shown. qRT-PCR analysis confirmed that

BOP2 transcripts were expressed at similar levels in both genotypes.

(A) *35S:BOP2/+ Col/+*.

(B) *35S:BOP2/+ ath1-3/+*.

Scale bars, 1 cm.

Figure 3.4 Effect of KNAT6 and ATH1 inactivation on vascular patterning in *bp-2* stems

Cross sections from the base of fully elongated primary stems were stained with phloroglucinol-HCl to detect lignin as described (Khan et al., 2012b). At least 50 sections from 4–5 plants per genotype were examined. Representative sections are shown.

(A) WT.

(B) *bp-2*.

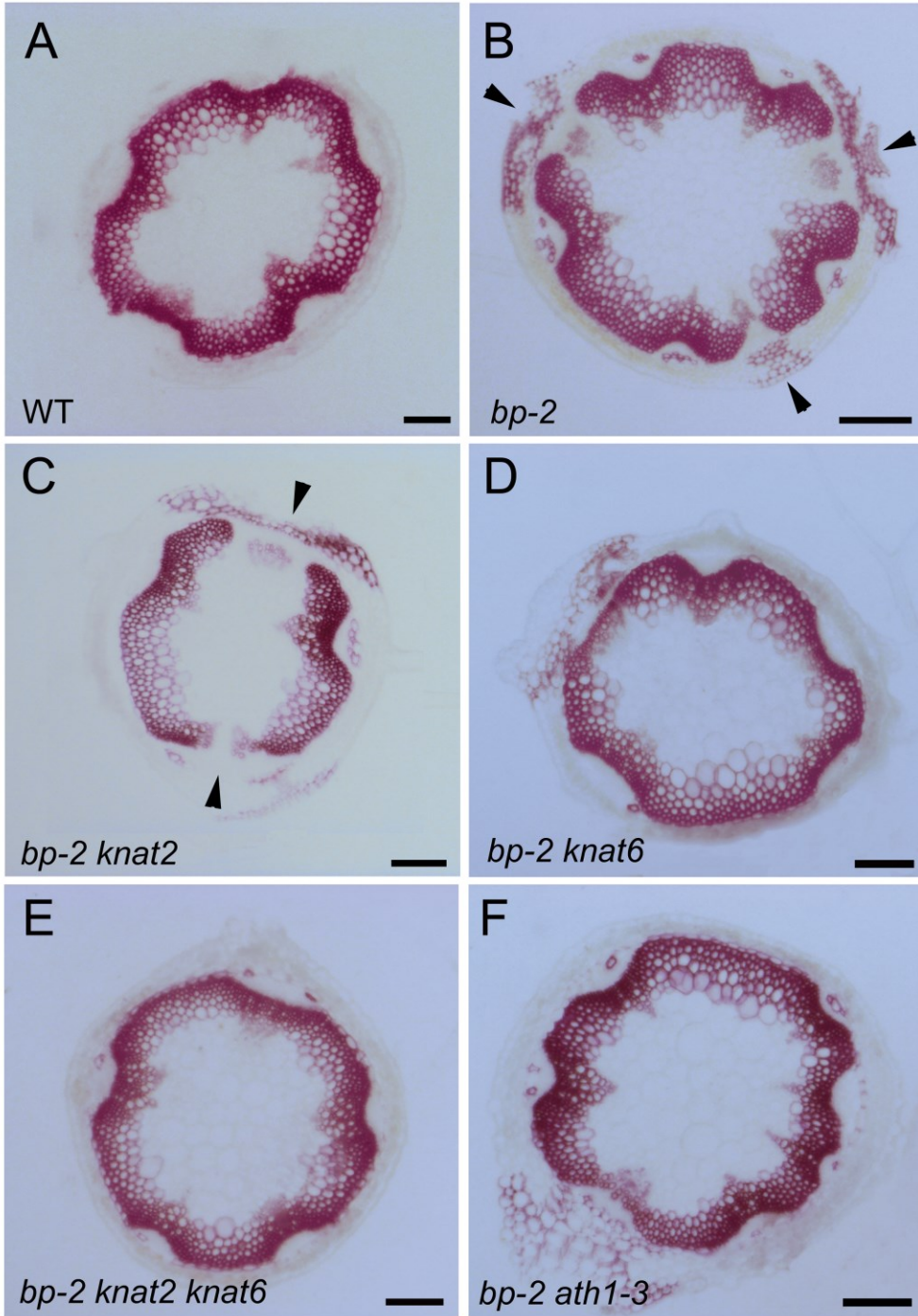
(C) *bp-2 knat2*.

(D) *bp-2 knat6*.

(E) *bp-2 ath1-3*.

(F) *bp-2 knat2 knat6*.

Arrowheads denote gaps in the vascular ring. Scale bars, 100 μ m.



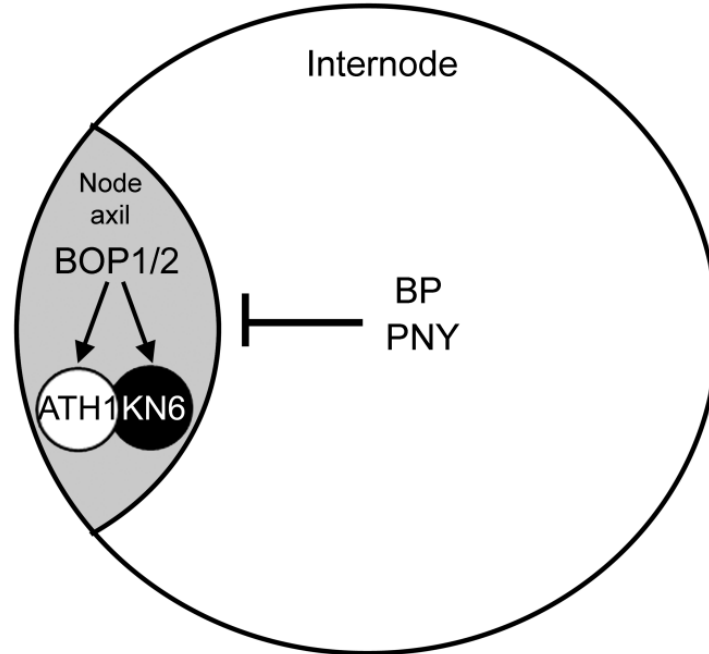


Figure 3.5 Summary of genetic interactions between BP-PNY, BOP1/2, and KNAT6-ATH1 in inflorescence patterning

BP and PNY restrict *BOP1/2* expression to the pedicel axil at nodes. *BOP1/2* in stems induces *KNAT6* and *ATH1* expression, permitting the formation of a KNOX-BELL complex whose potential activity is antagonistic to BP and PNY. Arrows represent transcriptional activation. Black T-bar represents transcriptional repression. Grey T-bar represents an opposing activity.

CHAPTER 4

PENNYWISE and POUNDFOOLISH coordinate flowering by antagonizing *BLADE-ON-PETIOLE1* and 2-mediated activation of *TALE* homeobox genes

This Chapter is presented as a manuscript in preparation for Journal of Experimental Botany

Madiha Khan, Paul Tabb, Alexander Edwards, and Shelley R. Hepworth

4.1 Abstract

In the model plant *Arabidopsis* (*Arabidopsis thaliana*), endogenous and exogenous signals acting on the meristem cause acquisition of inflorescence meristem (IM) fate. This results in new patterns of aerial development, seen as the transition from making leaves to the production of flowers separated by internodes. Competence to respond to floral inductive signals requires two BEL1-like (BELL) homeodomain proteins, PENNYWISE (PNY) and POUNDFOODLISH (PNF) in the meristem. Loss-of-function *pny pnf* mutations block floral evocation. Previous work showed that PNY and its binding partner BREVIPEDICELLUS (BP) controlled patterning in the inflorescence by confining lateral organ boundary genes *BLADE-ON-PETIOLE 1* and *2* (*BOP1/2*) to boundaries in the axil of the floral pedicel. Misexpression of *BOP1/2* is the cause of *pny* defects in phyllotaxy, apical dominance, and internode elongation. This study examines interactions between *BOP1/2* and PNY/PNF in the IM. We provide evidence that misexpression of *BOP1/2* and downstream effectors, *ARABIDOPSIS THALIANA HOMEBOX GENE1* (*ATH1*) and *KNOTTED1-LIKE FROM ARABIDOPSIS THALIANA6* (*KNAT6*), in the meristem blocks floral evocation. Compatible with this, inactivation of *BOP1/2*, *ATH1* and *KNAT6* restores flowering in *pny pnf* mutants. A steroid-induction system is used to show that BOP1 directly activates lateral boundary genes, including *ATH1*. We further identify TGA1 and TGA4 as bZIP transcription factors required by *BOP1/2* to exert changes in inflorescence architecture. These data reveal that PNY/PNF promote competence to flower by antagonizing *BOP1/2*-dependent activation of lateral organ boundary genes *ATH1* and *KNAT6* in the IM.

4.2 Introduction

Transition to reproductive development in land plants is a highly regulated event evolved to ensure successful propagation. In angiosperms, the shoot apical meristem (SAM) functions as a continuous source of new cells for organogenesis. During vegetative development, the SAM generates leaves. At the end of the vegetative phase, the SAM transitions to an inflorescence meristem (IM) that produces lateral branches and flowers separated by internodes (Bowman and Eshed, 2000; Fletcher, 2002; Barton, 2010). Flowers are crucial for success of angiosperm reproduction. Hence, the timing of the transition of a SAM to an IM is regulated by both endogenous and environmental factors that initiate flowering at the time of year which will ensure maximum reproductive success in respective environments. Early studies have identified five main factors that include photoperiod, vernalization, autonomous, gibberellin and light quality pathways that are required to regulate flowering time (reviewed in Boss et al., 2004; Amasino and Michaels, 2010; Srikanth and Schmid, 2011).

In the model plant *Arabidopsis* (*Arabidopsis thaliana*), the switch to flowering results in changes in the rate and patterning of cell division in the SAM, halting the production of rosette leaves and initiating the transformation to an IM in a process known as floral evocation (Bernier, 1988). Early in the switch to inflorescence fate, the meristem elongates internodes and initiates lateral branches from indeterminate axillary meristems. At subsequent nodes, the meristem initiates flowers from determinate axillary meristems (Benlloch et al., 2007). Following their elongation, internodes are fortified through the secondary lignification of interfascicular fibres to provide mechanical support and protection against pathogens (Nieminen et al., 2004; Ehlting et al., 2005). Although

flowering time has been studied for decades, a lot is still unknown about how the meristem becomes competent to flower.

In Arabidopsis, the three-amino-acid loop-extension (TALE) homeodomain proteins play a central role in meristem identity and maintenance. The TALE superfamily contains KNOTTED1-like HOMEBOX (KNOX) and BEL1-like (BELL) subclasses, whose products function as heterodimers (Bellauoi et al., 2001; reviewed in Hamant and Pautot, 2010; Hay and Tsiantis, 2010). Heterodimerization can be important for nuclear localization of the KNOX partner and influence binding-site selection (Bhatt et al., 2004; Cole et al., 2006; Smith et al., 2002). KNOX proteins SHOOTMERISTEMLESS (STM) and BREVIPEDICELLUS (BP; formerly KNOTTED1-LIKE FROM ARABIDOPSIS THALIANA1 [KNAT1]) function with three BELL proteins to maintain the vegetative SAM: PENNYWISE (PNY; also called BELLRINGER, REPLUMLESS, and VAMAANA), POUNDFOODLISH (PNF) and ARABIDOPSIS THALIANA HOMEBOX GENE1 (ATH1) (Byrne et al., 2003; Smith and Hake, 2003; Kanrar et al., 2006; Rutjens et al., 2009). Triple mutants of *pnf pnf ath1-1* phenocopy weak *stm* mutants most likely due to depletion of STM in the nucleus (Rutjens et al., 2009).

Significant re-organization of *KNOX-BELL* expression occurs at the transition to flowering in support of new patterns of aerial development (Lincoln et al., 1994; Gómez-Mena and Sablowski, 2008; Bryne et al., 2003; Smith et al., 2003; Smith et al., 2004). Meristem expression of *BP* and *ATH1* is down-regulated at the floral transition (Lincoln et al., 1994; Gómez-Mena and Sablowski, 2008). *BP* expression relocates to the stem cortex where it promotes vascular patterning, internode elongation, and delays lignification by excluding lateral organ boundary genes from the stem (Smith et al., 2003;

Mele et al., 2003; Ragni et al., 2008; Khan et al., 2012ab). *PNY* expression remains in the IM but expands to the stem cortex where it has functions similar to BP (Smith et al., 2003; Peaucelle et al., 2011; Etchells et al., 2012; Khan et al., 2012b). *ATH1* is expressed at the base of cauline leaves and at the base of floral organs where it promotes abscission (Gómez-Mena and Sablowski, 2008). STM and PNY-PNF remain in the IM to promote its organization and maintenance (Long et al., 1996; Smith et al., 2004).

The meristem of *pnf pnf* double mutants fails to complete the transition from vegetative SAM to reproductive IM (Smith et al., 2004). The meristem changes shape and inflorescence identity genes *SUPPRESSOR OF OVEREXPRESSION OF CONSTANS1* (*SOCI*) and *FRUITFULL* (*FUL*) are upregulated but there is no expression of floral meristem identity genes, *LEAFY* (*LFY*) and *APETALAI* (*API*) (Smith et al., 2004). The basis of this defect is only partly understood. Evidence suggests that STM-PNY/PNF are required for the flower specification function of FLOWERING LOCUS T (*FT*) which forms a complex with *FD* (Abe et al., 2005; Wigge et al., 2005; Kobayashi and Weigel, 2007; Kanrar et al., 2008; Turck et al., 2008; Zeevaart, 2008; Smith et al., 2011). STM-PNY/PNF also promote SQUAMOSA PROMOTER-BINDING PROTEIN-LIKE (*SPL*) transcription factors in response to hormonal and age-related signals. *SPL* proteins function in parallel with *FT-FD* to specify flowers (Wang et al., 2009; Yamaguchi et al., 2009). *SPL3*, 4 and 5 functions are dependent upon and their expression is promoted by PNY/PNF through negative regulation of microRNA 156 (*miR156*), a miRNA that antagonizes *SPL* transcript accumulation during vegetative development (Wang et al., 2009; Yamaguchi et al., 2009; Lal et al., 2011). Interestingly, loss-of-function *ATH1* (*ath1-1*) partially restores flowering and internode elongation in *pnf pnf* mutants

suggesting that down-regulation of *ATH1* is essential for completing the floral evocation (Rutjens et al., 2009).

Previous research showed that loss-of-function *bp* and *pny* defects in inflorescence architecture are caused by stem misexpression of lateral organ boundary genes *BLADE-ON-PETIOLE1/2* (*BOPI/2*) and their downstream effectors, *KNAT6* and *ATH1*, whose products form a complex. *KNAT2* is also misexpressed in *bp* and *pny* stems but plays a minor role (Ragni et al., 2008; Rutjens et al., 2009; Khan et al., 2012a; Khan et al., 2012b; Li et al., 2012). *BOP1/2* gain-of-function mimics *bp*, *pny*, and *bp pny* phenotypes showing that phenotypic variation in inflorescence architecture is determined by the domain and level of *BOPI/2* misexpression (Khan et al., 2012). *BOPI/2* belong to the *NONEXPRESSOR OF PATHOGENESIS-RELATED GENES1* (*NPR1*)-like gene family of BTB-ankyrin transcriptional co-activators in Arabidopsis (Ha et al., 2004; Hepworth et al., 2005; Norberg et al., 2005). BTB-ankyrin proteins bind to DNA and exert their function through TGA (TGACG-motif binding) bZIP transcriptional factors (Zhang et al., 1999; Zhou et al., 2000; Després et al., 2003; Zhang et al., 2003; Hepworth et al., 2005).

BOP1/2 function is antagonistic to *BP* and *PNY*. The mechanism of this antagonism is still unknown, but it does not seem to involve transcriptional repression of *BP* or *PNY* (Khan et al., 2012b). Rather, antagonism may instead involve the reciprocal regulation of common downstream target genes. *BP* is a direct repressor of lignin biosynthetic genes. One of its predicted targets is *PRXR9GE* (*PRXR9*), a class III peroxidase that catalyzes the polymerization of lignin monomers for deposition during stem maturation (Boerjan et al., 2003; Mele et al., 2003; Khan et al., 2012b). Previously, we showed that *BOPI/2* promote *KNAT6* and *ATH1* expression and require the activities of these downstream

genes to regulate inflorescence architecture and to promote lignin deposition (Khan et al., 2012a; Khan et al., 2012b). We hypothesize that a complex of KNAT6-ATH1 activated by BOP1/2 has affinity for some of the same direct transcriptional targets as BP or PNY (Khan et al., 2012a; Khan et al., 2012b).

In this study, we show that PNY and PNF repress *BOP1/2* and its downstream effectors, *ATH1* and *KNAT6*, in the IM. Misexpression of this boundary module in *pnf pny* meristems blocks floral evocation, as evidenced by rescue of flowering by inactivation of *BOP1/2*, *ATH1*, or *KNAT6*. Compatible with this, BOP1/2 gain-of-function delays the floral transition (Tabb, 2012). Using a steroid-induction system, we identify lateral organ boundary genes, *ATH1* and *PRXR9*, as direct downstream targets of BOP1. Finally, we provide evidence that BOP1/2 require the activities of bZIP TGA factors TGA1 and TGA4 to exert changes in inflorescence architecture. These data shed light on how PNY and PNF promote competence to flower and identify new developmental roles for TGA1 and TGA4. Collectively, these data provide new evidence that BOP1/2 antagonism of KNOX-BELL factors is a conserved module, essential in embryo development (Jun et al., 2010), inflorescence architecture (Khan et al., 2012ab), abscission (McKim et al., 2008; Gómez-Mena and Sablowski, 2008; Shi et al., 2011) and at the transition to flowering, as shown here.

4.3 Materials and methods

4.3.1 Plant material and growth conditions

Plants were grown in growth chambers on agar plates and/or in soil at 21°C in 24 h light (100 $\mu\text{mol m}^{-2}\text{s}^{-1}$). Wild-type was the Columbia-0 (Col-0) ecotype of Arabidopsis. The

bop1-3 bop2-1 double mutant (SALK_012994; SALK_075879), and *pnf-40126* (SALK_40126), *pnf_96116* (SALK_96116); *knat6-2* (SALK_054482) and *ath1-3* (SALK_113353) mutant alleles used in this study were as previously described (Hepworth et al., 2005; Smith et al., 2003; Belles-Boix et al., 2006; Gómez-Mena and Sablowski, 2008; Smith et al., 2004). *35S:BOP2* and *bop1-6D* overexpression lines (Norberg et al., 2012b) and the *BOP2:GUS* reporter line were previously described (Xu et al., 2010). Mutant alleles *tga1-1* (SALK_028212), *tga4-1* (SALK_127923) and the double mutant were kindly provided by Pierre Fobert (Shearer et al., 2012). The *ATH1:GUS* reporter line was kindly provided by Marcel Proveniers (Proveniers et al., 2007). All mutant combinations were constructed by crossing and confirmed by PCR genotyping. Constructs were used to transform wild-type plants by floral dipping (Clough and Bent, 1998) using the *Agrobacterium* strain C58C1 pGV101 pMP90 (Koncz and Schell, 1986).

4.3.2 Primers and genotyping

The strategy and primers used for genotyping *bop1-3*, *bop2-1*, *pnf-40126*, *knat6-*, *ath1-3* (Khan et al., 2012b) and *pnf_96116* alleles (Smith et al., 2004) were as previously described. Primers for qRT-PCR analysis of *ATH1* and *KNAT6* transcripts were as listed in Khan et al., 2012a; Khan et al., 2012b). All other primers for plasmid construction, transcript analysis, and genotyping were as listed in Table S4.2.

4.3.3 Construction of *4CL:BOP1-GR*, *D35S:BOP1-GR*, *35S:BOP1-GR* and *PRXR9:GUS* transgenic lines

To make p4CLprom:BOP1-GR and pD35S:BOP1-GR constructs for overexpression of inducible BOP1 in plants, *BOP1* was fused in-frame to the steroid-binding domain of the rat glucocorticoid receptor (Lloyd et al., 1994). This fusion gene was amplified by PCR using pBOP1prom:BOP1-GR as the template, CDS-BOP1-F and GR-R as the primers, and iProof (Biorad, CA) as the polymerase. dATP overhangs were added to the resulting fragment, which was transferred to the Gateway-compatible entry vector pCR8/GW/TOPO (Invitrogen, Carlsbad, CA) and sequenced to ensure fidelity. LR clonase © (Invitrogen, Carlsbad, CA) was used to move the insert to pSM-3 based destination vectors containing either a double 35S promoter (D35S) or the promoter of a lignin biosynthetic gene 4-coumarate:Coenzyme A ligase from parsley (4CL) (Carl Douglas lab, unpublished). *Hygromycin*-resistant primary transformants were selected on agar plates containing 10 µm dexamethasone (DEX) by exposing seeds to light for 8 hours then incubating them in the dark for 48 hours. Seedlings were then exposed to low-light for 8 hours before incubation in continuous light for 6 additional days before the transfer of *hygromycin*-resistant seedlings to soil. Seedlings resistant to *hygromycin* developed elongated hypocotyls. Primary transformants on soil were sprayed daily with 10 µm DEX (Sigma) to induce nuclear localization of the BOP1-GR fusion protein. Phenotypes were scored in T1 generation.

To make p35S:BOP1-GR, *BOP1* coding sequence was amplified from cloned cDNA template using iProof as the polymerase (BioRad, Hercules, CA) and 4H-GR-F1 and BOP1-GR-R2+linker incorporating *NheI* and *BamHI* restriction sites respectively, as the

primers. The resulting product was cloned into pCR-BluntII-TOPO (Invitrogen, Carlsbad, CA). After sequencing, the insert was excised by digestion with *NheI* and *BamHI* restriction enzymes and ligated the corresponding compatible *XbaI* and *BamHI* sites of pBI-ΔGR (Lloyd et al., 1994). Wild-type plants were transformed. Kanamycin-resistant seedlings were selected on agar plates containing 10 μm DEX. Following transfer to soil, transformants were sprayed daily with DEX solution (as above). Phenotypes were scored in T1 generation.

To create the *PRXR9:GUS* reporter line, ~2-kb of promoter sequence including the start site of translation was amplified by PCR from a genomic DNA template and used to create a translational fusion with the GUS gene (*uidA*). In this reaction, BAC MSD21 was the template, 2-kbPRXRproF1 and PRXRproR1 incorporating *BamHI* and *NcoI* restriction sites were the primers, and iProof (BioRad, CA) was the polymerase. The resulting product was cloned into pCR-BluntII-TOPO (Invitrogen, Carlsbad, CA) and sequenced to ensure fidelity. The insert was then released by digestion with *BamHI* and *NcoI* and ligated into the corresponding sites of pGCO:GUS (Hepworth et al., 2002). *Agrobacterium* was co-transformed with pSOUP (Hellens et al., 2000). Wild-type plants were transformed and glufosinate-ammonium resistant primary transformants were selected on soil using the herbicide Finale (distributed by Farnham Companies Inc, Phoenix, AZ). Cloning primers are listed in Table S4.2.

4.3.4 Histological analysis of GUS localization

To monitor *BOP2:GUS* expression in vegetative shoot apices, *BOP2:GUS* in wild-type and *pnx pnf/+* seedlings were grown on agar plates in short-day conditions (8 hours light,

16 hours dark). Seedlings from both populations (n>20) were stained at 10-days-old as described in Khan et al., 2012b. About one quarter of seedlings in the *pnf pnf/+* population showed staining in the meristem. To monitor *BOP2:GUS*, *ATH1:GUS* and *PRXR9:GUS* expression at later stages of development, plants were grown on soil for 4 weeks in continuous light before staining. When required, tissues were fixed, embedded, sectioned, and photographed as described in Khan et al., 2012b.

4.3.5 qRT-PCR

Total RNA was isolated from internodes of 4-week-old flowering plants using Trizol © reagent (Invitrogen, Carlsbad, CA). Internode tissue was harvested from primary and secondary inflorescences of 5-6 plants, starting above the first silique from the bottom and all the way up to where the internodes were too small (less than 0.2cm long) to collect. Tissue for analysis was excised with a new razor blade on parafilm, quickly frozen in liquid nitrogen, and stored at -80°C until extraction. cDNA was synthesized using 1 ug of RNA and qRT-PCR (qPCR) was performed as previously described (Khan et al., 2012b). Plants homozygous for a *D35S:BOP1-GR* transgene (line 9) were treated continuously with Mock (1L H₂O + 1.2ml Anhydrous ethanol), 30 µm DEX, 50 µm cycloheximide (CHX) or 30 µm DEX + 50 µm CHX for 2, 4, 24 hours. For long-term treatment, seedlings were germinated on 10 µm DEX plates. Once transplanted to soil, they were sprayed daily for 4 weeks until RNA was extracted. For qPCR on *D35S:BOP1-GR* internodes, values were normalized to *EIFA* and then to Mock control in case of DEX treatment and to CHX in case of DEX+CHX treatments (Nakamichi et al., 2010). This was done because Jun et al., 2010 had previously shown transcripts of *AS2*, a direct target of BOP1, went down after treatments with CHX in plants transformed with BOP1-GR as

well as untransformed *bop* mutant plants indicating CHX had negative effect on BOP1 target genes which was independent of BOP1 function. Data shown represent the average of three biological replicates. Bars indicate standard error of the mean. Gene specific primers for qPCR analysis are listed in Table S4.2.

4.3.6 Accession numbers

Sequence data for genes described in this article can be found in the GenBank/EMBL data libraries under the accession numbers: At2g41370 (BOP1), At3g57130 (BOP2), At1g23380 (KNAT6), At5g02030 (PNY), At3g04120 (GAPC), At3g21770 (AtPRXR9GE), At5g65210 (TGA1), At5g10030 (TGA4), At2g27990 (PNF) and At4g32980 (ATH1).

4.4 Results

4.4.1 Inactivation of BOP1/2, KNAT6, or ATH1 rescues the *pnf pnf* phenotype

The strong *BOP-ox* line *bop1-6D* shows a 10-day delay in flowering compared to wild-type (Tabb, 2012). Based on our previous results, we reasoned that misexpression of *BOP1/2* in the *pnf pnf* meristem might antagonize the floral transition. Given that *BOP1/2* exert changes in inflorescence architecture through *ATH1* and *KNAT6*, we reasoned that misexpression of these additional genes play a role. To test this hypothesis, *bop1 bop2 pnf pnf*, *knat6 pnf pnf*, and *ath1-3 pnf pnf* mutants were generated and their phenotypes analyzed relative to WT and parental controls. *pnf pnf* mutants remained in a vegetative state and were unable to elongate internodes or initiate flowering (Smith et al., 2004; Kanrar et al., 2008; Rutjens et al., 2009; Ung et al., 2011). As anticipated,

inactivation of *BOP1/2* or its downstream effectors *KNAT6* and *ATH1* dramatically rescued flowering and internode elongation in *pnf pnf* mutants. The morphology of inflorescences in *bop1 bop2 pny pnf*, *knat6 pny pnf*, and *ath1 pny pnf* plants was similar to wild-type (Fig. 4.1, A-E). Quantitative phenotypic analysis of plant height, paraclade numbers, and internode length of 20 plants per genotype showed little or no difference compared to wild-type control plants (Tabb, 2012).

4.4.2 *BOP1/2*, *ATH1*, and *KNAT6* expression domains are expanded in *pnf pnf* meristems

Given that PNY restricts *BOP1/2* expression to the axils of pedicels, we examined *BOP1/2* expression in *pnf pnf* meristems before and after floral induction. Since *pnf pnf* mutants initiate leaves prior to floral evocation, we anticipated that misexpression of *BOP1/2* might only occur after floral induction in *pnf pnf* meristems given the continued presence of STM-ATH1 activity in the SAM. Surprisingly, *BOP2* was expressed throughout the central, peripheral, and rib zones of the *pnf pnf* SAM suggesting that ATH1 does not repress *BOP1/2* nor does *BOP1/2* interfere with SAM function (Fig. 4.2, A and B). This might be due to an abundance of KNOX-ATH1 heterodimers or the absence of a critical binding partner such as TGA factors, without which *BOP1/2* may not be functional (Lincoln et al., 1994; Long et al., 1996; Hepworth et al., 2005; Xu et al., 2010; Khan et al., 2012b; Khan and Hepworth, 2013).

During reproductive development, *BOP1/2* expression is excluded from the IM and restricted to determinate axillary meristems with floral fate (Xu et al., 2010). In *pnf pnf* mutants, *BOP1/2* expression expands into the central and rib zones of the meristem (Fig.

4.2, C and D; *BOP1* data not shown). *KNAT6* is misexpressed in an identical pattern (unpublished results by Veronique Pautot). *ATH1* misexpression is confined to the rib zone (Fig. 4.2, E and F). These data are consistent with the model that *BOP1/2* and its downstream effectors function in the same genetic pathway to block competence to flower when misexpressed in the meristem of *pnf pnf* mutants.

4.4.3 *PRXR9* is co-expressed with other lateral organ boundary genes

Previously, we showed that *KNAT6*, *ATH1*, and the lignin biosynthetic gene *PRXR9* are upregulated in *BOP*-ox internodes (Khan et al., 2012b). While *KNAT6* is well-established as a lateral organ boundary gene (Belles-Boix et al., 2006; Ragni et al., 2008), the expression patterns of *ATH1* and *PRXR9* in the literature are incomplete. To confirm that these genes are indeed expressed at lateral organ boundaries in the inflorescence in a pattern that overlaps with *BOP1/2* in the axil of pedicels, the base of floral organ and in the receptacle and valve margins of the fruit, we analyzed the patterns of *ATH1:GUS* and *PRXR9:GUS* expression in these tissues. This analysis showed that *ATH1:GUS* expression is not as confined to the lateral organ boundary as *BOP1/2* or *KNAT6* (Khan et al., 2012b). Expression is diffuse at the base of pedicel (Fig. 4.3A) consistent with its role in restricting cell elongation at the basal boundary of shoot organs (Gómez-Mena and Sablowski, 2008). Previous work showed that *ATH1:GUS* expression occurs at the base of floral organs, and in the receptacle (Gómez-Mena and Sablowski, 2008). In *35S:BOP2* lines, *ATH1:GUS* expression was up-regulated stems and pedicels confirming previous qPCR data (Fig. 4.3, A and B; Khan et al., 2012a). *PRXR9:GUS* was sometimes expressed in vasculature of wild-type stems and pedicels but mainly concentrated in the axils of pedicels (Fig. 4.4, A and B). *PRXR9:GUS* expression also occurs at the base of

floral organs prior to abscission (Fig.4.4C), in the fruit receptacle after abscission (Fig. 4.4D), and in the valve margins of fruits (Fig. 4.4E). All of these cell-types are fortified with lignin as a normal part of development (Patterson, 2001; Roberts et al., 2002). These data show that *KNAT6*, *PRXR9*, *ATH1* and *BOPI/2* have overlapping expressions in lateral organ boundaries of the inflorescence (Fig. 4.3; Fig. 4.4; Gómez-Mena and Sablowski, 2008; McKim et al., 2008; Ragni et al., 2008; Khan et al., 2012b).

4.4.4 BOP1/2 directly activates lateral organ boundary genes *ATH1* and *PRXR9*

Given that *PRXR9*, *KNAT6*, and *ATH1* co-expressed with *BOPI/2* and are upregulated in *BOP*-ox internodes (Fig. 4.3, A and B; Fig. 4.5H; Khan et al., 2012ab) we next tested if any of these genes are direct transcriptional targets of BOP1. For this, we generated a translational fusion of BOP1 to the steroid binding domain of the rat glucocorticoid receptor which was expressed in wild-type plants. Treatment with Dexamethasone (DEX) leads to translocation of the GR fusion protein from the cytoplasm to the nucleus as a way of controlling post-translational activity (Lloyd et al., 1994). This system was used previously to show that BOP1 directly activates the transcription of *AS2* in leaves (Jun et al., 2010). Three separate gain-of-function *BOPI-GR* lines were created: *35S:BOPI-GR*; *D35S:BOPI-GR*, and *4CL:BOPI-GR* under the control of three different constitutive promoters: single CaMV enhancer, double CaMV enhancer, or the promoter of *4CL*, lignin biosynthetic gene from parsley that is expressed in cell walls (Hauffe et al., 1991). Transformants with strong gain-of-function phenotypes similar to *bop1-6D* were obtained in the T1 generation (Supplemental Table S4.1). Homozygous progeny from one *D35S:BOPI-GR* line with a strong phenotype was identified for further analysis. *D35S:BOPI-GR* plants treated with DEX for four weeks had shortened internodes and

clustered siliques similar to *bop1-6D* overexpression lines (Fig. 4.5, A-D). After 2 hours of DEX treatment, transcript levels of *ATH1* and *PRXR9* were almost 2-fold higher but *KNAT6* did not show an increase relative to Mock-treated control plants (Fig.4.5E). After 4 hours of DEX treatment, *ATH1* transcripts remained 2-fold higher and *PRXR9* levels were 8-fold higher (Fig. 4.5F). *KNAT6* transcript levels after 4 hour of DEX treatment remained unchanged relative to Mock-treated control plants (Fig. 4.5F). Continuous DEX treatments for 4 weeks resulted in 6-fold higher levels of *ATH1* transcript and 38-fold higher levels of *PRXR9* transcript relative to Mock-treated control plants (Fig. 4.5G). *KNAT6* transcript levels remained unchanged even after continuous treatment with DEX (Fig. 4.5G). These data are consistent with *ATH1* and *PRXR9* being immediate targets of BOP1 and *KNAT6* being an indirect target.

Rapid activation of *ATH1* and *PRXR9* suggested that their induction by BOP1 may be independent of protein synthesis. We tested this by analyzing *ATH1*, *PRXR9*, and *KNAT6* expression in response to DEX induction in the presence of protein synthesis inhibitor cycloheximide (CHX). After 2 hours of combined treatment with DEX and CHX, *ATH1* transcript was increased 5-fold and *PRXR9* was increased 4-fold relative to CHX-treated control plants (Fig 4.5E). After 4 hours of combined treatment, transcripts of *ATH1* increased 7.5-fold and transcripts of *PRXR9* increased 5-fold (Fig. 4.5F). *KNAT6* showed up to a 2-fold increase after combined DEX and CHX treatment for 2 and 4 hours (Fig. 4.5, E and F). The differences in transcripts of *ATH1*, *KNAT6* and *PRXR9* treated with DEX + CHX in comparison to those treated with DEX alone might be due to the different controls used (see materials and methods).

4.4.5 BOP1/2 promote *TGA1* and *TGA4* expression

BOP1/2 lack a DNA binding domain and are likely recruited to DNA via interactions with TGA bZIP transcription factors (Hepworth et al., 2005; Xu et al., 2010; reviewed in Khan and Hepworth, 2013). TGA8/PAN mediates BOP function in the floral meristem (Hepworth et al., 2005; Xu et al., 2010). Microarray results provided by Raju Datla showed that *TGA4* was upregulated ~3.2-fold in *bop1-6D* internodes suggesting the potential for functional importance. qRT-PCR results on *bop1-6D* internodes confirmed this data, showing a 3-fold increase of *TGA1* and 5-fold increase of *TGA4* (Fig. 4.5H). However, steroid-induced induction of *D35S:BOP1-GR* lines revealed no increase in *TGA1* and *TGA4* transcript after 2 or 4 hour treatments with DEX or DEX+CHX (Fig. 4.5, E and F). After DEX treatment for 4 weeks, transcript levels of *TGA4* were increased 2.3-fold but *TGA1* remained the same (Fig. 4.5G). These data indicate that *TGA1/4* are probably not direct targets of BOP1 activation. However, since *TGA1/4* transcripts are higher over the long term in *bop1-6D* lines, they might be required by BOP1/2 to exert function.

4.4.6 BOP1/2 exert their function through TGA1/4

To test if BOP1/2 require TGA1/4 for function, we examined the effects of *tga1*, *tga4* and *tga1 tga4* loss-of-function on the phenotype of a strong *35S:BOP2* gain-of-function line with short compact inflorescences (Norberg et al., 2005; Khan et al., 2012ab). In this experiment, plants that were homozygous for the *35S:BOP2* transgene were crossed to wild-type control plants or to lines homozygous for *tga1*, *tga4*, or *tga1 tga4* mutations. The phenotypes of F1 progeny from three to five independent crosses per genotype were

examined (Supplemental Fig. S4.1). These results showed that partial loss-of-function in TGA1 or TGA4 individually (*tga1/+* or *tga4/+*) had no effect on the *35S:BOP2* phenotype (Fig. 4.6, A-C; Supplemental Fig. S4.1). In contrast, combined TGA1 and TGA4 inactivation (*tga1/+ tga4/+*) restored internode elongation in the majority of *35S:BOP2* plants (Fig. 4.6D; Supplemental Fig. S4.1). These data show that TGA1/4 work redundantly and are required by BOP1/2 to exert changes in inflorescence architecture.

4.5 Discussion

During the vegetative phase of Arabidopsis development, the SAM generates leaves without internode elongation resulting in a compact basal rosette of leaves. Endogenous and environmental signals acting on the SAM promotes its conversion to an IM. Only the IM is competent to initiate the production of reproductive structures including lateral branches and flowers, separated by internodes (Bowman and Eshed, 2000; Fletcher, 2002; Barton, 2010). The timing of flowering and the subsequent patterning of the inflorescence is tightly regulated to ensure optimal reproductive success. Previously, we showed that BP and PNY in the stem cortex confines *BOP1/2* expression to the axil of pedicels to regulate growth patterns and differentiation in the developing inflorescence stem (Khan et al., 2012b). BP-PNY function in part to maintain indeterminacy in the stem so that lignification occurs when internode elongation is complete. This work also showed that BOP1/2 promote the expression of lateral organ boundary genes *ATH1* and *KNAT6* which form a KNOX-BELL complex that potentially antagonizes BP/PNY activity to regulate inflorescence architecture. The class III peroxidase *PRXR9* was

identified as a potential target of antagonistic regulation by BP and PNY during secondary cell wall biosynthesis (Khan et al., 2012a; Khan et al., 2012b).

This study concentrates on the KNOX-BELL and BOP1/2 interactions during floral evocation. Proper allocation of cells into the developing primordia and perpetuation of pluripotent cells in the central zone are important for maintaining the SAM (Vollbrecht et al., 2000). *PNY* and *PNF* are required for SAM competence to respond to floral inductive signals which is required for new patterns of growth that promote the display of flowers (Smith et al., 2004, Rutjens et al., 2009). In *pnf pny* mutants, the SAM display defects in the allocation of cells, thereby failing to complete the morphological changes necessary for restructuring of the SAM into IM. This results in plants that do not flower and produce only leaves (Smith et al., 2004). To examine this further, we used a genetics approach to show that PNY and PNF are negative regulators of *BOP1/2*, *KNAT6* and *ATH1* during floral evocation. We also showed that inactivation of *bop1 bop2*, *ath1* and *knat6* rescues the no flowering defects of *pnf pny* double mutants. A glucocorticoid-based induction was used to identify *ATH1* and *PRXR9* as direct targets of BOP1 activity. Since BOP1/2 do not contain DNA binding domain, they may require TGA transcription factors to bind to their target genes (Hepworth et al., 2005). TGA1 and TGA4 were identified as potential transcription factors required by BOP1/2 to bind to their targets and exert changes during flowering and inflorescence development.

4.5.1 PNY and PNF in the meristem repress BOP1/2 to promote floral evocation

Significant reorganization of KNOX and BELL expression in the meristem occurs during the transition to flowering. *ATH1* and *BP* expression dissipates from the SAM. *BP*

expression moves to the stem cortex and *ATH1* is expressed at the base of shoot and in lateral organ boundaries (Lincoln et al., 1994; Long et al., 1996; Long and Barton, 2000; Byrne, 2003; Smith and Hake, 2003; Smith et al., 2004; Gómez-Mena and Sablowski, 2008; Takano et al., 2010). STM remains in the IM where its function is dependent on BELL factors, PNY and PNF (Bhatt et al., 2004; Cole et al., 2006; Kanrar et al., 2006; Rutjens et al., 2009).

Our data show that PNY and PNF repress *BOPI/2* in the SAM (Fig. 4.2, A and B) and *BOPI/2*, *ATH1* (Fig. 4.2, C-F) and *KNAT6* (based on unpublished data by Veronique Pautot) in the IM. Interestingly, IM misexpression of *ATH1* is confined to the rib zone, where cell division increases following the floral transition to provide cells for incorporation into internodes (Carles and Fletcher, 2003). This misexpression in *pnf pny* is functionally important since *bop1 bop2*, *ath1*, and *knat6* mutations restore both internode elongation and flowering (Fig. 4.1, A-E). These events are synchronized in Arabidopsis and understanding the role of *ATH1* may shed light on this mechanism. Collectively, our data suggest that ectopic expression of *BOPI/2* and its downstream effectors, *KNAT6* and *ATH1*, block competence to flower. STM is likely also required for repression but this is difficult to test genetically since *stm* mutants do not maintain a functional meristem into the reproductive stage of development (Long et al., 1996). In *stm* embryos, *BOPI/2* expands into the junction between the fused cotyledons consistent with STM repression (Jun et al., 2010).

Previous work in the C24 ecotype of Arabidopsis identified *ATH1* as a positive regulator of the floral repressor *FLOWERING LOCUS C (FLC)* but has no substantial effect on the expression of other *FLC*-clade members *FLOWERING LOCUS M (FLM)* and *MADS*

AFFECTING FLOWERING 2 (MAF2) (Proveniers et al., 2007). Strong *35S:FLC* lines have a non-flowering phenotype similar to *pnf pnf* (Michaels and Amasino, 1999). It is possible that ectopic ATH1-KNAT6 activity in *pnf pnf* meristem blocks down-regulation of *FLC* but this remains to be tested. FLC-clade members play a major role in repressing *FT* (reviewed in Jarillo, 2011). It has been suggested that the flower specification function of *FT* is impaired in *pnf pnf* (Smith et al., 2004). PNY-PNF also promote the expression of *SPL3*, *4* and *5* which function in the autonomous pathway to promote flowering in response to endogenous hormone and age-related signals (Kanrar et al., 2006; Kobayashi and Weigel, 2007; Kanrar et al., 2008; Turck et al., 2008; Zeevaart, 2008; Lal et al., 2011). Further tests are required to determine the transcriptional targets of BOP1/2 and/or ATH1-KNAT6 that block flowering in the IM. Understanding these targets will shed light on how the meristem responds to floral inductive signals to direct changes in plant architecture.

4.5.2 BOP1/2 are direct transcriptional regulators of lateral organ boundary genes

ATH1* and *PRXR9

In developing leaves, BOP1 directly promotes *AS2*, whose product directly mediates stable repression of *KNOX* genes to maintain simple leaf shape (Jun et al., 2010). We identify lateral organ boundary genes *ATH1* and *PRXR9* as additional direct targets of BOP1 activation.

ATH1 is the best candidate for direct regulation of *KNAT6*. *35S:ATH1* lines display shortened internodes and clustered siliques, similar to *35S:BOPs* (Gómez-Mena and Sablowski, 2008). Induction using *35S:ATH1-GR* lines shows upregulation of *KNAT6*

after 4 hours of DEX treatment and boundary expression of *KNAT6:GUS* expression is lost in *ath1-3* embryos (personal communication by Marcel Proveniers). While *KNAT6* transcript is increased over the long term in *bop1-6D* internodes, its induction is small and not reproducible using the milder *D35S:BOP1-GR* system. Li et al., 2012 have shown that *KNAT6* transcript levels are significantly down-regulated in double mutants of *ath1-4* and *isoginchaku-2D*, a gain of function *ASYMMETRIC LEAVES 2* mutant, compared to *iso-2D* alone. Combined, these results suggest that BOP1/2 promote *KNAT6* expression indirectly via activation of *ATH1*.

PRXR9 encodes a cell wall peroxidase for the polymerization of lignin monomers. Transcripts are dramatically up-regulated in *bp* and *BOP-ox* stems (Mele et al., 2003; Khan et al., 2012a). We show here that *PRXR9:GUS* expression is localized to lateral organ boundaries and that its transcript is directly activated by BOP1. Mele et al., 2003 speculated that polymerization of monolignols is a key node for developmental regulation of stem maturation. Following organ detachment, floral organ abscission zones in the plant after shedding takes place are also fortified with lignin to provide a protective surface that resists dehydration and pathogen attack (Bleeker et al., 2002). The valve margin of fruits contains a similar layer of lignified cells that promotes pod shatter (Girin et al., 2009). Thus, BOP promotion of lignin biosynthesis in stems likely reflects its natural function at lateral organ boundaries.

4.5.3 BOP1/2 activity is dependent on TGA1 and TGA4

There are 10 TGA factors in Arabidopsis with overlapping functions in defense, stress, and development (reviewed in Jakoby et al., 2002; Gatz, 2013). Similar to NPR1,

BOP1/2 form complexes in yeast two-hybrids with most TGA proteins (Hepworth et al., 2005). Additionally, BOP1/2 and TGA8/PERIANTHIA (PAN) form a nuclear complex that controls sepal number in flowers and chromatin immunoprecipitation (ChIP) assays showed enrichment of BOP1-GFP at two potential TGA binding sites in the *API* promoter (Xu et al., 2010; Hepworth et al., 2005). Mapping of the *ATH1* and *PRXR9* promoters has also identified potential TGA binding sites (data not shown). Our data have identified TGA1 and TGA4 as prime targets for recruitment of BOP1/2 onto target DNA during flowering and inflorescence development.

TGA1 and TGA4 comprise clade I TGA factors with experimental evidence for roles in both basal defense and development. Basal plant defense is based on preformed chemical and physical barriers, such as lignin, that resist pathogen attack (reviewed in Gatz, 2013). TGA1 and TGA4 interact with NPR1 in a redox-dependent manner (Després et al., 2003). Transcript profiling shows upregulation of *TGA1* in developing stems (Ehltling et al., 2005) whereas *TGA4* is expressed in leaves (Song et al., 2008). TGA4 was identified biochemically as interacting with CONSTANS (CO), a positive regulator of floral induction in the photoperiodic pathway (Song et al., 2008). CO and TGA4 then promote the expression of *FT*, a key floral integrator required to promote flowering, by binding directly to its promoter (Song et al., 2008). In addition, similar to *CO*, *TGA4* mRNA also follows the 24 h oscillation in a circadian clock dependent manner supporting its role in the floral transition pathway (Suarez-Lopez et al., 2001; Song et al., 2008).

BOP1/2 promotion of TGA1 and TGA4 in stems seems to be indirect. Although transcripts are upregulated in *bop1-6D* internodes, the use of *D35S:BOPI-GR* lines, showed that transcript levels were not obviously induced by DEX even after prolonged

treatment (Fig. 4.5E-H). However, shortened internodes and late flowering in *35S:BOP2* line was rescued by partial inactivation of TGA1 and TGA4 (*tga1/+ tga4/+*) (Fig. 4.6, A-D). These data provide evidence that BOP1/2 requires TGA1/4 to exert changes to flowering time and inflorescence architecture. The next step is to test if BOP1/2 bind via TGA1/4 to the *ATH1* and *PRXR9* promoters. It would also be interesting to see if ectopic lignification of the vasculature and cortex in *35S:BOP2* lines (Khan et al., 2012b) is rescued by *tga1 tga4* loss-of-function and if flowering is restored in *pnf pnf* lines.

In conclusion, this study provides evidence that PNY/PNF repression of *BOP1/2* and their downstream effectors *ATH1* and *KNAT6* is necessary for competence to flower (Fig. 4.7). A pattern of antagonistic interactions between KNOX-BELL transcription factors and BOP1/2 regulates inflorescence architecture (Khan et al., 2012ab). Future studies will identify direct targets of BOP1/2-ATH1/KNAT6 that block competence to flower in *pnf pnf* mutants. Ultimately, this work will provide a deeper understanding of the mechanisms that allow the meristem to initiate new patterns of aerial growth in response to floral inductive signals.

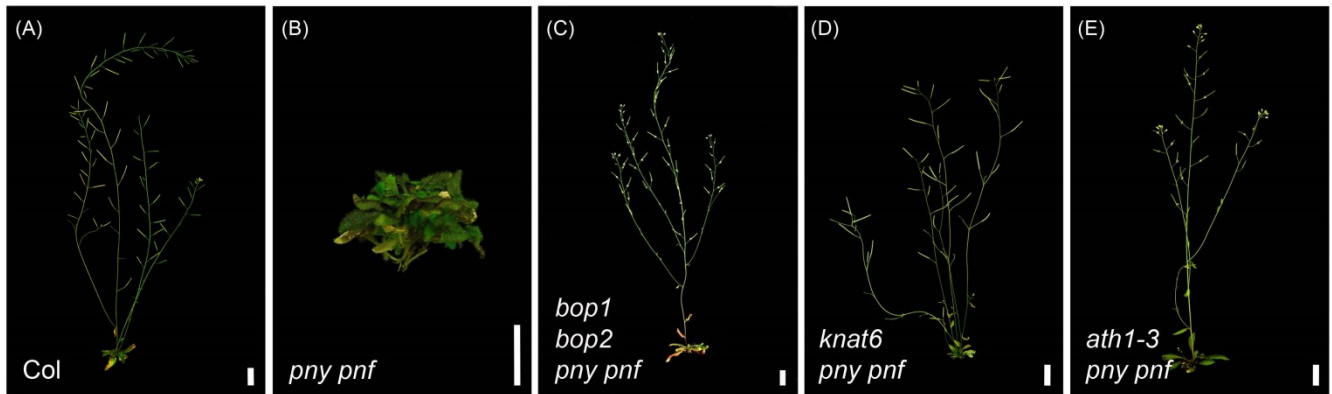


Figure 4.1 Phenotypic suppression of *pny pnf* loss of flowering by *bop1 bop2*, *knat6* and *ath1-3*

(A) WT control

(B) *pny pnf*; loss of flowering.

(C) *bop1 bop2 pny pnf*; rescue of *pny pnf* phenotypes; similar to wild-type.

(D) *pny pnf knat6*; rescue of *pny pnf* phenotypes, similar to wild-type.

(E) *ath1-3 pny pnf*; rescue of *pny pnf* phenotypes; similar to wild-type.

Scale bar, 2cm.

Figure 4.2 *BOP2:GUS* and *ATH1:GUS* expression in the meristems of *pnf pnf* plants

(A, B) *BOP2:GUS* expression in the SAM of 10-day old seedlings grown in SD

(A) in WT; expression limited to the lateral organ primordia.

(B) in *pnf pnf*; expression expanded into the meristem.

(C-F) *BOP2:GUS* and *ATH1:GUS* expressions in the IM of 4-weeks old *pnf pnf* plants.

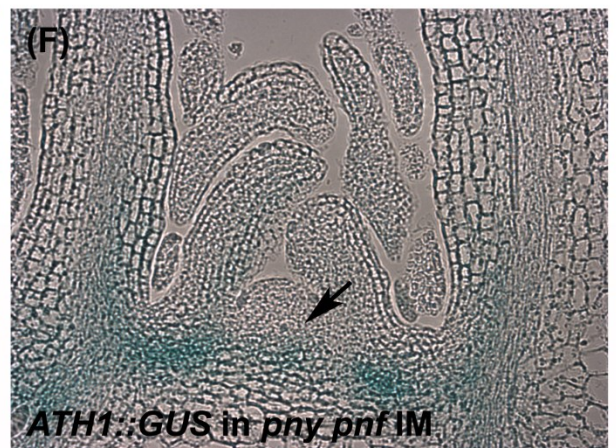
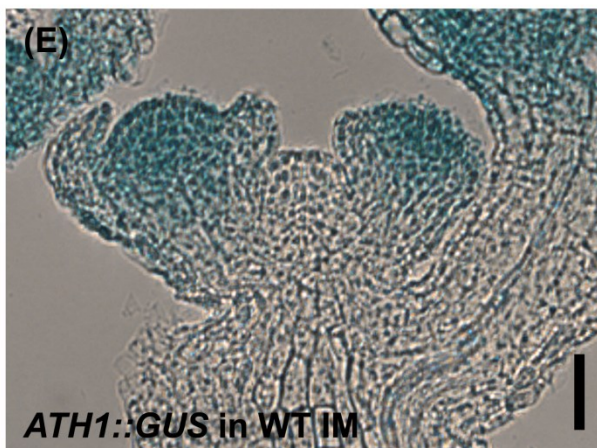
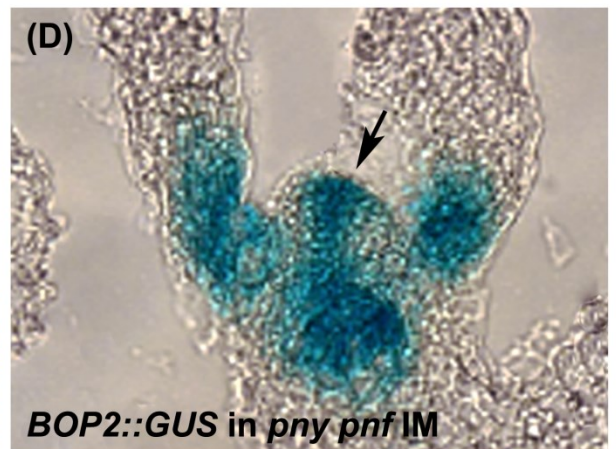
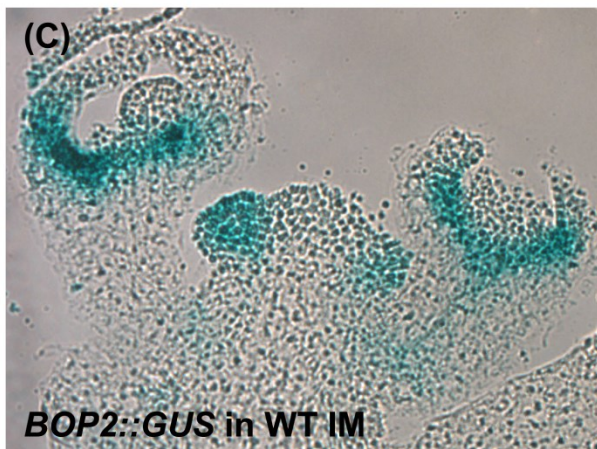
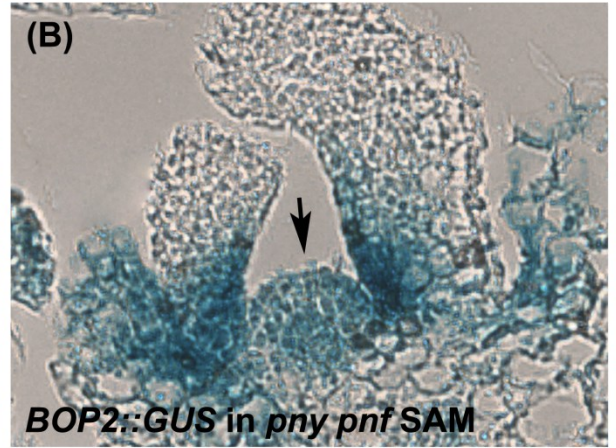
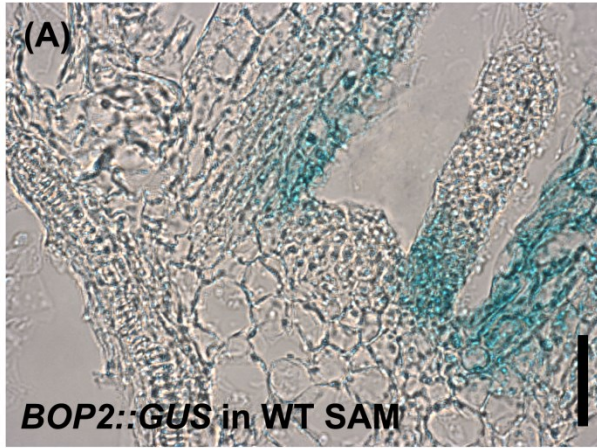
(C) *BOP2:GUS* in WT; expression limited to the floral meristem.

(D) *BOP2:GUS* in *pnf pnf*; expression expanded into the central and rib zone (arrow).

(E) *ATH1:GUS* in WT; expression limited to the floral meristem.

(F) *ATH1:GUS* in *pnf pnf*; expression expanded in to the ribzone (arrow)

Scale bar, 0.1mm.



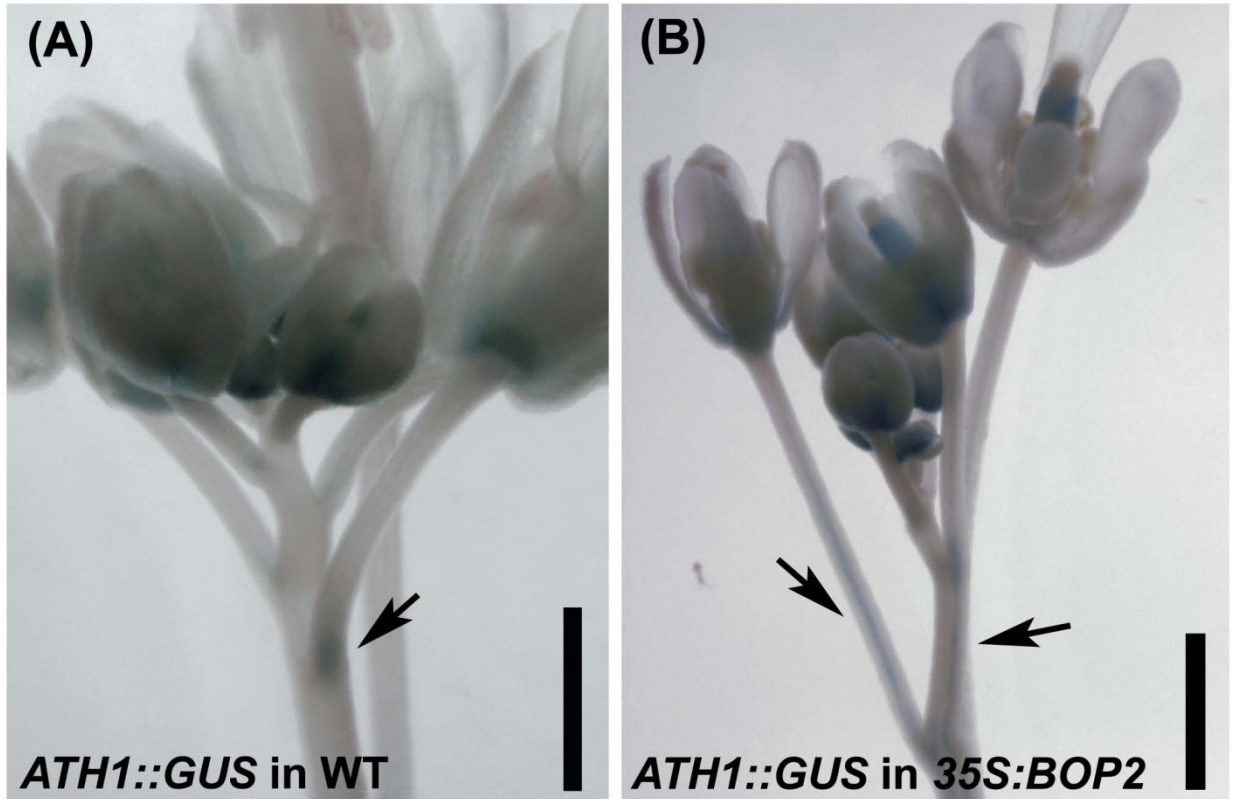


Figure 4.3 *ATH1::GUS* expression in inflorescence apices of WT and *35S::BOP2*

(A) *ATH1::GUS* in WT.

(B) *ATH1::GUS* in *35S::BOP2*.

ATH1::GUS expression in WT is confined to the axils of pedicels and base of the flowers but in *35S::BOP2* expression expands into stems and pedicels.

Scale bar, 1mm.

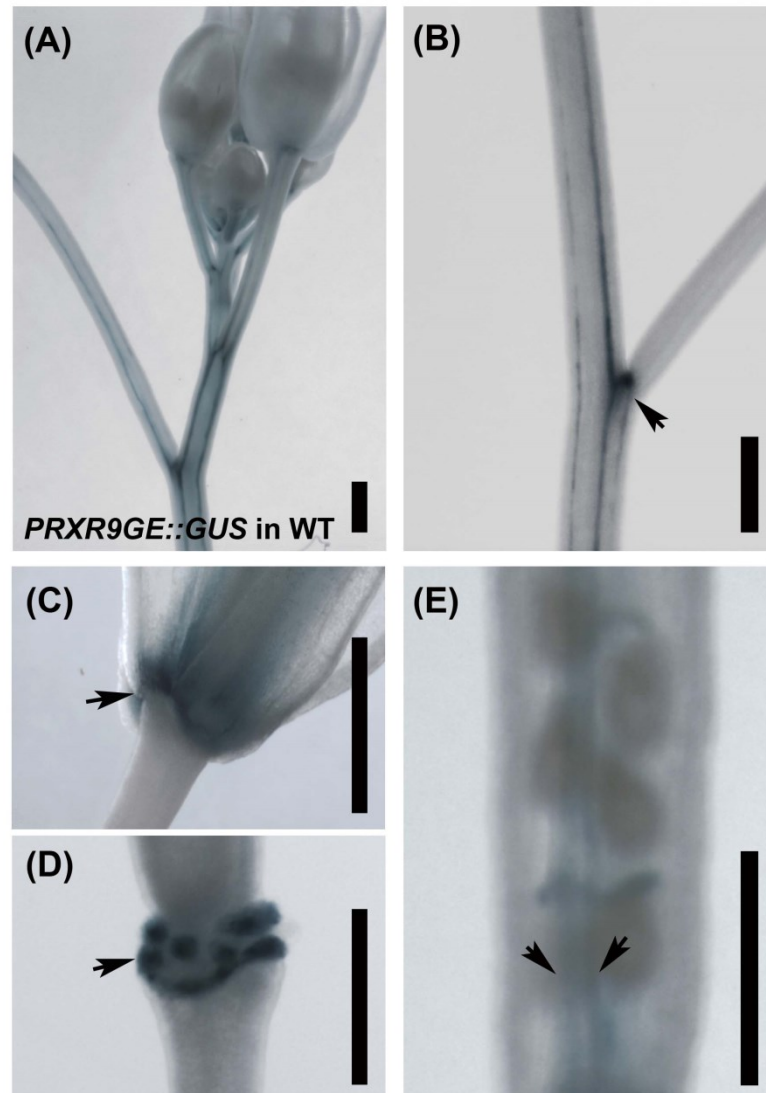


Figure 4.4 *PRXR9:GUS* expression in boundaries

(A) Inflorescence; expression in vasculature of the stems and pedicels.

(B) Close up of inflorescence; expression concentrated in the axil at the base of the pedicel (arrow).

(C) Base of flower; expression in the abscission zone prior to abscission.

(D) Base of fruit; expression in the abscission zone after abscission.

(E) Silique; expression in the valve margins (arrows).

Scale bars, 1mm.

Figure 4.5 Transcript level comparisons of *ATH1*, *PRXR9*, *KNAT6*, *TGA1* and *TGA4* in *D35S:BOPI-GR* lines

(A-D) Phenotypic comparison of *D35S:BOPI-GR* in Col treated with 10um DEX continuously for 3-weeks in comparison to *bop1-6D*.

(A) WT control.

(B) *bop1-6D*; shortened plants with irregular internodes.

(C) *D35S:BOPI-GR* in Col (Mock treated); WT-like plants.

(D) *D35S:BOPI-GR* in Col (DEX treated); phenocopy *bop1-6D*.

(E-G) qRT-PCR analysis in internodes of *D35S:BOPI-GR* in Col plants treated with Mock, 30um DEX, 50um CHX and 30um DEX + 50um CHX to check for transcript levels of *ATH1*, *PRXR9*, *KNAT6*, *TGA1* and *TGA4* in plants after:

(E) 2 hours of treatment.

(F) 4 hours of treatment.

(G) Continuous long-term treatment.

(H) qRT-PCR analysis on internodes of Col WT and *bop1-6D* overexpression lines.

Scale bar, 2cm.

Error bars, SEM

Asterisks - transcripts in DEX significantly different from Mock (E-G); transcripts in DEX + CHX significantly different from CHX (E, F); and transcripts in *bop1-6D* significantly different from wild type (H) (Student's *t* tests, $P < 0.1$).

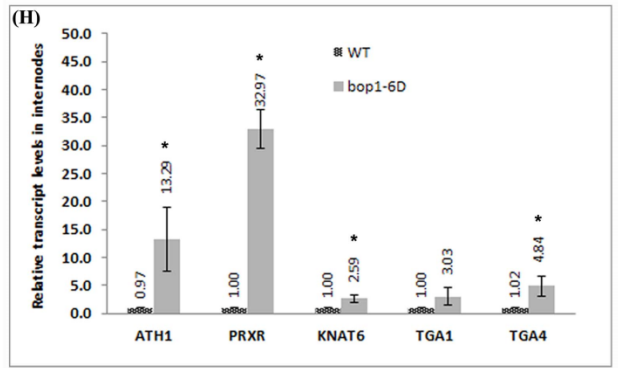
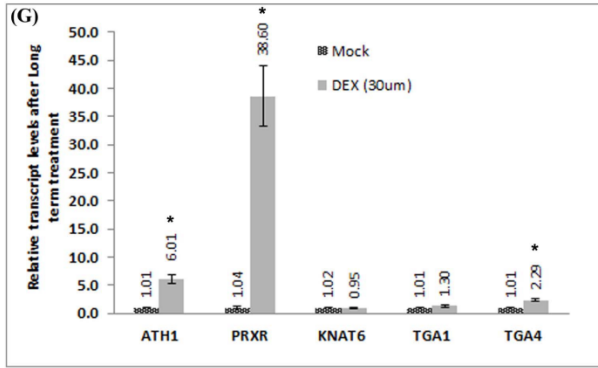
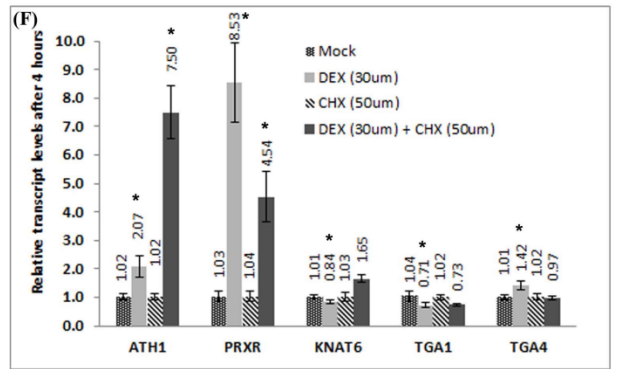
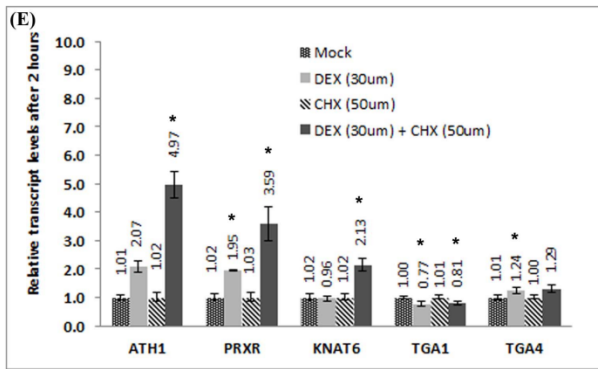


Figure 4.6 BOP1/2 require TGA1 and TGA4 to exert changes in inflorescence architecture

(A) *35S:BOP2/+ x Col/+*; shortened internodes and clustered siliques.

(B) *35S:BOP2/+ x tga1/+*; phenocopy of *35S:BOP2/+ x Col/+*.

(C) *35S:BOP2/+ x tga4/+*; phenocopy of *35S:BOP2/+ x Col/+*.

(D) *35S:BOP2/+ x tga1/+ tga4/+*; plant looks like Col wild-type.

Scale bar, 2cm.



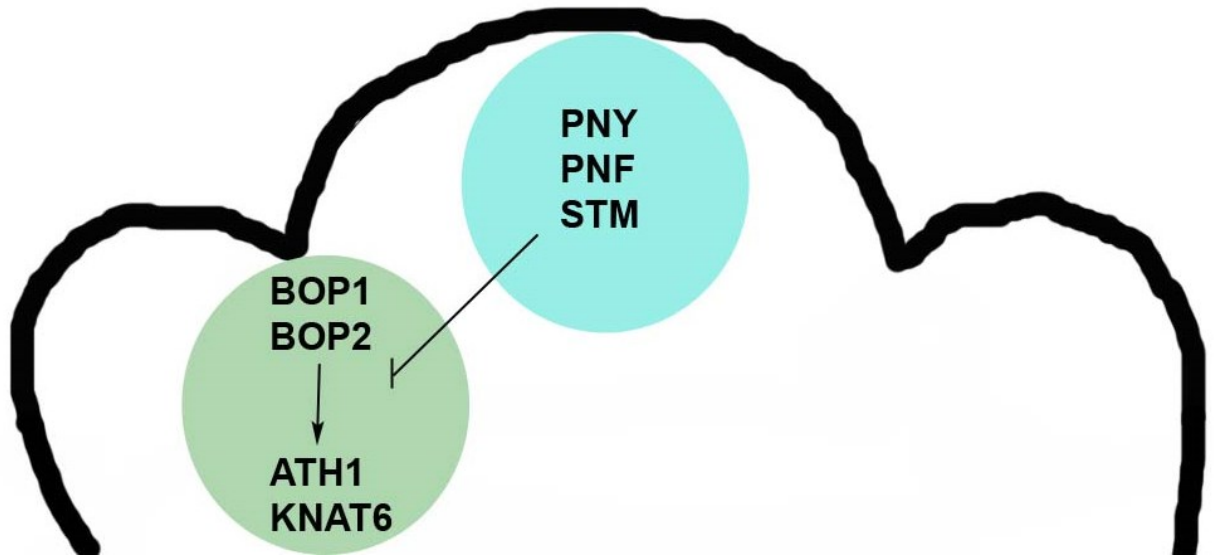


Figure 4.7 Summary of genetic interactions between *PNY/PNF-STM*, *BOP1/2*, *ATH1* and *KNAT6*

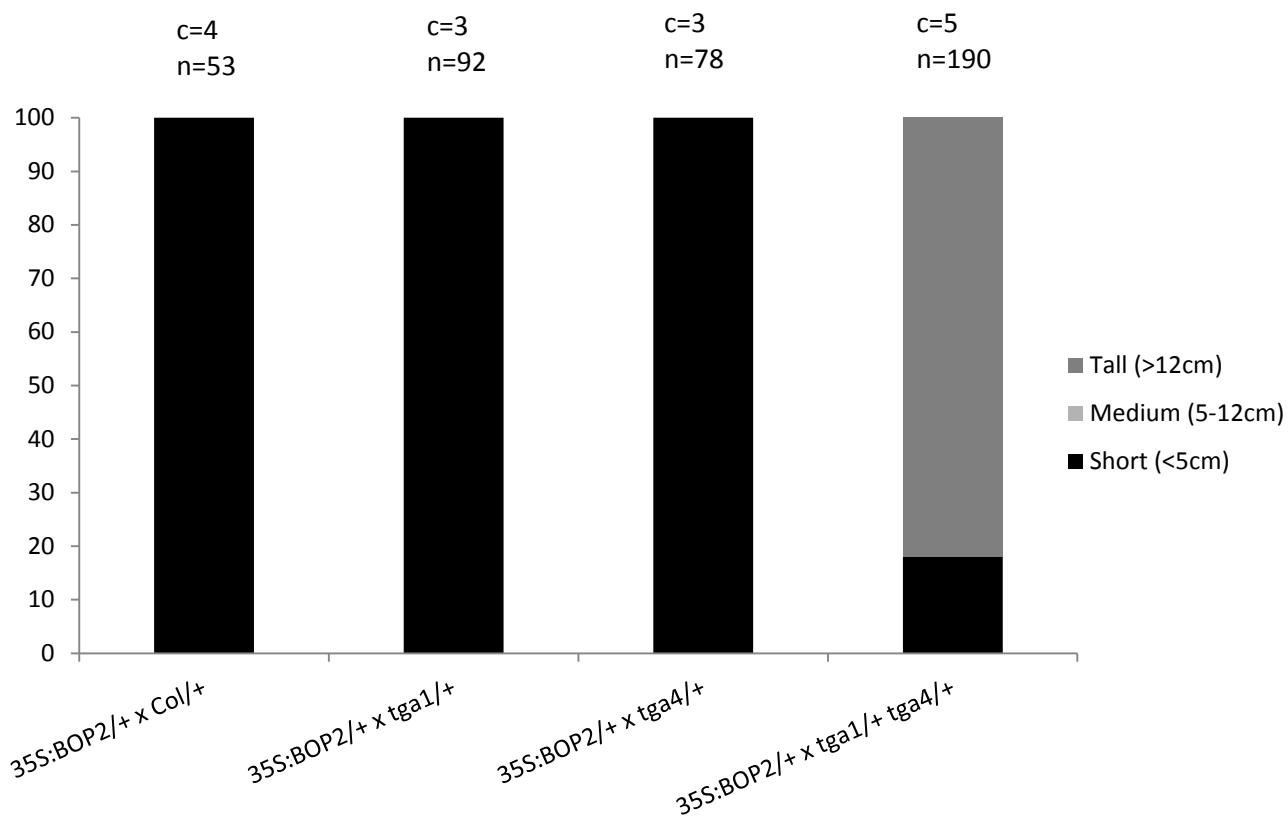
PNY/PNF in the meristem forms heterodimers with STM. These heterodimers function to exclude the expression of boundary genes *BOP1/2*, *ATH1* and *KNAT6* from the meristem. BOP1/2 promote *ATH1* and *KNAT6*, thereby antagonizing PNY and PNF.

Supplemental Table S4.1 Summary of inflorescence defects in plants overexpressing *BOP1-GR*

Transgene	WT-like	<i>pnv</i>-like	<i>bop1-6D</i>-like	Total # of Transformants
		%		
<i>35S:BOP1-GR</i>	69.49	25.42	5.08	59
<i>4CL:BOP1-GR</i>	43.75	50.00	6.25	16
<i>D35S:BOP1-GR</i>	68.75	18.75	12.50	16

Supplemental Table S4.2 List of general primers

Description	Primer	Sequence 5' – 3'	Reference
Genotyping			
<i>tga1-1</i>	tga1 Salk RP	TAGGGAATCTCCGTGTCCTCTCG	This study
	tga1 Salk LP	TTCAAAACCTGGATTCATGGTTCC	
<i>tga4-1</i>	tga4 Salk RP	GAAGGTTTGAAGTTTACGAGCCTCT	This study
	tga4 Salk LP	GCTCTGCTGAAGTTTCCACATTCC	
<i>pnf</i>	pnf Salk RP	TGCATGAGTTCCATATATATAGCAA	This study
	pnf Salk LP	TCCGATCGGTATGTGTTGTGTTCC	
Cloning			
<i>4CL/D35S:BOPI-GR</i>	CDSAtBOP1F	Restriction endonuclease site is <u>underlined</u> ATGAGCAATACTTTCGAAGAATC	This study
	GR-R	CTATTTTGGATGAAACAG	
<i>PRXR9GE:GUS</i>	2Kb PRXR pro F1	GGATCCGTAAGTGGAAAAGAATTTGTTAGT	This study
	PRXR pro R1 NcoI	CCCATGGCCATCTAGTAGTTACCTCGATTTTG	
<i>35S:BOPI-GR</i>	4H GR F1	AAAGCTAGCTATGAGCAATACTTTCGAAGA	This study
	BOPI GR + linker	AAAGGATCCGCGCCGGTGCCGACGGCAGCGG CAGCGAAATGGTGGTGGTGGTGATG	
qPCR			
<i>ATH1</i>	ATH1-qPCR-F1	ATACTCGCTCGATTATTCATCTCGA	This study
	ATH1-R1	ATCGATCATCCACCATTTGAAGAAG	
<i>TGA1</i>	TGA1-SRDX-F	ATGAATTCGACATCGACACATTTTG	This study
	TGA1-qPCR-R	ATCCTCTGACACGTTGTTGTCTAG	
<i>TGA4</i>	TGA4-SRDX-F	ATGAATACAACCTCGACACATTTTG	This study
	TGA4-qPCR-R	AAGTATCCTCTGACAAGCTGTCTGG	
<i>EIFA</i>	EIFA-qPCR-F1	AAACTCAATGAAGTACTTGAGGGAC	This study
	EIFA-qPCR-R1	TCTCAAACCATAAGCATAAATACCC	



Supplemental Figure S4.1

Quantitative analysis of inflorescence height in populations of F1 plants for the genotypes indicated. c is the # of crosses; n is the # of plants measured.

CHAPTER 5

General conclusions and future directions

5.1 General conclusions

This thesis investigated the interactions between *BOP1/2* and *TALE* homeobox genes in regulating inflorescence development. The first aim of this thesis was to test if antagonistic interactions between BP/PNY and BOP1/2 in stems regulate inflorescence architecture. The second aim was to test if BOP1/2 regulate inflorescence architecture by activating the lateral organ boundary genes *ATH1* and *KNAT6*. The third aim was to test if antagonistic interactions between PNY/PNF and BOP1/2 in the meristem regulate competence to flower. The major findings from testing these hypotheses were as follows:

1. Test if antagonistic interactions between BP/PNY and BOP1/2 in stems regulate inflorescence architecture

BOP1/2 were found to be expressed at lateral organ boundaries in embryos, the SAM, inflorescence stems, and fruits. *BOP1/2* gain-of-function displayed *bp pny*-like mutant phenotypes. Phenotypes of *bp* and *pny* single mutants were due to misexpression of *BOP1/2* outside of the boundaries and inactivation of *BOP1/2* rescued these defects. *BOP1/2* were shown to promote *KNAT6* expression and require *KNAT6* to exert their changes in inflorescence architecture. A role for *BOP1/2* in secondary cell wall formation through promoting lignin biosynthesis genes was identified. Overall, our findings showed that *BOP1/2* antagonize BP/PNY in stems through reciprocal regulation of *KNAT6* and lignin biosynthesis genes to regulate inflorescence architecture.

2. Determine if *BOP1/2* regulate inflorescence architecture by activating *ATH1* and *KNAT6*

BOP1/2 were shown to promote *ATH1* expression and like *KNAT6*, BOP1/2 required *ATH1* activity to exert changes in inflorescence architecture. It was observed that *bp* and *pnf* defects were in part due to misexpression of *ATH1* and that inactivation of *ATH1* rescued *bp* and *pnf* mutant phenotypes. Partial rescue of *bp* and *pnf* lignin patterning defects by *ath1* and *knat6* mutations identified a role for *KNAT6* and *ATH1* in secondary stem development which was previously uncharacterized. These findings suggested that BOP1/2 positively regulate lateral organ boundary genes *KNAT6* and *ATH1*, which form a heterodimer whose function is antagonistic to BP-PNF in control of inflorescence architecture.

3. Test if antagonistic interactions between PNY/PNF and BOP1/2 in the meristem regulate competence to flower

A novel role for BOP1/2 in competence to flower was identified through gain-of-function BOP1/2 plants which display delayed flowering. Furthermore, misexpression of *BOP1/2*, *KNAT6* and *ATH1* resulted in loss of flowering in *pnf pnf* mutants and inactivation of these genes rescued *pnf pnf* mutant defects. It was observed that BOP1/2 are direct transcriptional regulators of lateral organ boundary genes *ATH1* and *PRXR9* but indirectly activate *KNAT6* most likely through *ATH1* during inflorescence and secondary cell wall development. Since BOP1/2 cannot directly bind to DNA, TGA1 and TGA4 were identified as possible transcriptional factors required by BOP1/2 to promote changes in the inflorescences. Overall, the findings identify antagonism in the meristem between PNY/ PNF and BOP1/2 and their downstream effectors *ATH1* and *KNAT6* during regulation of competence to flower.

Together this thesis identifies conserved antagonistic relationships between BOP1/2 and BP/PNY in stems and PNY/PNF in meristems. Misexpression of BOP1/2 antagonizes meristem activity through reciprocal regulation of target genes thereby causing changes in flowering time and inflorescence architecture.

5.2 Future directions

1. How do BOP1/2 associate with promoters of their downstream targets?

Through glucocorticoid based transcriptional induction, *ATH1* and *PRXR9* as direct targets of BOP1 were identified. After a 2 hour induction with DEX, transcripts of *ATH1* and *PRXR9* were upregulated in *D35S:BOP1-GR* stems. The next step would be to identify if epitope-tagged BOP1 directly bind to the promoters of *ATH1* and *PRXR9* through chromatin immunoprecipitation. Since BOP cannot bind to DNA directly, potential TGA transcription factor binding sites have been identified on the promoters of *ATH1* and *PRXR9*. These binding sites would be the potential regions where BOP-TGA complexes assemble at the promoter. TGA1 and TGA4 are required by BOP1/2 to exert changes in flowering time and inflorescence architecture. A yeast one-hybrid system or EMSAs could be employed to test if these or other TGAs bind to the promoters of *ATH1* and *PRXR9*.

2. How do BOP1/2 antagonize competence to flower?

Since gain-of-function BOP1/2 in the meristem delays flowering in conjunction with *KNAT6* and *ATH1*, it is expected that these proteins target flowering-time pathway(s). *ATH1* was identified as an activator of the floral repressor *FLC* (Proveniers et al., 2007).

Thus, it is plausible that BOP1/2 function through ATH1 to up-regulate *FLC* and other floral repressors or to prevent activation of flowering activators. This can be tested using a candidate gene approach through qRT-PCR and *in situ* hybridization in the meristems of *pny pnf* and *35S:BOP2* plants.

3. Identify orthologs of BOP1/2 in *Populus trichocarpa*

BOP1/2 have been shown to function in secondary cell wall biosynthesis. Gain-of-function BOP1/2 promotes lignin biosynthesis genes leading to ectopic lignification in stems and inactivation of *BOP1/2* rescues the ectopic lignification in *bp* and *pny* mutants. It would be interesting to identify if orthologs of *BOP1/2* in a tree, *Populus trichocarpa* (Poplar), play a similar role. Two orthologs of BOP1/2 expressed in xylem are found in Poplar (*PtBPL1/2*) (Khan et al., 2012b; Khan and Hepworth, 2013). The functions of *PtBPL1/2* can be tested in *bop1 bop2* mutants in Arabidopsis to see if Poplar BOPs complement the Arabidopsis BOP functions. In parallel, it can be tested if knockdown or overexpression of *PtBPL1/2* alters wood formation in trees.

4. Role of BOP1/2 in fruit boundaries

Release of seeds in advance of harvest (“pod shatter”) is a difficulty in some commercial crops. *BOP1/2* are expressed in the valve margins, a lateral organ boundary that regulates pod shatter. Loss-of-function *pny* mutants lack a replum, which is a meristematic region in the fruits separated from the leafy valves by the valve margins. The replum cells in *pny* mutants are converted to valve margin-like cells and this phenotype is enhanced in *bp pny* mutants (Alonso-Cantabrana et al., 2007). It would be interesting to see if BOP1/2

activate a boundary module consisting of ATH1 and KNAT6 to pattern in the valve margins in fruits.

Despite all the research done on *BOP1/2* genes in the last decade, there is much more to learn about the role of these genes in plant development and plant defense. This thesis alone has identified novel roles for BOP1/2 in flowering time, inflorescences, secondary cell wall biosynthesis and fruit patterning. Hence, their importance in plants is indisputable. Further studies are needed to fully understand their function in *Arabidopsis* and to transfer this knowledge to economically relevant plant species.

REFERENCES

- Abe M, Kobayashi Y, Yamamoto S, Daimon Y, Yamaguchi A, Ikeda Y, Ichinoki H, Notaguchi M, Goto K, Araki T** (2005) FD, a bZIP protein mediating signals from the floral pathway integrator FT at the shoot apex. *Science* **309**: 1052–1056
- Achard P, Genschik P** (2009) Releasing the brakes of plant growth: how GAs shutdown DELLA proteins. *J Exp. Bot.* **60**: 1085–1092
- Aida M, Ishida T, Tasaka M** (1999) Shoot apical meristem and cotyledon formation during *Arabidopsis* embryogenesis: interaction among the *CUP-SHAPED COTYLEDON* and *SHOOT MERISTEMLESS* genes. *Development* **126**: 1563–1570
- Aida M, Tasaka M** (2006) Morphogenesis and patterning at the organ boundaries in the higher plant shoot apex. *Plant Mol. Biol.* **60**: 915–928
- Alonso-Cantabrana H, Ripoll JJ, Ochando I, Vera A, Ferrándiz C, Martínez-Laborda A** (2007) Common regulatory networks in leaf and fruit patterning revealed by mutations in the *Arabidopsis ASYMMETRIC LEAVES1* gene. *Development* **134**: 2663–2671
- Amasino RM, Michaels SD** (2010) The timing of flowering. *Plant Physiol.* **154**: 516–520
- Barton MK** (2010) Twenty years on: the inner workings of the shoot apical meristem, a developmental dynamo. *Dev. Biol.* **341**: 95–113
- Barton MK, Poethig RS** (1993) Formation of the shoot apical meristem in *Arabidopsis thaliana*: an analysis of development in the wild type and in the shoot meristemless mutant. *Development* **831**: 823–831
- Bastow R, Mylne JS, Lister C, Lippman Z, Martienssen RA, Dean C** (2004) Vernalization requires epigenetic silencing of FLC by histone methylation. *Nature* **427**: 164–167
- Baucher M, El Jaziri M, Vandeputte O** (2007) From primary to secondary growth: origin and development of the vascular system. *J Exp. Bot.* **58**: 3485–3501
- Bäurle I, Laux T** (2003) Apical meristems: the plant's fountain of youth. *BioEssays* **25**: 961–970
- Bell AD, Bryan A** (2008) *Plant Form: An illustrated guide to flowering plant morphology*. Timber press, London, pp 170-173
- Bellaoui M, Pidkowich MS, Samach A, Kushalappa K, Kohalmi SE, Modrusan Z, Crosby WL, Haughn GW** (2001) The *Arabidopsis* BELL1 and KNOX TALE homeodomain proteins interact through a domain conserved between plants and animals. *Plant Cell* **13**: 2455–2470

- Belles-Boix E, Hamant O, Witiak SM, Morin H, Traas J** (2006) *KNAT6*: An Arabidopsis homeobox gene involved in meristem activity and organ separation. *Plant Cell* **18**: 1900–1907
- Benlloch R, Berbel A, Serrano-Mislata A, Madueño F** (2007) Floral initiation and inflorescence architecture: a comparative view. *Ann. Bot.* **100**: 659–676
- Bernier G** (1988) The control of floral evocation and morphogenesis. *Annual Review of Plant Physiol. and Plant Mol. Biol.* **39**: 175–219
- Bhatt AM, Etchells JP, Canales C, Lagodienko A, Dickinson H** (2004) VAAMANA-- a BEL1-like homeodomain protein, interacts with KNOX proteins BP and STM and regulates inflorescence stem growth in Arabidopsis. *Gene* **328**: 103–111
- Boerjan W, Ralph J, Baucher M** (2003) Lignin biosynthesis. *Annu. Rev. Plant Biol.* **54**: 519–546
- Bonawitz ND, Chapple C** (2010) The genetics of lignin biosynthesis: connecting genotype to phenotype. *Annu. Rev. Gen.* **44**: 337–363
- Boss PK, Bastow RM, Mylne JS, Dean C** (2004) Multiple pathways in the decision to flower : enabling , promoting , and resetting. *Plant Cell* **16**: S18–32
- Bowman JL, Alvarez J, Weigel D, Meyerowitz EM, Smyth DR** (1993) Control of flower development in *Arabidopsis thaliana* by *APETALA1* and interacting genes. *Development* **119**: 721–743
- Bowman JL, Eshed Y** (2000) Formation and maintenance of the shoot apical meristem. *Trends Plant Sci.* **5**: 110–115
- Boyle P, Le Su E, Rochon A, Shearer HL, Murmu J, Chu JY, Fobert PR, Després C** (2009) The BTB/POZ domain of the Arabidopsis disease resistance protein NPR1 interacts with the repression domain of TGA2 to negate its function. *Plant Cell* **21**: 3700–3713
- Brand U, Fletcher JC, Hobe M, Meyerowitz EM, Simon R** (2000) Dependence of stem cell fate in Arabidopsis on a feedback loop regulated by CLV3 activity. *Science* **289**: 617–619
- Byrne ME, Groover AT, Fontana JR, Martienssen RA** (2003) Phyllotactic pattern and stem cell fate are determined by the Arabidopsis homeobox gene *BELLRINGER*. *Development* **130**: 3941–3950
- Byrne ME, Simorowski J, Martienssen RA** (2002) ASYMMETRIC LEAVES1 reveals *knox* gene redundancy in Arabidopsis. *Development* **129**: 1957–1965
- Capron A, Chatfi S, Provart N, Berleth T** (2009) Embryogenesis: Pattern formation from a single cell. *The Arabidopsis Book* **7**: e0126. doi:10.1199/tab.0126

- Carles CC, Fletcher JC** (2003) Shoot apical meristem maintenance: the art of a dynamic balance. *Trends Plant Sci.* **8**: 394–401
- Chuck G, Lincoln C, Hake S** (1996) KNAT1 induces lobed leaves with ectopic meristems when overexpressed in Arabidopsis. *Plant Cell* **8**: 1277–1289
- Clark SE, Jacobsen SE, Levin JZ, Meyerowitz EM** (1996) The CLAVATA and SHOOT MERISTEMLESS loci competitively regulate meristem activity in Arabidopsis. *Development* **122**: 1567–1575
- Clark SE, Running MP, Meyerowitz EM** (1993) CLAVATA1, a regulator of meristem and flower development in Arabidopsis. *Development* **119**: 397–418
- Clough SJ, Bent AF** (1998) Floral dip: a simplified method for Agrobacterium-mediated transformation of *Arabidopsis thaliana*. *Plant J.* **16**: 735–743
- Cole M, Nolte C, Werr W** (2006) Nuclear import of the transcription factor SHOOT MERISTEMLESS depends on heterodimerization with BLH proteins expressed in discrete sub-domains of the shoot apical meristem of *Arabidopsis thaliana*. *Nucleic Acids Res.* **34**: 1281–1292
- Corbesier L, Vincent C, Jang S, Fornara F, Fan Q, Searle I, Giakountis A, Farrona S, Gissot L, Turnbull C, Coupland G** (2007) FT protein movement contributes to long-distance signaling in floral induction of Arabidopsis. *Science* **316**: 1030–1033
- Cosio C, Dunand C** (2010) Transcriptome analysis of various flower and silique development stages indicates a set of class III peroxidase genes potentially involved in pod shattering in *Arabidopsis thaliana*. *BMC Genomics* **11**: 528–544
- Couzigou J-M, Zhukov V, Mondy S, Abu el Heba G, Cosson V, Ellis THN, Ambrose M, Wen J, Tadege M, Tikhonovich I, Mysore KS, Putterill J, Hofer J, Borisov AY, Ratet P** (2012) NODULE ROOT and COCHLEATA maintain nodule development and are legume orthologs of Arabidopsis *BLADE-ON-PETIOLE* genes. *Plant Cell* **24**: 4498–4510
- Dean G, Casson S, Lindsey K** (2004) *KNAT6* gene of Arabidopsis is expressed in roots and is required for correct lateral root formation. *Plant Mol. Biol.* **54**: 71–84
- Després C, Chubak C, Rochon A, Clark R, Bethune T, Desveaux D, Fobert PR** (2003) The Arabidopsis NPR1 Disease Resistance Protein Is a Novel Cofactor That Confers Redox Regulation of DNA Binding Activity to the Basic Domain / Leucine Zipper Transcription Factor TGA1. *Plant Cell* **15**: 2181–2191
- Douglas SJ, Chuck G, Dengler RE, Pelecanda L, Riggs CD** (2002) KNAT1 and ERECTA regulate inflorescence architecture in Arabidopsis. *Plant Cell* **14**: 547–558
- Ehlting J, Mattheus N, Aeschliman DS, Li E, Hamberger B, Cullis IF, Zhuang J, Kaneda M, Mansfield SD, Samuels L, Ritland K, Ellis BE, Bohlmann J,**

- Douglas C** (2005) Global transcript profiling of primary stems from *Arabidopsis thaliana* identifies candidate genes for missing links in lignin biosynthesis and transcriptional regulators of fiber differentiation. *Plant J.* **42**: 618–640
- Emery JF, Floyd SK, Alvarez J, Eshed Y, Hawker NP, Izhaki A, Baum SF, Bowman JL** (2003) Radial patterning of Arabidopsis shoots by class III *HD-ZIP* and *KANADI* genes. *Curr. Biol.* **13**: 1768–1774
- Endrizzi K, Moussian B, Haecker A, Levin JZ, Laux T** (1996) The *SHOOTMERISTEMLESS* gene is required for maintenance of undifferentiated cells in Arabidopsis shoot and floral meristems and acts at a different regulatory level than the meristem genes *WUSCHEL* and *SWILLE*. *Plant J.* **10**: 967–979
- Ethells JP, Moore L, Jiang WZ, Prescott H, Capper R, Saunders NJ, Bhatt AM, Dickinson HG** (2012) A role for *BELLRINGER* in cell wall development is supported by loss-of-function phenotypes. *BMC Plant Biol.* **12**: 212-224
- Fletcher JC** (2002) Shoot and floral meristem maintenance in Arabidopsis. *Annu. Rev. Plant Biol.* **53**: 45–66
- Fletcher JC, Meyerowitz EM** (2000) Cell signaling within the shoot meristem. *Curr. Opin. Plant Biol.* **3**: 23–30
- Furutani M, Vernoux T, Traas J, Kato T, Tasaka M, Aida M** (2004) *PIN-FORMED1* and *PINOID* regulate boundary formation and cotyledon development in Arabidopsis embryogenesis. *Development* **131**: 5021–5030
- Gallavotti A** (2013) The role of auxin in shaping shoot architecture. *J Exp. Bot.* **64**: 2593–2608
- Gallois J-L, Woodward C, Reddy GV, Sablowski R** (2002) Combined *SHOOT MERISTEMLESS* and *WUSCHEL* trigger ectopic organogenesis in Arabidopsis. *Development* **129**: 3207–3217
- Gatz C** (2013) From Pioneers to Team Players: TGA Transcription Factors Provide a Molecular Link Between Different Stress Pathways. *Mol. Plant Microbe Interact.* **26**: 151–159
- Gazzani S, Gendall AR, Lister C, Dean C** (2003) Analysis of the Molecular Basis of Flowering Time Variation in Arabidopsis Accessions. *Plant Physiol.* **132**: 1107–1114
- Gendall AR, Levy YY, Wilson A, Dean C** (2001) The *VERNALIZATION 2* gene mediates the epigenetic regulation of vernalization in Arabidopsis. *Cell* **107**: 525–535

- Gómez-Mena C, Sablowski R (2008)** ARABIDOPSIS THALIANA HOMEODOMAIN GENE1 establishes the basal boundaries of shoot organs and controls stem growth. *Plant Cell* **20**: 2059–2072
- Gourlay CW, Hofer JM, Ellis TH (2000)** Pea compound leaf architecture is regulated by interactions among the genes *UNIFOLIATA*, *cochleata*, *afila*, and *tendrill-lessn*. *Plant Cell* **12**: 1279–1294
- Guo M, Thomas J, Collins G, Timmermans MCP (2008)** Direct repression of *KNOX* loci by the ASYMMETRIC LEAVES1 complex of Arabidopsis. *Plant Cell* **20**: 48–58
- Ha CM, Jun JH, Fletcher JC (2010)** Control of Arabidopsis leaf morphogenesis through regulation of the YABBY and KNOX families of transcription factors. *Genetics* **186**: 197–206
- Ha CM, Jun JH, Nam HG, Fletcher JC (2004)** *BLADE-ON-PETIOLE1* encodes a BTB/POZ domain protein required for leaf morphogenesis in *Arabidopsis thaliana*. *Plant Cell Physiol.* **45**: 1361–1370
- Ha CM, Jun JH, Nam HG, Fletcher JC (2007)** *BLADE-ON-PETIOLE1* and 2 control Arabidopsis lateral organ fate through regulation of LOB domain and adaxial-abaxial polarity genes. *Plant Cell* **19**: 1809–1825
- Ha CM, Kim G-T, Kim BC, Jun JH, Soh MS, Ueno Y, Machida Y, Tsukaya H, Nam HG (2003)** The *BLADE-ON-PETIOLE1* gene controls leaf pattern formation through the modulation of meristematic activity in Arabidopsis. *Development* **130**: 161–172
- Hackbusch J, Richter K, Müller J, Salamini F, Uhrig JF (2005)** A central role of *Arabidopsis thaliana* ovate family proteins in networking and subcellular localization of 3-aa loop extension homeodomain proteins. *Proc. Nat. Acad. Sci.* **102**: 4908–4912
- Harmer SL, Hogenesch JB, Straume M, Chang H-S, Han B, Zhu T, Wang X, Kreps JA, Kay SA (2000)** Orchestrated transcription of key pathways in Arabidopsis by the circadian clock. *Science* **290**: 2110–2113
- Hartmann U, Ho S, Nettlesheim K, Wisman E, Saedler H, Huijser P (2000)** Molecular cloning of SVP : a negative regulator of the floral transition in Arabidopsis. *Plant J.* **21**: 351–360
- Hauffe KD, Paszkowski U, Schulze-Lefert P, Hahlbrock K, Dangl JL, Douglas CJ (1991)** A parsley *4CL-1* promoter fragment specifies complex expression patterns in transgenic tobacco. *Plant Cell* **3**: 435–443

- Hay A, Kaur H, Phillips A, Hedden P, Hake S, Tsiantis M** (2002) The gibberellin pathway mediates KNOTTED1-type homeobox function in plants with different body plans. *Curr. Biol.* **12**: 1557–1565
- He Y, Amasino RM** (2005) Role of chromatin modification in flowering-time control. *Trends Plant Sci.* **10**: 30–35
- Hellens RP, Edwards EA, Leyland NR, Bean S, Mullineaux PM** (2000) pGreen: a versatile and flexible binary Ti vector for *Agrobacterium*-mediated plant transformation. *Plant Mol. Biol.* **42**: 819–832
- Hepworth SR, Valverde F, Ravenscroft D, Mouradov A, Coupland G** (2002) Antagonistic regulation of flowering-time gene *SOC1* by CONSTANS and FLC via separate promoter motifs. *The EMBO journal* **21**: 4327–4337
- Hepworth SR, Zhang Y, McKim S, Li X, Haughn GW** (2005) BLADE-ON-PETIOLE – dependent signaling controls leaf and floral patterning in Arabidopsis. *Plant Cell* **17**: 1434–1448
- Hibara K, Takada S, Tasaka M** (2003) *CUC1* gene activates the expression of SAM-related genes to induce adventitious shoot formation. *Plant J.* **36**: 687–696
- Ichihashi Y, Kawade K, Usami T, Horiguchi G, Takahashi T, Tsukaya H** (2011) Key proliferative activity in the junction between the leaf blade and leaf petiole of Arabidopsis. *Plant Physiol.* **157**: 1151–1162
- Irish VF** (2010) The flowering of Arabidopsis flower development. *Plant J.* **61**: 1014–1028
- Jakoby M, Weisshaar B, Dröge-Laser W, Vicente-Carbajosa J, Tiedemann J, Kroj T, Parcy F** (2002) bZIP transcription factors in Arabidopsis. *Trends Plant Sci.* **7**: 106–111
- Jarillo JA, Piñeiro M** (2011) Timing is everything in plant development. The central role of floral repressors. *Plant Sci.* **181**: 364–378
- Johanson U, West J, Lister C, Michaels S, Amasino R, Dean C** (2000) Molecular analysis of FRIGIDA, a major determinant of natural variation in Arabidopsis flowering time. *Science* **290**: 344–347
- Jun JH, Ha CM, Fletcher JC** (2010) BLADE-ON-PETIOLE1 coordinates organ determinacy and axial polarity in Arabidopsis by directly activating ASYMMETRIC LEAVES2. *Plant Cell* **22**: 62–76
- Kanrar S, Bhattacharya M, Arthur B, Courtier J, Smith HMS** (2008) Regulatory networks that function to specify flower meristems require the function of homeobox genes *PENNYWISE* and *POUND-FOOLISH* in Arabidopsis. *Plant J.* **54**: 924–937

- Kanrar S, Onguka O, Smith HMS** (2006) Arabidopsis inflorescence architecture requires the activities of KNOX-BELL homeodomain heterodimers. *Planta* **224**: 1163–1173
- Karim MR, Hirota A, Kwiatkowska D, Tasaka M, Aida M** (2009) A role for Arabidopsis PUCHI in floral meristem identity and bract suppression. *Plant Cell* **21**: 1360–1372
- Kayes JM, Clark SE** (1998) CLAVATA2, a regulator of meristem and organ development in Arabidopsis. *Development* **125**: 3843–3851
- Khan M, Hepworth SR** (2013) *BLADE-ON-PETIOLE* genes: setting boundaries in development and defence. Submitted to *Plant Sci.*
- Khan M, Tabb P, Hepworth SR** (2012a) BLADE-ON-PETIOLE1 and 2 regulate Arabidopsis inflorescence architecture in conjunction with homeobox genes *KNAT6* and *ATH1*. *Plant Signal. Behav.* **7**: 788–792
- Khan M, Xu M, Murmu J, Tabb P, Liu Y, Storey K, McKim SM, Douglas CJ, Hepworth SR** (2012b) Antagonistic interaction of BLADE-ON-PETIOLE1 and 2 with BREVIPEDICELLUS and PENNYWISE regulates Arabidopsis inflorescence architecture. *Plant Physiol.* **158**: 946–960
- Kim D-H, Doyle MR, Sung S, Amasino RM** (2009) Vernalization: winter and the timing of flowering in plants. *Annu. Rev. Cell Dev. Biol.* **25**: 277–299
- Kinkema M, Fan W, Dong X** (2000) Nuclear localization of NPR1 is required for activation of PR gene expression. *Plant Cell* **12**: 2339–2350
- Kobayashi Y, Kaya H, Goto K, Iwabuchi M, Araki T** (1999) A pair of related genes with antagonistic roles in mediating flowering signals. *Science* **286**: 1960–1962
- Kobayashi Y, Weigel D** (2007) Move on up, it's time for change--mobile signals controlling photoperiod-dependent flowering. *Genes Dev.* **21**: 2371–2384
- Koncz C, Schell J** (1986) The promoter of TL-DNA gene 5 controls the tissue-specific expression of chimaeric genes carried by a novel type of Agrobacterium binary vector. *Mol. Gen. Genet.* **204**: 383–396
- Koornneef M, Hanhart CJ, Van der Veen JH** (1991) A genetic and physiological analysis of late flowering mutants in *Arabidopsis thaliana*. *Mol. Gen. Genet.* **229**: 57–66
- Lal S, Pacis LB, Smith HMS** (2011) Regulation of the *SQUAMOSA PROMOTER-BINDING PROTEIN-LIKE* genes/microRNA156 module by the homeodomain proteins PENNYWISE and POUND-FOOLISH in Arabidopsis. *Mol. Plant* **4**: 1123–32

- Lavagi I, Estelle M, Weckwerth W, Beynon J, Bastow RM** (2012) From bench to bountiful harvests: a road map for the next decade of Arabidopsis research. *Plant Cell* **24**: 2240–2247
- Lee J, Oh M, Park H, Lee I** (2008a) SOC1 translocated to the nucleus by interaction with AGL24 directly regulates leafy. *Plant J.* **55**: 832–843
- Lee JH, Park SH, Lee JS, Ahn JH** (2007) A conserved role of SHORT VEGETATIVE PHASE (SVP) in controlling flowering time of Brassica plants. *Biochim. Biophys. Acta* **1769**: 455–461
- Lee Y, Derbyshire P, Knox JP, Hvoslef-Eide AK** (2008b) Sequential cell wall transformations in response to the induction of a pedicel abscission event in *Euphorbia pulcherrima* (poinsettia). *Plant J.* **54**: 993–1003
- Lewis MW, Leslie ME, Liljegren SJ** (2006) Plant separation: 50 ways to leave your mother. *Curr. Opin. Plant Biol.* **9**: 59–65
- Li D, Liu C, Shen L, Wu Y, Chen H, Robertson M, Helliwell CA, Ito T, Meyerowitz E, Yu H** (2008) A repressor complex governs the integration of flowering signals in Arabidopsis. *Dev. Cell* **15**: 110–120
- Li Y, Pi L, Huang H, Xu L** (2012) ATH1 and KNAT2 proteins act together in regulation of plant inflorescence architecture. *J Exp. Bot.* **63**: 1423–1433
- Liljegren SJ, Gustafson-Brown C, Pinyopich A, Ditta GS, Yanofsky MF** (1999) Interactions among APETALA1, LEAFY, and TERMINAL FLOWER1 specify meristem fate. *Plant Cell* **11**: 1007–1018
- Lincoln C, Long J, Yamaguchi J, Serikawa K, Hake S** (1994) A *knotted1*-like homeobox gene in Arabidopsis is expressed in the vegetative meristem and dramatically alters leaf morphology when overexpressed in transgenic plants. *Plant Cell* **6**: 1859–1876
- Liu C, Chen H, Er HL, Soo HM, Kumar PP, Han J-H, Liou YC, Yu H** (2008) Direct interaction of AGL24 and SOC1 integrates flowering signals in Arabidopsis. *Development* **135**: 1481–1491
- Lloyd AM, Shena M, Walbot V, Davis RW** (1994) Epidermal cell fate determination in Arabidopsis: patterns define by a steroid-inducible regulator. *Science* **266**: 436–439
- Lodha M, Marco CF, Timmermans, MC** (2013) The ASYMMETRIC LEAVES complex maintains repression of *KNOX* homeobox genes via direct recruitment of Polycomb-repressive complex 2. *Genes Dev.* **27**: 596–601
- Long JA, Barton MK** (1998) The development of apical embryonic pattern in Arabidopsis. *Development* **125**: 3027–3035

- Long J, Barton MK** (2000) Initiation of axillary and floral meristems in Arabidopsis. *Dev. Biol.* **218**: 341–353
- Long JA, Moan EI, Medford JI, Barton MK** (1996) A member of the KNOTTED class of homeodomain proteins encoded by the *STM* gene of Arabidopsis. *Nature* **379**: 66–69
- Mayer KFX, Schoof H, Haecker A, Lenhard M, Ju G, Laux T, Morgenstern A, Tu D-** (1998) Role of WUSCHEL in regulating stem cell fate in the Arabidopsis shoot meristem. *Cell* **95**: 805–815
- McKim SM, Stenvik G-E, Butenko M a, Kristiansen W, Cho SK, Hepworth SR, Aalen RB, Haughn GW** (2008) The *BLADE-ON-PETIOLE* genes are essential for abscission zone formation in Arabidopsis. *Development* **135**: 1537–1546
- Mele G, Ori N, Sato Y, Hake S** (2003) The knotted1-like homeobox gene *BREVIPEDICELLUS* regulates cell differentiation by modulating metabolic pathways. *Genes Dev.* **17**: 2088–2093
- Meyerowitz EM** (1987) *Arabidopsis thaliana*. *Annu. Rev. Gen.* **21**: 93–111
- Michaels SD** (2009) Flowering time regulation produces much fruit. *Curr. Opin. Plant Biol.* **12**: 75–80
- Michaels SD, Amasino RM** (1999) *FLOWERING LOCUS C* encodes a novel MADS domain protein that acts as a repressor of flowering. *Plant Cell* **11**: 949–956
- Michaels SD, Amasino RM** (2001) Loss of *FLOWERING LOCUS C* activity eliminates the late-flowering phenotype of *FRIGIDA* and autonomous pathway mutations but not responsiveness to vernalization. *Plant Cell* **13**: 935–941
- Michaels SD, He Y, Scortecci KC, Amasino RM** (2003) Attenuation of *FLOWERING LOCUS C* activity as a mechanism for the evolution of summer-annual flowering behavior in Arabidopsis. *Proc. Nat. Acad. Sci.* **100**: 10102–10107
- Mou Z, Fan W, Dong X** (2003) Inducers of plant systemic acquired resistance regulate NPR1 function through redox changes. *Cell* **113**: 935–944
- Murray JH, Jones A, Godin C, Traas J** (2012) Systems analysis of shoot apical meristem growth and development: integrating hormonal and mechanical signaling. *Plant Cell* **24**: 3907–3919
- Nieminen KM, Kauppinen L, Helariutta U** (2004) A weed for wood? Arabidopsis as a genetic model for xylem development. *Plant Physiol.* **135**: 653–659
- Norberg M, Holmlund M, Nilsson O** (2005) The *BLADE ON PETIOLE* genes act redundantly to control the growth and development of lateral organs. *Development* **132**: 2203–2213

- Ogawa M, Shinohara H, Sakagami Y, Matsubayashi Y** (2008) Arabidopsis CLV3 peptide directly binds CLV1 ectodomain. *Science* **319**: 294
- Onouchi H, Igeño MI, Périlleux C, Graves K, Coupland G** (2000) Mutagenesis of plants overexpressing *CONSTANS* demonstrates novel interactions among Arabidopsis flowering-time genes. *Plant Cell* **12**: 885–900
- Parcy F, Nilsson O, Busch MA, Lee I, Weigel D** (1998) A genetic framework for floral patterning. *Nature* **395**: 561–566
- Passardi F, Penel C, Dunand C** (2004) Performing the paradoxical: how plant peroxidases modify the cell wall. *Trends Plant Sci.* **9**: 534–540
- Patterson SE** (2001) Cutting loose. Abscission and dehiscence in Arabidopsis. *Plant Physiol.* **126**: 494–500
- Pautler M, Tanaka W, Hirano H-Y, Jackson D** (2013) Grass meristems I: shoot apical meristem maintenance, axillary meristem determinacy and the floral transition. *Plant Cell Physiol.* **54**: 302–312
- Pautot V, Dockx J, Hamant O, Kronenberger J, Grandjean O, Jublot D, Traas J** (2001) KNAT2: evidence for a link between knotted-like genes and carpel development. *Plant Cell* **13**: 1719–1734
- Peaucelle A, Louvet R, Johansen JN, Salsac F, Morin H, Fournet F, Belcram K, Gillet F, Höfte H, Laufs P** (2011) The transcription factor BELLRINGER modulates phyllotaxis by regulating the expression of a pectin methylesterase in Arabidopsis. *Development* **138**: 4733–4741
- Proveniers M, Rutjens B, Brand M, Smeekens S** (2007) The Arabidopsis TALE homeobox gene *ATH1* controls floral competency through positive regulation of *FLC*. *Plant J.* **52**: 899–913
- Putterill J, Laurie R, Macknight R** (2004) It's time to flower: the genetic control of flowering time. *BioEssays* **26**: 363–373
- Ragni L, Belles-Boix E, Günl M, Pautot V** (2008) Interaction of KNAT6 and KNAT2 with BREVIPEDICELLUS and PENNYWISE in Arabidopsis inflorescences. *Plant Cell* **20**: 888–900
- Ratcliffe OJ, Amaya I, Vincent C, Rothstein S, Carpenter R, Coen ES, Bradley DJ** (1998) A common mechanism controls the life cycle and architecture of plants. *Development* **125**: 1609–1615
- Reddy GV, Meyerowitz EM** (2005) Stem-cell homeostasis and growth dynamics can be uncoupled in the Arabidopsis shoot apex. *Science* **310**: 663–667

- Robert Wyatt** (1982) Inflorescence architecture: How flower number, arrangement, and phenology affect pollination and fruit-set. *Am. J. Bot.* **69**: 585–594
- Roberts JA, Elliott KA, González-Carranza ZH** (2002) Abscission, dehiscence, and other cell separation processes. *Annu. Rev. Plant Biol.* **53**: 131–158
- Rochon A, Boyle P, Wignes T, Fobert PR, Després C** (2006) The coactivator function of Arabidopsis NPR1 requires the core of its BTB/POZ domain and the oxidation of C-terminal cysteines. *Plant Cell* **18**: 3670–3685
- Rutjens B, Bao D, Van Eck-Stouten E, Brand M, Smeekens S, Proveniers M** (2009) Shoot apical meristem function in Arabidopsis requires the combined activities of three BEL1-like homeodomain proteins. *Plant J.* **58**: 641–654
- Sablowski R** (2007) Flowering and determinacy in Arabidopsis. *J Exp. Bot.* **58**: 899–907
- Saleh O, Issman N, Seumel GI, Stav R, Samach A, Reski R, Frank W, Arazi T** (2011) MicroRNA534a control of *BLADE-ON-PETIOLE 1* and *2* mediates juvenile-to-adult gametophyte transition in *Physcomitrella patens*. *Plant J.* **65**: 661–674
- Samach A, Onouchi H, Gold SE, Ditta GS, Schwarz-Sommer Z, Yanofsky MF, Coupland G** (2000) Distinct roles of CONSTANS target genes in reproductive development of Arabidopsis. *Science* **288**: 1613–1616
- Sassi M, Vernoux T** (2013) Auxin and self-organization at the shoot apical meristem. *J Exp. Bot.* **64**: 2579–2592
- Schmid M, Uhlentaut NH, Godard F, Demar M, Bressan R, Weigel D, Lohmann JU** (2003) Dissection of floral induction pathways using global expression analysis. *Development* **130**: 6001–6012
- Schoof H, Lenhard M, Haecker A, Mayer KF, Jürgens G, Laux T** (2000) The stem cell population of Arabidopsis shoot meristems is maintained by a regulatory loop between the *CLAVATA* and *WUSCHEL* genes. *Cell* **100**: 635–644
- Schultz EA, Haughn GW** (1991) *LEAFY*, a homeotic gene that regulates inflorescence development in Arabidopsis. *Plant Cell* **3**: 771–781
- Schultz EA, Haughn GW** (1993) Genetic analysis of the floral initiation process (FLIP) in Arabidopsis. *Development* **119**: 745–765
- Schwechheimer C, Willige BC** (2009) Shedding light on gibberellic acid signalling. *Curr. Opin. Plant Biol.* **12**: 57–62
- Searle I, He Y, Turck F, Vincent C, Fornara F, Kröber S, Amasino RA, Coupland G** (2006) The transcription factor FLC confers a flowering response to vernalization by

- repressing meristem competence and systemic signaling in Arabidopsis. *Genes Dev.* **20**: 898–912
- Sexton R** (1976) Some ultrastructural observations on the nature of foliar abscission in *Impatiens sultani*. *Planta* **128**: 49–58
- Shearer HL, Cheng YT, Wang L, Liu J, Boyle P, Després C, Zhang, Y, Li X, Fobert PR** (2012) Arabidopsis clade I TGA transcription factors regulate plant defenses in an NPR1-independent fashion. *Mol. Plant Microbe Interact.* **25**: 1459-1468
- Sheldon CC, Rouse DT, Finnegan EJ, Peacock WJ, Dennis ES** (2000) The molecular basis of vernalization: the central role of FLOWERING LOCUS C (FLC). *Proc. Nat. Acad. Sci.* **97**: 3753–3758
- Shi C-L, Stenvik G-E, Vie AK, Bones AM, Pautot V, Proveniers M, Aalen RB, Butenko MA** (2011) Arabidopsis class I KNOTTED-like homeobox proteins act downstream in the IDA-HAE/HSL2 floral abscission signaling pathway. *Plant Cell* **23**: 2553–2567
- Sieburth LE, Meyerowitz EM** (1997) Molecular dissection of the AGAMOUS control region shows that cis elements for spatial regulation are located intragenically. *Plant Cell* **9**: 355–365
- Simon R, Igeño MI, Coupland G** (1996) Activation of floral meristem identity genes in Arabidopsis. *Nature* **384**: 59-62
- Smith HMS, Campbell BC, Hake S** (2004) Competence to respond to floral inductive signals requires the homeobox genes *PENNYWISE* and *POUND-FOOLISH*. *Curr. Biol.* **14**: 812–817
- Smith HMS, Hake S** (2003) The interaction of two homeobox genes, *BREVIPEDICELLUS* and *PENNYWISE*, regulates internode patterning in the Arabidopsis inflorescence. *Plant Cell* **15**: 1717–1727
- Smith HMS, Ung N, Lal S, Courtier J** (2011) Specification of reproductive meristems requires the combined function of SHOOT MERISTEMLESS and floral integrators FLOWERING LOCUS T and FD during Arabidopsis inflorescence development. *J Exp. Bot.* **62**: 583–593
- Smith RS, Guyomarc'h S, Mandel T, Reinhardt D, Kuhlemeier C, Prusinkiewicz P** (2006) A plausible model of phyllotaxis. *Proc. Nat. Acad. Science* **103**: 1301–1306
- Song YH, Song NY, Shin SY, Kim HJ, Yun D, Lim CO** (2008) Isolation of CONSTANS as a TGA4/OBF4 interacting protein. *Mol. Cells* **25**: 559–565
- Srikanth A, Schmid M** (2011) Regulation of flowering time: all roads lead to Rome. *Cell. Mol. Life Sci.* **68**: 2013–2037

- Steeves TA, Sussex IM** (1989) Patterns in plant development. Academic, New York.
- Suárez-López P, Wheatley K, Robson F, Onouchi H, Valverde F, Coupland G** (2001) CONSTANS mediates between the circadian clock and the control of flowering in *Arabidopsis*. *Nature* **410**: 1116–1120
- Sung S, Amasino RM** (2004) Vernalization and epigenetics: how plants remember winter. *Curr. Opin. Plant Biol.* **7**: 4–10
- Sussex IM, Kerk NM** (2001) The evolution of plant architecture. *Curr. Opin. Plant Biol.* **4**: 33–37
- Tabb P** (2012) Genetic analysis of co-ordination of flowering and regulation of inflorescence architecture in *Arabidopsis thaliana*. Carleton University, Ottawa, pp 1–97. M.Sc. thesis.
- Takada S, Goto K** (2003) TERMINAL FLOWER2, an *Arabidopsis* homolog of HETEROCHROMATIN PROTEIN1, counteracts the activation of FLOWERING LOCUS T by CONSTANS in the vascular tissues of leaves to regulate flowering time. *Plant Cell* **15**: 2856–2865
- Takada S, Hibara K, Ishida T, Tasaka M** (2001) The *CUP-SHAPED COTYLEDON1* gene of *Arabidopsis* regulates shoot apical meristem formation. *Development* **128**: 1127–1135
- Takano S, Niihama M, Smith HMS, Tasaka M, Aida M** (2010) *gorgon*, a novel missense mutation in the *SHOOT MERISTEMLESS* gene, impairs shoot meristem homeostasis in *Arabidopsis*. *Plant Cell Physiol.* **51**: 621–634
- Talbert PB, Adler HT, Parks DW, Comai L** (1995) The *REVOLUTA* gene is necessary for apical meristem development and for limiting cell divisions in the leaves and stems of *Arabidopsis thaliana*. *Development* **121**: 2723–2735
- Tamaki S, Matsuo S, Wong HL, Yokoi S, Shimamoto K** (2007) Hd3a protein is a mobile flowering signal in rice. *Science* **316**: 1033–1036
- Turck F, Fornara F, Coupland G** (2008) Regulation and identity of florigen: FLOWERING LOCUS T moves center stage. *Annu. Rev. Plant Biol.* **59**: 573–594
- Ung N, Lal S, Smith HMS** (2011) The role of PENNYWISE and POUND-FOOLISH in the maintenance of the shoot apical meristem in *Arabidopsis*. *Plant Physiol.* **156**: 605–614
- Ung N, Smith HMS** (2011) Regulation of shoot meristem integrity during *Arabidopsis* vegetative development. *Plant Signal. Behav.* **6**: 1250–1252

- Vaughan JG** (1954) The morphology and growth of the vegetative and reproductive apices of *Arabidopsis thaliana* (L.) Heynh., *Capsella bursa-pastoris* (L.) Medic. and *Anagallis arvensis* L. Bot. J. Linn. Soc. **55**: 279–301
- Venglat SP, Dumonceaux T, Rozwadowski K, Parnell L, Babic V, Keller W, Martienssen R, Selvaraj G, Datla R** (2002) The homeobox gene *BREVIPEDICELLUS* is a key regulator of inflorescence architecture in *Arabidopsis*. Proc. Nat. Acad. Sci. **99**: 4730–4735
- Vernoux T, Besnard F, Traas J** (2010) Auxin at the shoot apical meristem. Cold Spring Harb. Perspect. Biol. **2**: a001487
- Vollbrecht E, Reiser L, Hake S** (2000) Shoot meristem size is dependent on inbred background and presence of the maize homeobox gene, *knotted1*. Development **127**: 3161–3172
- Vroemen CW, Mordhorst AP, Albrecht C, Kwaaitaal MACJ, de Vries SC** (2003) The *CUP-SHAPED COTYLEDON3* gene is required for boundary and shoot meristem formation in *Arabidopsis*. Plant Cell **15**: 1563–1577
- Wagner D, Sablowski R, Meyerowitz EM** (1999) Transcriptional activation of *APETALA1* by *LEAFY*. Science **285**: 582–584
- Wang J-W, Czech B, Weigel D** (2009) miR156-regulated SPL transcription factors define an endogenous flowering pathway in *Arabidopsis thaliana*. Cell **138**: 738–749
- Werner JD, Borevitz JO, Uhlentaut NH, Ecker JR, Chory J, Weigel D** (2005) *FRIGIDA*-independent variation in flowering time of natural *Arabidopsis thaliana* accessions. Genetics **170**: 1197–1207
- Wigge PA, Kim MC, Jaeger KE, Busch W, Schmid M, Lohmann JU, Weigel D** (2005) Integration of spatial and temporal information during floral induction in *Arabidopsis*. Science **309**: 1056–1059
- William DA, Su Y, Smith MR, Lu M, Baldwin DA, Wagner D** (2004) Genomic identification of direct target genes of *LEAFY*. Proc. Nat. Acad. Science **101**: 1775–1780
- Wu X-M, Yu Y, Han L-B, Li C-L, Wang H-Y, Zhong N-Q, Yao Y, Xia G-X** (2012a) The tobacco *BLADE-ON-PETIOLE2* gene mediates differentiation of the corolla abscission zone by controlling longitudinal cell expansion. Plant Physiol. **159**: 835–850
- Wu Y, Zhang D, Chu JY, Boyle P, Wang Y, Brindle ID, De Luca V, Després C** (2012b) The *Arabidopsis* NPR1 protein is a receptor for the plant defense hormone salicylic acid. Cell Rep. **1**: 639–647

- Xu M** (2011) Role of BLADE-ON-PETIOLE1 and 2 in patterning the *Arabidopsis thaliana* leaf and inflorescence architecture. Carleton University, Ottawa pp 1-158. Ph.D. thesis.
- Xu L, Xu Y, Dong A, Sun Y, Pi L, Xu Y, Huang H** (2003) Novel as1 and as2 defects in leaf adaxial-abaxial polarity reveal the requirement for ASYMMETRIC LEAVES1 and 2 and ERECTA functions in specifying leaf adaxial identity. *Development* **130**: 4097–4107
- Xu M, Hu T, McKim SM, Murmu J, Haughn GW, Hepworth SR** (2010) Arabidopsis BLADE-ON-PETIOLE1 and 2 promote floral meristem fate and determinacy in a previously undefined pathway targeting APETALA1 and AGAMOUS-LIKE24. *Plant J.* **63**: 974–989
- Yadav RK, Perales M, Gruel J, Girke T, Jönsson H, Reddy GV** (2011) WUSCHEL protein movement mediates stem cell homeostasis in the Arabidopsis shoot apex. *Genes Dev.* **25**: 2025–2030
- Yamaguchi A, Kobayashi Y, Goto K, Abe M, Araki T** (2005) TWIN SISTER OF FT (TSF) acts as a floral pathway integrator redundantly with FT. *Plant Cell Physiol.* **46**: 1175–1189
- Yamaguchi A, Wu M-F, Yang L, Wu G, Poethig RS, Wagner D** (2009) The microRNA regulated SBP-box transcription factor SPL3 is a direct upstream activator of LEAFY, FRUITFUL, and APETALA1. *Dev. Cell* **17**: 268–278
- Yaxley JR, Ross JJ, Sherriff LJ, Reid JB** (2001) Gibberellin biosynthesis mutations and root development in pea. *Plant Physiol.* **125**: 627–633
- Zeevaart JAD** (2008) Leaf-produced floral signals. *Curr. Opin. Plant Biol.* **11**: 541–547
- Zhang Y, Fan W, Kinkema M, Li X, Dong X** (1999) Interaction of NPR1 with basic leucine zipper protein transcription factors that bind sequences required for salicylic acid induction of the PR-1 gene. *Proc. Nat. Acad. Sci.* **96**: 6523–6528
- Zhang Y, Tessaro MJ, Lassner M, Li X** (2003) Knockout analysis of Arabidopsis transcription factors TGA2, TGA5, and TGA6 reveals their redundant and essential roles in systemic acquired resistance. *Plant Cell* **15**: 2647–2653
- Zhao Q, Dixon RA** (2011) Transcriptional networks for lignin biosynthesis: more complex than we thought? *Trends Plant Sci.* **16**: 227–233
- Zhou JM, Trifa Y, Silva H, Pontier D, Lam E, Shah J, Klessig DF** (2000) NPR1 differentially interacts with members of the TGA/OBF family of transcription factors that bind an element of the *PR-1* gene required for induction by salicylic acid. *Mol. Plant Microbe Interact.* **13**: 191–202